

NUMERICAL STUDIES ON ECCENTRICALLY BRACED FRAMES

A THESIS SUBMITTED TO
THE GRADUATE SCHOOL OF NATURAL AND APPLIED SCIENCES
OF
MIDDLE EAST TECHNICAL UNIVERSITY

BY

AHMET KUŞYILMAZ

IN PARTIAL FULFILLMENT OF THE REQUIREMENTS
FOR
THE DEGREE OF DOCTOR OF PHILOSOPHY
IN
CIVIL ENGINEERING

MAY 2014

Approval of the thesis:

NUMERICAL STUDIES ON ECCENTRICALLY BRACED FRAMES

submitted by **AHMET KUŞYILMAZ** in partial fulfillment of the requirements for the degree of **Doctor of Philosophy in Civil Engineering Department, Middle East Technical University** by,

Prof. Dr. Canan Özgen
Dean, Graduate School of **Natural and Applied Sciences**

Prof. Dr. Ahmet Cevdet Yalçın
Head of Department, **Civil Engineering**

Prof. Dr. Cem Topkaya
Supervisor, **Civil Engineering Dept., METU**

Assoc.Prof. Dr. Afşin Sarıtaş
Co-Supervisor, **Civil Engineering Dept., METU**

Examining Committee Members:

Prof. Dr. Polat Gülkan
Civil Engineering Dept., Çankaya University

Prof. Dr. Cem Topkaya
Civil Engineering Dept., METU

Prof. Dr. Mehmet Utku
Civil Engineering Dept., METU

Assoc. Prof. Dr. Altuğ Erberik
Civil Engineering Dept., METU

Assoc. Prof. Dr. Eray Baran
Civil Engineering Dept., Atılım University

Date:

23.05.2014

I hereby declare that all information in this document has been obtained and presented in accordance with academic rules and ethical conduct. I also declare that, as required by these rules and conduct, I have fully cited and referenced all material and results that are not original to this work.

Name, Last Name : Ahmet KUŞYILMAZ

Signature :

ABSTRACT

NUMERICAL STUDIES ON ECCENTRICALLY BRACED FRAMES

Kuşylmaz, Ahmet

Ph.D., Department of Civil Engineering

Supervisor : Prof. Dr. Cem Topkaya

Co-Supervisor : Assoc. Prof. Dr. Afşin Sarıtaş

May 2014, 158 pages

Numerical studies were performed on eccentrically steel braced frames to ascertain seismic performance factors and to examine dynamic characteristics of eccentrically braced frames (EBF). Pursuant to this goal a computer program which facilitates EBF designs was developed. In the first phase, the approximate period formula given in ASCE7-10 was evaluated and a technique based on global deformation characteristics was developed to improve the fundamental period estimates for EBFs. The results indicate that the developed method accurately predicts the fundamental period and reduces the scatter by a significant amount when compared with the estimations of the approximate formula. In the second phase, an analytical study on the design overstrength of EBFs was performed. The results reveal that designed frames have on average higher overstrength values when compared with the codified value. Afterwards, a numerical study was

performed to evaluate the displacement amplification factor (C_d) given in ASCE7-10 for EBFs and the rigid-plastic mechanism used for calculating link rotation angles. Based on the results, EBFs were redesigned and analyzed using a new set of C_d factors and a more accurate procedure to estimate link rotation angles. Finally, response modification factors of EBFs were evaluated utilizing a novel procedure given in FEMA P695. The results reveal that collapse probability of link sections go beyond fifty percent for procedure defined in FEMA P695. Six archetypes were redesigned using the proposed modifications to C_d factor and re-evaluated using FEMA P695 methodology. The results indicate that proposed modifications are adequate to satisfy the target collapse probability.

Keywords: Structural Steel, Eccentrically Braced Frame, Overstrength, Fundamental Period, Displacement Amplification Factor

ÖZ

DIŐMERKEZLİ ÇAPRAZ ÇERÇEVELER ÜZERİNDE SAYISAL ÇALIŐMALAR

KuŐyılmaz, Ahmet

Doktora, İnaŐat MühendisliĐi Bölümü

Tez Yöneticisi : Prof. Dr. Cem Topkaya

Ortak Tez Yöneticisi : Doç. Dr. AfŐin SarıtaŐ

Mayıs 2014, 158 sayfa

DıŐmerkezli çelik çapraz çerçevelerin (DÇÇ) sismik performans faktörlerini deĐerlendirmek ve dinamik davranıŐlarını incelemek amacıyla sayısal çalıŐmalar yapılmıŐtır. Bu amaç doĐrultusunda DÇÇin tasarımı hızlandıran bir bilgisayar programı geliştirilmiŐtir. İlk fazda, ASCE 7-10'da belirtilen yaklaşık periyot denklemi irdelenmiŐ ve DÇÇlerin hakim periyot tahminlerini iyileŐtirmek için deformasyon özelliklerine baĐlı bir teknik geliştirilmiŐtir. Sonuçlar geliştirilen metodla hesaplanan periyot deĐerlerinin gerçek periyotlara mevcut yaklaşık periyot denkleminde daha çok yakınsadıĐını göstermektedir. İkinci aşamada, DÇÇin tasarım dayanım fazlalıĐı katsayısı üzerine analitik bir çalıŐma yapılmıŐtır. Sonuçlar tasarlanan çerçevlerdeki ortalama dayanım fazlalıĐı deĐerinin şartnamede öngörülen deĐerden fazla olduĐunu göstermektedir. Ayrıca, ASCE 7-10'da verilen deplasman artırım katsayısının ve rijit-plastik deformasyon yoluyla elde edilen baĐ kiriŐ dönmelerinin deĐerlendirilmesi için sayısal bir çalıŐma yapılmıŐtır. Elde edilen sonuçlar doĐrultusunda yeni bir C_d profili ve daha kesin

bağ kiriş dönme prosedürü kullanarak tasarımlar ve analizler yinelenmiştir. Son olarak, DÇÇ'in davranış katsayıları güncel bir prosedür olan FEMA P695 yöntemi ile incelenmiştir. Sonuçlar FEMA P695 yöntemiyle bulunan bağ kiriş çökme oranlarının yüzde ellinin üzerinde olduğunu göstermektedir. Altı model çerçeve önerilen C_d değişiklikleriyle yeniden tasarlanmış ve FEMA P695 prosedürüne göre yeniden değerlendirilmiştir. Sonuçlar önerilen değişikliklerin hedeflenen çökme olasılıklarını sağlamada yeterli olduğunu göstermektedir.

Anahtar Kelimeler: Yapısal Çelik, Dışmerkezli Çapraz Çerçeveler, Dayanım Fazlalığı, Doğal Periyot, Deplasman Büyütme Katsayısı

To My Family

ACKNOWLEDGMENTS

This study was conducted under the supervision of Prof. Dr. Cem Topkaya. I would like to express my earnest thanks and gratitude for his support, guidance, encouragement and criticisms at all levels of this research. It was a great honor and pleasure for me to work under his kind and enlightening supervision.

Also, I would like to express my deepest appreciation to my co-supervisor Assoc. Prof. Dr. Afşin Sarıtaş for his support, advice and comments throughout the thesis work.

I would like to thank to my family for their endless support and love. During my study, I felt their encouragement and guidance all the time. Their enthusiasm about this study was always my main source of motivation. The patience and support shown by them are thankfully acknowledged.

Special thanks go to Professor Oh-Sung Kwon of University of Toronto for providing data on apparent building periods.

I want to extend my thanks to my office mates Mustafa Can Yücel, Müge Özgenoğlu, Alper Özge Gür, Kaan Kaatsız, Elif Ün, Fırat Soner Alıcı, Duygu Güleyen, Başar Mutlu, Sadun Tanışer and Aksel Fenerci. The joyful times that we shared in Room Z01 and their enormous support will always be remembered with pleasure.

I want to thank to Cihangir Dikici, Serkan Şahin, İpek Yılmaz, Gizem Mestav Sarıca, Meltem Bayram, Eda Fitoz and Ceren Satioğlu for their help and friendship.

TABLE OF CONTENTS

ABSTRACT.....	v
ÖZ.....	vii
ACKNOWLEDGMENTS.....	x
TABLE OF CONTENTS.....	xi
LIST OF TABLES.....	xv
LIST OF FIGURES.....	xvii
LIST OF SYMBOLS AND ABBREVIATIONS.....	xxi
CHAPTERS	
1. INTRODUCTION.....	1
1.1. GENERAL.....	1
1.2. REVIEW OF PREVIOUS STUDIES.....	3
1.2.1. Experimental Studies.....	3
1.2.2. Numerical Studies.....	5
1.3. OBJECTIVE AND SCOPE.....	8
1.4. ORGANIZATION OF THE THESIS.....	10
2. DEVELOPMENT OF COMPUTER PROGRAM FOR SEISMIC DESIGN OF EBFs.....	13
2.1. DESIGN OF EBFs ACCORDING TO US PROVISIONS.....	13
2.2. EBF DESIGN PROCEDURE AND ITS IMPLEMENTATION.....	18

2.2.1.	Formation of a Library of Sub-assemblages	19
2.2.2.	Design Algorithm	24
2.3.	VERIFICATION OF THE DEVELOPED PROGRAM	27
3.	FUNDAMENTAL PERIODS OF STEEL ECCENTRICALLY BRACED FRAMES	33
3.1.	BACKGROUND	33
3.2.	IMPACT OF USING COMPUTED PERIODS	36
3.3.	DEVELOPMENT OF A METHOD TO DETERMINE FUNDAMENTAL PERIODS	43
3.4.	A PARAMETRIC STUDY ON PERIOD ESTIMATION OF EBFs.....	47
3.4.1.	Verification of the Method Using Actual Top Story Drift Ratios....	55
3.4.2.	Evaluation of the Method Using Estimated Roof Drift Ratios.....	56
3.4.3.	Verification of the Method Using Data Published in Literature	58
3.5.	DEVELOPMENT OF NEW PERIOD-HEIGHT RELATIONSHIPS AND THEIR VERIFICATION WITH APPARENT PERIODS.....	61
4.	DESIGN OVERSTRENGTH OF STEEL ECCENTRICALLY BRACED FRAMES	65
4.1.	BACKGROUND	65
4.2.	A PARAMETRIC STUDY ON DESIGN OVERSTRENGTH OF EBFs	68
4.2.1.	Details of Parametric Study	68
4.2.2.	Results of the Parametric Study	73
4.2.2.1.	Influence of Link Length to Bay Width Ratio (e/L) on Design Overstrength	75
4.2.2.2.	Influence of Building Height (h_n) on Design Overstrength	75

4.2.2.3.	Influence of Bay Width (L) on Design Overstrength.....	77
4.2.2.4.	Influence of Seismic Hazard Level on Design Overstrength....	78
4.2.2.5.	Evaluation of Structural Overstrength (Ω_o).....	79
5.	DISPLACEMENT AMPLIFICATION FACTORS FOR STEEL ECCENTRICALLY BRACED FRAMES	81
5.1.	BACKGROUND	81
5.2.	VERIFICATION OF NUMERICAL MODELS	84
5.3.	A PARAMETRIC STUDY ON DISPLACEMENT FACTORS OF EBFs	87
5.3.1.	Details of Parametric Study.....	87
5.3.2.	Results of the Parametric Study	92
5.3.2.1.	Evaluation of the Displacements from ETHA and ITHA, and Design Displacements	95
5.3.2.2.	Evaluation of the Displacement Amplification Factor (C_d).....	96
5.3.2.3.	Evaluation of the Link Rotation Angle Calculation Procedure Given in AISC341 (2005)	98
5.3.2.4.	Evaluation of the Link Rotation Angles.....	99
5.4.	PROPOSED MODIFICATIONS	100
5.4.1.	Modification of the C_d Factor.....	101
5.4.2.	Modifications for the Procedure for Link Rotation Angle Calculation	102
5.5.	VERIFICATION OF PROPOSED MODIFICATIONS	110
6.	EVALUATION OF SEISMIC RESPONSE FACTORS FOR EBFs USING FEMA P695 METHODOLOGY.....	113
6.1.	BACKGROUND	113

6.2.	NON-SIMULATED COLLAPSE CRITERIA.....	114
6.3.	DESCRIPTION OF ARCHETYPES.....	119
6.4.	MODELING AND ANALYSIS.....	124
6.5.	EVALUATION OF SEISMIC RESPONSE FACTORS.....	127
6.6.	PROPOSED MODIFICATIONS	131
6.7.	RE-EVALUATION OF SEISMIC RESPONSE FACTORS	134
7.	CONCLUSIONS AND RECOMMENDATIONS.....	141
7.1.	SUMMARY	141
7.2.	CONCLUSIONS	143
7.3.	RECOMMENDATIONS FOR FURTHER RESEARCH.....	146
	REFERENCES	147
	CURRICULUM VITAE	157

LIST OF TABLES

TABLES

Table 2.1 Comparisons of Developed Program Output with Data Published by Özhendekci and Özhendekci (2008) (Frame ID : S-9-800-7-90).....	29
Table 2.2 Comparisons of Developed Program Output with Data Published by Özhendekci and Özhendekci (2008) (Frame ID : S-9-800-7-120).....	30
Table 2.3 Comparisons of Developed Program Output with Data Published by Özhendekci and Özhendekci (2008) (Frame ID : I-9-450-8-150).....	30
Table 2.4 Comparisons of Developed Program Output with Data Published by Özhendekci and Özhendekci (2008) (Frame ID : I-9-450-8-180).....	31
Table 2.5 Comparisons of Developed Program Output with Data Published by Becker and Ishler (1996)	32
Table 3.1 Comparative Designs of an Example EBF	42
Table 3.2 Spectral Ground Motion Parameters S_s and S_1 for 16 Regions in USA	50
Table 3.3 Statistical Analysis of the Ratios of Computed Period to Estimated Period	55
Table 3.4 Properties of Instrumented EBF Buildings	63
Table 4.1 Summary of Pushover Analysis Results	72
Table 4.2 Statistical Analysis of Design Overstrength Values.....	74

Table 5.1 Member sizes of the Example EBF	90
Table 6.1 Archetype Properties and Scaling Factors.....	120
Table 6.2 Member Sizes of Archetypes and Link Rotation Angles from Design and Analysis	123
Table 6.3 Member Sizes of Revised Archetypes and Link Rotation Angles from Design and Analysis	139

LIST OF FIGURES

FIGURES

Figure 1.1 Typical EBF arrangements.....	2
Figure 2.1 Free body diagram and deformation mechanism of EBF	16
Figure 2.2 Free body diagram of lateral forces and link force distribution.....	25
Figure 3.1 Floor plan used in the parametric study	36
Figure 3.2 Typical elevation view of a plane EBF and illustration of linear displaced shape.....	38
Figure 3.3 Typical deformation pattern of an EBF	49
Figure 3.4 Normalized link length versus link length to bay width ratio.....	52
Figure 3.5 Variation of roof drift ratio with the product of link rotation angle and link length to bay width ratio.....	52
Figure 3.6 Comparison of calculated and predicted normalized link lengths	54
Figure 3.7 Comparison of computed and estimated periods using the proposed method	57
Figure 3.8 Comparison of computed and estimated periods using Equation (3.1)	58
Figure 3.9 Comparison of computed and estimated periods for published data	60

Figure 3.10 Histograms for roof drift ratio by proposed method in this thesis	64
Figure 4.1 General structural response	66
Figure 4.2 Floor plan used in parametric study	69
Figure 4.3 Pushover analysis of representative frames	72
Figure 4.4 Variation of design overstrength for the entire data set	73
Figure 4.5 Variation of design overstrength for different link length and bay width ratios	76
Figure 4.6 Variation of design overstrength for different bay widths	77
Figure 4.7 Variation of design overstrength for different seismic hazards	78
Figure 5.1 Test setups used in the studies of Okazaki et al. (2006) and Roeder & Popov (1978)	85
Figure 5.2 Comparison of numerical simulations with experimental results	86
Figure 5.3 Comparison of response spectra	91
Figure 5.4 Response of a 9 story EBF	93
Figure 5.5 Evaluation of inelastic, elastic and design displacements	96
Figure 5.6 Evaluation of the C_d factor and link rotation angle calculation procedure	98
Figure 5.7 Ratio of actual and design link rotation angles	99
Figure 5.8 Elastic displacements of example EBF using various assumptions....	104
Figure 5.9 Deformation of EBF components	106
Figure 5.10 Verification of proposed modifications for the example EBF	109

Figure 5.11 Link rotation angles for redesigned EBF	111
Figure 6.1 Experimental behavior of moment connection (Engelhardt, 1998)....	115
Figure 6.2 Experimental behavior of shear link beam (Okazaki et al., 2005).....	116
Figure 6.3 Typical time history of link rotation angle.....	118
Figure 6.4 Ordered cycles from rainflow counting procedure	118
Figure 6.5 Floor plan	121
Figure 6.6 Far field record set response spectra	126
Figure 6.7 Anchored response spectra to SDC D_{max} at 1 second	126
Figure 6.8 Response of 3 story archetype with $e/L=0.1$	128
Figure 6.9 Response of 6 story archetype with $e/L=0.1$	128
Figure 6.10 Response of 9 story archetype with $e/L=0.1$	129
Figure 6.11 Response of 3 story archetype with $e/L=0.15$	129
Figure 6.12 Response of 6 story archetype with $e/L=0.15$	130
Figure 6.13 Response of 9 story archetype with $e/L=0.15$	130
Figure 6.14 Variation of deflection amplification factor.....	134
Figure 6.15 Response of 3 story redesigned archetype with $e/L=0.1$	136
Figure 6.16 Response of 6 story redesigned archetype with $e/L=0.1$	136
Figure 6.17 Response of 9 story redesigned archetype with $e/L=0.1$	137
Figure 6.18 Response of 3 story redesigned archetype with $e/L=0.15$	137

Figure 6.19 Response of 6 story redesigned archetype with $e/L=0.15$ 138

Figure 6.20 Response of 9 story redesigned archetype with $e/L=0.15$ 138

LIST OF SYMBOLS AND ABBREVIATIONS

ACMR	Adjusted Collapse Margin Ratio
ACMR _{20%}	Adjusted Collapse Margin Ratio of 20% Collapse Probability
A _d	Area of Brace Member
AISC	American Institute of Steel Construction
ASCE	American Society of Civil Engineers
ATC	Applied Technology Council
B ₁	Multiplier to Account for P- δ Effects
C ₁ ,C ₂ ,C ₃ ,C ₄	Regression Coefficients for Normalized Link Length Model
C _b	Lateral-torsional Buckling Modification Factor
CBF	Centrically Braced Frame
CGS	California Geological Survey
C _m	Coefficient for Non-Uniform Moment
C _s	Seismic Response Coefficient
CSA	Canadian Standards Association
CSMIP	California Strong Motion Instrumentation Program
C _u	Upper Limit on Calculated Period
d	Depth of Link/Beam
DF _{beam}	Moment Distribution Factor for Beam
DF _{brace}	Moment Distribution Factor for Brace
d _i	Displacement at i th Story
E	Modulus of Elasticity
e	Length of the Link
e/L	Link Length to Bay Width Ratio
EBF	Eccentrically Braced Frame
e _N	Normalized Link Length
ETHA	Elastic Time History Analysis
FEMA	Federal Emergency Management Agency
F _i	Earthquake Force at i th Story
F _x	Seismic Lateral Force
F _y	Yield Strength

h_i	Height of i^{th} Story from Base
h_n	Height of Building
h_s	Story Height
I_{beam}	Strong Axis Moment of Inertia of Beam
I_{brace}	Strong Axis Moment of Inertia of Brace
I_e	Importance Factor
ITHA	Inelastic Time History Analysis
K	Effective Length Factor
k	Distribution Exponent
L	Bay Width
L_{beam}	Length of Beam
L_{brace}	Length of Brace
M_{beam}	Bending Moment of Beam at Brace-Beam Joint
M_{brace}	Bending Moment of Brace at Brace-Beam Joint
MCE	Maximum Considered Earthquake
MCE_R	Risk Adjusted Maximum Considered Earthquake
m_i	Mass of i^{th} Story
M_{link}	Bending Moment at Link End
M_p	Plastic Moment Capacity
MRF	Moment Resisting Frame
N	Number of Story
NEHRP	National Earthquake Hazards Reduction Program
n_s	Number of Story
P_{beam}	Axial Force in Beam
P_{brace}, P_d	Axial Force in Brace
P_{link}	Axial Force in Link
R	Response Modification Factor
RD_R	Roof Drift Ratio
R_y	Actual to Expected Yield Strength Ratio
R_{μ}	Ductility Reduction Factor
S_i	Mapped Spectral Acceleration at 1 sec Period
S_{D1}	Design Spectral Acceleration at 1 sec Period
SDC	Seismic Design Category
S_{DS}	Design Spectral Acceleration at Short Period (0.2 sec)
S_{M1}	Site Adjusted Spectral Acceleration at 1 sec Period

S_{MS}	Site Adjusted Spectral Acceleration at Short Period (0.2 sec)
S_S	Mapped Spectral Acceleration at Short Period (0.2 sec)
SSF	Spectral Shape Factor
STMf	Special Truss Moment Frames
T	Fundamental Period
T_a	Approximate Fundamental Period
t_f	Flange thickness of Link/Beam
T_{max}	Maximum Period
T_{min}	Minimum Period
t_w	Web thickness of Link/Beam
UBC	Uniform Building Code
USGS	United States Geological Survey
V	Design Story Force
V_{beam}	Shear Force in Beam
V_e	Ultimate Elastic Base Shear
V_{link}	Shear Force in Link
V_n	Nominal Shear Strength
V_p	Plastic Shear Capacity
V_s	Base Shear at First Significant Yield
V_y	Base Shear at Structural Collapse Level
W	Effective Seismic Weight
Z_{beam}	Plastic Section Modulus of Link/Beam
α	Angle Between Brace and Beam
β_{DR}	Collapse Uncertainty Related to Design Requirements
β_{MDL}	Collapse Uncertainty Related to Modeling
β_{RTR}	Record-to-record Collapse Uncertainty
β_{TD}	Collapse Uncertainty Related to Test Data
β_{TOT}	Total System Collapse Uncertainty
γ, γ_{total}	Total Link Rotation Angle
γ_c	Link Rotation Angle due to Column Axial Deformation
γ_{da}	Link Rotation Angle due to Brace Axial Deformation
γ_{dbb}	Link Rotation Angle due to Brace and Beam Bending Deformation
γ_m	Modified Link Rotation Angle
γ_p	Plastic Link Rotation Angle

Δ	Design Story Drift
Δ_L	Vertical Deflection of Left Column
Δ_{\max}	Maximum Amount of Drift
Δ_p	Plastic Story Drift
Δ_R	Vertical Deflection of Right Column
Δ_s	Drift at First Significant Yield
δ_{TSE}	Elastic Roof Displacement
δ_{xe}	Elastic Story Deflection
Δ_y	Drift at Structural Collapse Level
θ_p	Column Rotation Angle
μ_s	Ductility Factor
μ_T	Period Based Ductility
ϕ	Resistance Factor
ϕ_i	Displacement Amplification Modifier at i^{th} Story
Ω_d	Design Overstrength Factor
Ω_m	Material Overstrength Factor
Ω_o	Structural Overstrength Factor

CHAPTER 1

INTRODUCTION

1.1. GENERAL

The design of structures located in seismic regions must ensure the ability of resisting considerable lateral internal loads. In steel structures, seismic resistant eccentrically braced frames (EBFs) are a lateral load resisting system that are capable of combining high stiffness in the elastic range with good ductility and energy dissipation capacity in the plastic range. EBFs can be regarded as a hybrid system between conventional concentrically braced frames (CBFs) and conventional moment resisting frames (MRFs) that combines the distinct advantages of each system such as the stiffness and strength of the CBFs and the ductility and stable energy dissipation of the MRFs while minimizing their respective disadvantages such as the poor ductility of the CBFs and the insufficient elastic stiffness of MRFs.

EBFs are characterized by an isolated segment of beam, which is referred to as link. The diagonal brace, at least at one end, is connected to the end of the link rather than the beam-column joint. Several EBF arrangements are illustrated in Figure 1.1. The EBF system employs deliberately large eccentricities between the brace-beam connection and beam-column joint, which are chosen to assure that the link yields in shear. The eccentric elements are designed to remain elastic at low excitation

levels, and to yield in shear under higher excitations. Therefore, these link elements act as a ductile fuse that dissipates large amount of energy while preventing buckling of brace. The length of the link, e , is a decisive parameter influencing the inelastic behavior of the link since yielding mechanism, energy dissipation capacity and the ultimate failure mechanism are associated with it. For short links, the shear response governs inelastic behavior, whereas for longer links, the flexure response governs inelastic behavior. Due to predictable and reliable nature of shear yielding mechanism, short links are preferred to flexural links in order to achieve ductile behavior during a seismic event. It is observed that the shear force will reach the ultimate shear resistance while end moments are still below the flexural resistance for short links. Since the shear force in the link is constant, inelastic shear strains are quite uniformly distributed along the length, which permits the development of large link deformations without excessively high local strains. For long links, flexural hinges form at the link ends when moments reach the ultimate link flexural resistance. The development of inelastic link rotation is accompanied by high flexural strains at link ends, which in turn can lead to premature failure of the link by fracture of the link flange at relatively low inelastic rotations.

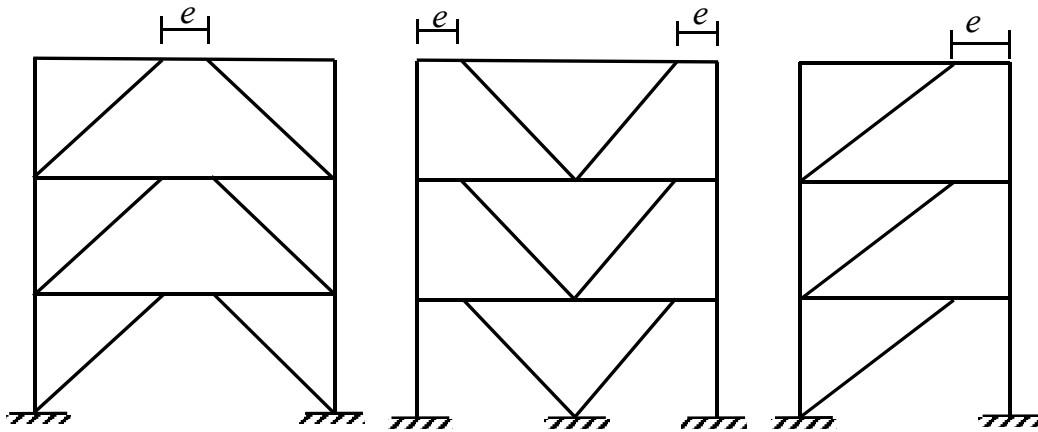


Figure 1.1 Typical EBF arrangements

During cyclic loading link elements act as structural fuses which limits transmitted forces to adjacent beam, brace and column elements. Therefore, these members outside of the link are expected to remain mainly elastic ensuring the stability of EBF system. In order to attain ductile hysteretic response, prevention of brace and column buckling is a significant factor for seismic resistant design of EBFs.

1.2. REVIEW OF PREVIOUS STUDIES

1.2.1. Experimental Studies

In order to examine dynamic characteristics of EBF under seismic action, extensive experimental studies on EBF were conducted since mid 1970's. The early tests were mostly undertaken at University of California at Berkeley.

Roeder and Popov (1977) and Manheim (1982) performed pseudo-static tests on one-third scale three story EBF. Afterwards, Yang (1982) tested a five story one-third scale EBF on shaking table. Experimental frames showed excellent inelastic response when subjected to various severe ground motions. Pseudo-dynamic testing was conducted on a full-scale six-story EBF building as part of the US-Japan Cooperative Program (Roeder, Foutch and Goel, 1987; Foutch, 1989). The building exhibited remarkable ductility and energy absorption capacity, although the energy absorption is concentrated mostly in lower three stories.

After verifying dynamic response of small frames subjected to seismic loads numerous studies were performed on isolated links. In these tests the behavior of short links was studied under monotonic and severe cyclic loading conditions and different boundary conditions were employed. Hjelmstad and Popov (1983) and Malley and Popov (1983, 1984) tested a number of twenty five full scale links

subjected to equal unsymmetrical end moments. In these experimental programs the size, spacing and amount of web stiffeners were altered to determine primary requirements for link length and web stiffeners. Various subassemblages consisting of link, beam, or slab were tested by Kasai and Popov (1986) and by Ricles and Popov (1987). Kasai and Popov (1986) stated that web buckling is the primary reason for link hysteretic response deterioration and since it is hard to assess post buckling behavior and collapse mechanism of EBF system, link web buckling is the most preferable failure mode for capacity design of EBFs. Ricles and Popov (1987) observed that the elastic shear force resisted by floor slab at the link is 8 to 12 percent of the total shear force and floor slabs above an interior link withstand larger shear forces than exterior links. Although, experimental results has shown that frames with shorter links possess remarkable ductility and stability under severe cyclic loading, architectural constraints forces engineers to employ longer links with flexural yielding mechanisms in design of EBFs. Engelhardt and Popov (1989, 1992) tested the subassemblages consisting of longer links, beam, and brace. Based on the findings of this investigation, preliminary design recommendations were proposed for EBF systems with longer links that are not attached to columns.

More recently, the shear links have been used for the retrofit and design of other structures such as long span bridges where the larger scale of these applications have led to the adoption of links that are built-up from plates instead of rolled wide flange beams to meet capacity demands. For two such example applications Itani et al. (1998) tested cyclic performance of built-up shear links utilized for retrofit of Richmond-San Rafael Bridge and McDaniel et al. (2003) examined two prototype steel shear links for the main tower of the new San Francisco-Oakland Bay self-anchored suspension bridge to evaluate the link force and deformation capacities. For both these tests, the maximum shear strength was nearly twice the expected yield shear strength which indicates an overstrength factor of 2 for shear links.

Okazaki (2004) and his coworkers examined seismic performance of links made from A992 steel with the tests conducted at University of Texas-Austin (Arce , 2002;

Gálvez, 2004; Ryu et al., 2004). For the experimental research performed by Arce (2002), a large number of shear links failed prematurely before achieving the inelastic rotation required in the AISC Seismic Provisions (2002), due to fracture of the link web. Richards and Uang (2003) suggested that shear links tested in those years were likely penalized by overly severe testing requirements defined by the AISC Seismic Provisions (2000, 2002) and proposed a revised loading protocol that realistically represents the demands caused by earthquake ground motions. In a subsequent study by Ryu et al. (2004), some of the same link specimens tested by Arce (2002) were retested using a revised loading protocol. Although the retested links still failed by web fracture in a manner identical to those observed by Arce (2002), the large rotations achieved by the retested links easily satisfied the rotation requirements of the AISC Seismic Provisions (2002).

Dusicka (2010) tested the links designed without stiffeners using low yield point steel as they attained shear deformations beyond 0.20 rad, surpassing the conventional designs that exhibited around 0.12 rad capacity. Mazzolani et al (2009) performed full scale tests of a real two-story reinforced concrete structure equipped with Y shaped eccentric braces using European wide flange shape (HE type). The results of this study indicates that the ratio between the link ultimate shear strength and its yielding strength can be significantly larger than 1.5.

1.2.2. Numerical Studies

Experimental inspection of structural behavior of eccentrically braced frames is much preferable for assessment of seismic hazard, nonetheless it is onerous and inefficient in use of time, effort and cost. Therefore, precise and efficient modeling of hysteretic behavior is essential to conduct static and inelastic analysis of EBFs.

Early models were simple models that were intended to predict gross overall behavior of link element of EBFs. One of the first was that by Gilbertson (1969) which utilizes two component model. The joint response of these two components creates bilinear flexural behavior with elastic and inelastic portions. Clough et al. (1966) also enhanced strain hardening to this formulation which arises when the elastic-perfectly plastic component yields. The amount of strain hardening equals to the elastic stiffness of the second component. The model proposed by Roeder (1977) utilizes inelastic shear effects. The element was based on sandwich beam theory that neglects interaction between axial force, shear force and bending moment, which is often crucial in the response of shear links in EBFs. It also ignores local effects such as web buckling, diagonal tension formation and progression of yielding.

The results of experimental studies (Kasai and Popov, 1986; Ricles and Popov, 1989) have revealed that the links attached to columns resists significant amount of bending moments along shear forces next to the column side. In order to reflect for this observation, a finite element model based on a stress resultant formulation was presented by Hjelmstad and Popov (1983) that uses a flexural-shear yield surface. However, this formulation has also some drawbacks as it neglects strain hardening and it demands considerable number of elements to achieve exact bending moments.

First efficient link element that was based on relatively accurate formulation was developed by Ricles and Popov (1987, 1994). It incorporates flexural-shear yielding, and utilizes anisotropic strain hardening and flexural kinematic hardening with combined isotropic kinematic shear hardening. The element consists of a single-component model of a linear elastic beam with nonlinear hinges at each end. Flexural and shear behavior of individual element was calibrated with experimental specimens tested under random cyclic loading (Ricles and Popov, 1987) and global response of element in an EBF was verified with the test frame of Roeder and Popov (1977).

Results of parametric studies (Ricles and Popov, 1987; Ricles and Bolin, 1991) has shown that the ratio of link capacity to demand (i.e. overstrength) was not identical

over the height of the EBF. Higher values of overstrength were attained in upper stories, and the damage was consistently larger in lower stories. Popov et al. (1992) pointed out that incorrect proportioning of links (non-uniform distribution of overstrength over the height) might result in an unfavorable response as energy dissipation and large inelastic deformation concentrates in only a few stories. However, Rossi and Lombardo (2007) stated that at the upper storeys of medium or high-rise structures the static approach provides overestimated values of the normalised overstrength factor of links. Also, this study concludes if normalised overstrength factors of links are restricted to the value offered by Eurocode 8 (1993) (i.e. 1.25), the seismic behavior of low-rise EBFs formed with links with high ultimate plastic rotation is almost always adequate and independent of the use of either static or modal analysis.

Goel (2005) proposed a new methodology for performance-based plastic design and validated the proposed design method by extensive nonlinear dynamic analyses. The results indicated that although most maximum link plastic rotations at each floor were well below the AISC 341-02 (2002) limitation, the plastic rotations at upper floors tended to increase rapidly and exceeded the 0.08 radian limitation during some of ground motions. Also, the roof level links exhibited only minor yielding.

Recently, Saritas and Filippou (2009) developed a beam finite element model for the analysis of shear critical members. The model follows the assumptions of Timoshenko beam theory for displacement field and uses a three-field variational formulation with independent displacement, stress and strain fields. The nonlinear response of the element is derived from the section integration of the multiaxial material stress-strain relation at several control points along the element, thus accounting for the interaction between normal and shear stress and the spread of inelastic deformations in the member. Moreover, the model does not possess shear locking problems and does not require mesh refinement for the accurate representation of inelastic deformations. Correlation studies of analytical results

with available experimental data of the hysteretic behavior of shear-yielding members confirm the capabilities of the proposed model.

1.3. OBJECTIVE AND SCOPE

There are several research programs conducted on EBF and its components in the literature as summarized in the preceding section. Monotonic and cyclic behavior of individual link elements, subassemblages and whole EBFs are investigated both experimentally and numerically. Although the outcomes of these studies led to improvement of ductile and economic design procedures in the specifications, there is a need to reevaluate code specified limits in the capacity design of EBFs. Moreover, these studies are mostly restricted to a narrow range in link length (usually links that yield in shear), bay width and height of EBF.

The aim of this research study is to ascertain seismic performance factors of EBFs numerically and to examine dynamic characteristics of EBFs. Pursuant to this goal a computer program which facilitates seismic resistant design of EBFs was developed. The algorithm of the program adopts the lightest uniform frame design and library of link-beam-brace sub-assemblages concepts. The design output from the program was compared with published solutions and the results indicate that the algorithm developed as a part of this study is capable of providing lighter framing solutions.

A formulation of a hand method which can be used to estimate the computed fundamental periods of vibration of building structures in general and steel eccentrically braced frames (EBFs) in particular is proposed as a part of this research. The developed method uses the Rayleigh's method as a basis and utilizes the roof drift ratio (RD_R) under seismic forces as a parameter. In order to obtain RD_R more than 4000 EBFs were designed by developed program. The method was

verified using design data produced as a part of this work as well as data published in literature. The verifications indicate that the proposed formulation is capable of providing acceptable estimates of the computed period. When compared with existing empirical period-height relationships the proposed formulation offers closer estimates with reduced scatter. The method was further refined to derive new period height relationships for particular seismicity regions. The accuracy of the relationship for high seismic regions was verified using measured periods of EBF buildings.

Furthermore, developed program was utilized to perform a parametric study to quantify design overstrength of steel eccentrically braced frames. The results indicate that the frames considered in this study have on average higher overstrength values when compared with the codified value even without considering potential increases due to material overstrength and strain hardening. The design overstrength was found to be influenced primarily by the link length to bay width ratio and the bay width, and secondarily by the building height and seismic hazard level.

As a part of this study a numerical study was undertaken to evaluate the displacement amplification factor given in ASCE7-10 (2010) for EBFs and link rotation angle estimation procedure given in AISC341 (2005). A total of 72 EBFs were designed by considering the number of stories, the bay width, the link length to bay width ratio, and the seismic hazard level as the prime variables. All structures were analyzed using elastic and inelastic time history analysis. Based on the results of the numerical study a new set of displacement amplification factors that vary along the height of the structure and more accurate procedures to estimate the link rotation angles were developed. In light of the proposed modifications, the EBFs were redesigned and analyzed using inelastic time history analysis.

Finally, a numerical study undertaken to evaluate seismic response factors for steel eccentrically braced frames (EBFs) using the FEMA P695 (2009) methodology. Six archetypes were designed by making use of the current US Specifications and their behavior was assessed by making use of non-simulated collapse models. A dual

criterion was adopted for performance assessment which includes the maximum and the cumulative link rotation angle experienced by the link beam. A modification to the deflection amplification factor was developed to bring the collapse probability of these archetypes to acceptable levels. The modifications result in deflection amplification factors that vary along the height of the structure. Six archetypes were redesigned using the proposed modifications and re-evaluated using the FEMA P695 (2009) methodology.

1.4. ORGANIZATION OF THE THESIS

This thesis consists of six chapters which follow the introduction. The brief contents of these chapters can be summarized as follows:

In Chapter 2, details of computer program that facilitates seismic design of EBFs that is developed as a part of this study are given. Also, this chapter introduces the design procedure of EBFs according to US provisions.

In Chapter 3, methodology of formulation to estimate computed fundamental periods of vibration of EBFs is described. Additionally, verification of this method with design data of parametric study and published data in literature is provided in this chapter.

In Chapter 4, details of parametric study to assess design overstrength of EBFs and results of this study are presented.

In Chapter 5, evaluation of displacement amplification factor given in ASCE7-10 (2010) for EBFs and link rotation angle estimation procedure given in AISC341 (2010) are provided. Results of elastic and inelastic numerical studies on both existing code designs and redesigned frames with proposed modifications are outlined.

In Chapter 6, assessment of seismic response modification factors of EBFs (namely response modification factor, R , and displacement modification factor, C_d) using a novel procedure provided by FEMA P695 (2009) are presented.

Finally, Chapter 7 summarizes the outcomes of all studies performed as a part of this research program and recommendations for use of the results of this work in future and ongoing research efforts are listed.

CHAPTER 2

DEVELOPMENT OF COMPUTER PROGRAM FOR SEISMIC DESIGN OF EBFs

In this chapter, the details of computer program that facilitates seismic resistant design of EBFs are presented. The program is capable of designing EBFs according to the US provisions and is based on the minimum frame weight principle. Because the seismic response modification factor values are directly dependent on the selected member sizes, the details of the developed program and specific constraints that present challenges during the design process are explained in detail.

2.1. DESIGN OF EBFs ACCORDING TO US PROVISIONS

Three main specifications namely, Minimum Design Loads for Buildings and Other Structures (ASCE7-10, 2010), Specification for Structural Steel Buildings (AISC 360-05, 2005) and Seismic Provisions for Structural Steel Buildings (AISC 341-05, 2005) are considered during the design of a typical EBF. In general, the seismic forces are computed by making use of ASCE7-10 (2010), specific rules for EBFs given in AISC 341-05 (2005) are followed, and member design checks are conducted in accordance with AISC 360-05 (2005). Design of EBFs presents a

variety of challenges because all the rules given in the aforementioned specifications have to be followed.

In general, links, beams, diagonal braces, and columns of an EBF must be sized considering the strength limit states. According to AISC 341-05 (2005) the diagonal braces, columns, and beam segments outside of the links shall be designed to remain essentially elastic under the maximum forces that can be generated by the fully yielded and strain hardened links. This implies that a capacity design procedure, which presents difficulties, must be adopted during the design of these members.

Sizing the links for strength is relatively straightforward. The effect of axial force on the link available shear strength need not be considered if the required axial strength is less than 15 percent of the nominal axial yield strength of the link. According to AISC 341-05 (2005) the plastic moment capacity of the link section (M_p) and plastic shear capacity (V_p) are determined as follows:

$$M_p = Z_{beam} F_y \quad (2.1)$$

$$V_p = 0.6 F_y t_w (d - 2t_f) \quad (2.2)$$

where t_w = web thickness of the link/beam, t_f = flange thickness of the link/beam, d = depth of the link/beam, Z_{beam} = plastic section modulus of the link/beam, F_y = yield strength.

The nominal shear strength (V_n) of the link is equal to the lesser of plastic shear capacity (V_p) or $(2M_p/e)$ where e is the link length.

Selecting link sections that satisfy link rotation angle limitations presents additional challenges. While a link that satisfies the strength limit states may be selected easily, a detailed frame analysis is required to check if the link rotation limits are satisfied. The link rotation angle (γ_p) is defined as the inelastic angle between the link and the beam outside of the link when the total story drift is equal to the design story drift.

According to AISC 341-05 the link rotation angle shall not exceed the following values:

(i) 0.08 radians for links of length $\frac{1.6M_p}{V_p}$ or less

(ii) 0.02 radians for links of length $\frac{2.6M_p}{V_p}$ or greater

(iii) The value determined by linear interpolation between the above values for links of length between $\frac{1.6M_p}{V_p}$ and $\frac{2.6M_p}{V_p}$.

The link rotation angle can be estimated using the procedure explained in the Commentary to AISC 341-05 (2005). As shown in Figure 2.1, an EBF deforms in a rigid-plastic mechanism and the link rotation angle can be expressed as a function of the column rotation angle (θ_p) as follows:

$$\gamma_p = \frac{L}{e} \theta_p \quad \text{where} \quad \theta_p = \frac{\Delta_p}{h_s} \quad (2.3)$$

where L = bay width, h_s = story height, Δ_p = plastic story drift which can be conservatively taken as the design story drift (Δ).

Like the link rotation limits the story drifts have to be checked in order to ensure that the design is satisfactory. According to ASCE 7-10 (2010) the design story drift shall be computed as the largest difference of the vertically aligned points at the top and bottom of the story under consideration. The deflection (δ_x) at any level can be determined as follows:

$$\delta_x = \frac{C_d \delta_{xe}}{I_e} \quad (2.4)$$

where δ_{xe} = the deflection at the level under consideration which is determined by an elastic analysis, I_e = the importance factor.

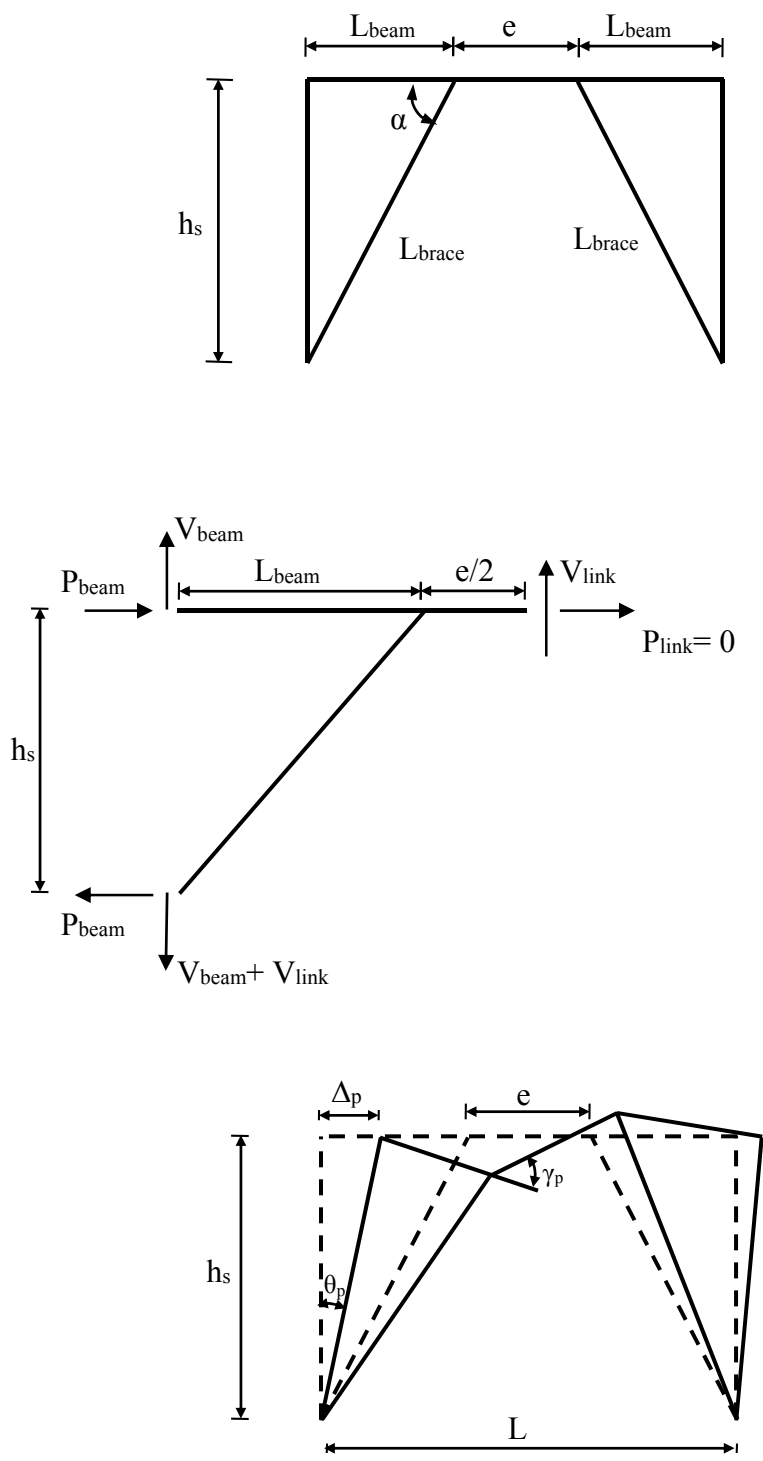


Figure 2.1 Free body diagram and deformation mechanism of EBF

For EBFs under Risk Category I and II the design story drift should satisfy the following:

$$\Delta \leq 0.02 h_s \quad (2.5)$$

Another challenge in the design of EBFs is the determination of the fundamental period of vibration (T). The ASCE 7-10 (2010) specification provides the following relationship for the approximate fundamental period (T_a) of EBFs:

$$T_a = 0.0731 h_n^{0.75} \quad (2.6)$$

where h_n = height of the building in meters.

Alternatively any properly substantiated analysis can be used to determine the fundamental period of vibration (T). However, the periods obtained from a rational analysis can be used to a different extent. For checking strength limit states the fundamental period shall not exceed the product of the coefficient for upper limit on calculated period (C_u) and the approximate fundamental period (T_a). The C_u coefficient ranges between 1.4 and 1.7 depending on the seismic hazard level. On the other hand, Clause 12.8.6.2 of ASCE 7-10 (2010) permits to determine the elastic drifts using seismic design forces based on computed fundamental period of the structure without the upper limit ($C_u T_a$) for checking story drift limits.

The aforementioned constraints must be tackled during the design of EBFs. Optimized designs are often difficult to obtain, due to member local buckling requirements, geometric constraints, the resistance of the beam outside of the link to flexure combined with axial effects (AISC Seismic Design Manual, AISC 327-05, 2005). The following section presents the details of a design approach developed as a part of this study and its implementation into a computer program.

2.2. EBF DESIGN PROCEDURE AND ITS IMPLEMENTATION

A design procedure has been developed as a part of this study and implemented into a MATLAB (MathWorks, 2010) program. As mentioned in the previous section, lateral drift values are needed for a satisfactory design and these can be obtained using a structural analysis code. In this case the structural analysis program, FedeasLab, developed by Filippou (2001) was adopted and its routines were integrated into the MATLAB program developed for the design of EBFs.

Several iterations are required in typical EBF designs to come up with a code compliant solution. The resulting solution is not unique and depends on the type of approach adopted by the designer. Usually link/beam, diagonal brace, and column members are treated separately and most optimal section sizes are found using an iterative procedure (Özhendekci and Özhendekci, 2008). The design philosophy developed as a part of this study differs from conventional methods. The idea behind the developed procedure is to minimize the weight of eccentrically braced framing by using a library of sub-assemblages and the concept of lightest uniform frame design. The sub-assemblages are composed of link/beam and diagonal brace members. The combination of link/beam and diagonal brace automatically satisfies the capacity design principles for braces.

The concept of lightest uniform frame design is developed to decrease the number of design iterations for designs where drift and link rotation limits control the selection of members. Usually designers have several options to fulfill the drift and link rotation limit requirements. In tall frames interstory drifts at top stories are usually high and must be reduced to code specified levels. Similarly, large interstory drifts result in large link rotation angles which in turn violate the limits. Reducing the drifts to acceptable levels presents challenges. There are several measures that can be taken to reduce the level of deformations at higher stories. One option is to stiffen the link/beam, brace and column sections at the stories experiencing high

level of deflections. This option may fail to be useful because the story drifts are influenced by the member sizes of the stories below the level of consideration. Therefore, the sizes of members in the stories below may need updating. Several different options were tried at the early stages of research and finally the concept of the lightest uniform frame design was developed to tackle stiffness related problems. As will be explained in the following sections, additional design steps are taken after the lightest uniform frame design is obtained. These steps aim at reducing the weight of the framing further.

2.2.1. Formation of a Library of Sub-assemblages

The design program uses a library of sub-assemblages for the design of link/beam and brace sections at any story. In typical EBF designs the link/beam sections are selected first based on the level of seismic forces at any given story. Later the braces are designed based on capacity design principles and considering strain hardening and overstrength that is present in the links. In this study an alternative approach is adopted which is based on the concept of using sub-assemblages. The idea here is to minimize the weight of the link-beam-brace assembly altogether rather than trying to optimize each member individually. Using the sub-assemblage concept helps reduce the weight of the framing and the number of design steps conducted to reach to the final member sizes. In the traditional design approach the link sections are selected by considering their weight and the applied forces. Although this design philosophy results in more optimized link sections for a given level of seismic action it usually disregards the effect of brace selection on the final weight of the seismic lateral load resisting system. Because capacity design principles are adopted for the design of braces some link sections can produce much larger shear and moments at link ends which in turn adversely affects the forces and moments on the brace. By

using the sub-assembly concept the problem is approached from a more holistic view.

American wide flange sections with a steel grade of A992 which has a yield strength of 345 MPa were considered in the design of link/beam members. A total of 220 seismically compact sections from AISC's shape database were taken into account. The library of sub-assemblages is dependent on the geometry of the framing used. For any selected geometry most optimum brace sections need to be found for all 220 link/beam sections. For the design of braces a single story of an EBF and the corresponding free body diagram shown in Figure 2.1 is considered. As shown in Figure 2.1 the geometry can be defined by three basic variables namely, the bay width (L), link length (e), and story height (h_s). The length of the beam outside of the link (L_{beam}), the length of braces (L_{brace}) and the brace angle (α) can be found by using these three basic variables.

Similar to the link/beam members the brace members were designed using American wide flange shapes having a steel grade of A992. All compact wide flange sections from AISC's shape database were considered. It was assumed that the braces are under strong axis bending for the configuration shown in Figure 2.1. In practice these braces can be connected to the link/beam members using a gusset plate therefore, no additional constraints are necessary to adjust the workpoints. A trial and error procedure was adopted for the selection of brace member sizes. For any given geometry and link/beam size, a brace section is selected starting from the one with the least weight. The adequacy of the selected brace member size is evaluated from a strength viewpoint using the procedure explained in the forthcoming text. The trial and error procedure is continued until the lightest brace member that satisfies the strength limit states is found.

A detailed structural analysis must be conducted to determine the forces and moments produced in the elements of an EBF. In order to facilitate the designs, a simplified method is employed to predict the amount of forces on the structural

members. This method was verified using structural analysis results and is based on the free body diagram shown in Figure 2.1.

The brace has to be designed to remain essentially elastic under the forces generated by the fully yielded and strain hardened link. These forces must be accurately determined to be able to apply the capacity design principles.

Depending on the link length, the link end moments and forces are determined using the following relationship:

$$\text{For } e < \frac{2M_p}{V_p} \quad V_{link} = V_p \quad M_{link} = \frac{eV_p}{2} \quad (2.7)$$

$$\text{For } e \geq \frac{2M_p}{V_p} \quad V_{link} = \frac{2M_p}{e} \quad M_{link} = M_p \quad (2.8)$$

where V_{link} = shear force produced at the link end, M_{link} = bending moment produced at the link end.

Moment distribution method is utilized to determine the moments acting on the beam and the brace. A similar method has been adopted in the past (AISC Seismic Design Manual, AISC 327-05, 2005) for the design of EBFs. This method requires calculation of moment distribution factors which can be determined as follows:

$$DF_{beam} = \frac{\frac{I_{beam}}{L_{beam}}}{\frac{I_{beam}}{L_{beam}} + \frac{I_{brace}}{L_{brace}}} \quad (2.9)$$

$$DF_{brace} = \frac{\frac{I_{brace}}{L_{brace}}}{\frac{I_{beam}}{L_{beam}} + \frac{I_{brace}}{L_{brace}}} \quad (2.10)$$

where DF_{beam} = moment distribution factor for the beam, DF_{brace} = moment distribution factor for the brace, I_{beam} = moment of inertia of the beam in the plane of bending, I_{brace} = moment of inertia of the brace in the plane of bending.

In the derivation of the distribution factors, it was assumed that the moments distribute according to the stiffness of each member. The far ends of the beam and brace were assumed to be pinned, in other words identical.

The bending moment produced by the link at the brace end (M_{link}) is distributed to the brace and the beam outside of the link. By utilizing the distribution factors, the bending moments on these members can be determined as follows:

$$M_{beam} = 1.1 DF_{beam} M_{link} \quad (2.11)$$

$$M_{brace} = 1.25 R_y DF_{brace} M_{link} \quad (2.12)$$

where M_{beam} = bending moment acting on the beam at the brace-beam joint, M_{brace} = bending moment acting on the brace at the brace-beam joint, R_y = ratio of expected yield stress to the specified minimum yield stress.

It is worthwhile to mention that the overstrength of the link is included in the design of the brace member by multiplying the forces produced on the brace by 1.25 and R_y as given in Equation (2.12). The recommended R_y factor of 1.1 for $F_y=345$ MPa is utilized. It should be emphasized that the R_y factor is not considered in calculating the beam axial force and bending moment. According to the AISC 341-05 (2005), if a continuous section with same properties is used for the beam and the link, the R_y factor can be omitted.

In the free body diagram shown in Figure 2.1, the axial force in the link (P_{link}) is assumed to be zero. The end moments of the beam and brace at the column location were taken equal to zero due to the pinned supports at these ends. By taking moments with respect to the supported end of the brace and considering link overstrength, the axial force in the beam (P_{beam}) can be found as:

$$P_{beam} = \frac{1.1V_{link}(L_{beam} + e/2)}{h_s} \quad (2.13)$$

After determining the bending moment acting on the beam the shear force in the beam (V_{beam}) can be determined as follows:

$$V_{beam} = \frac{M_{beam}}{L_{beam}} \quad (2.14)$$

The axial force in the brace (P_{brace}) can be calculated using the axial force and the shear force in the beam as follows:

$$P_{brace} = 1.25 R_y \left[\frac{P_{beam}}{1.1} \cos(\alpha) + \left(V_{link} + \frac{V_{beam}}{1.1} \right) \sin(\alpha) \right] \quad (2.15)$$

After determining the axial force and bending moment on the brace, the strength of the brace section is checked using the provisions given in AISC 360-05 (2005). The brace member is considered as a beam-column and equations H1-1a and H1-1b of AISC 360-05 (2005) specification are used to check the strength of the brace member. The second order effects on the brace member are taken into account by making use of the moment amplification factor, B_1 given in AISC 360-05 (2005). A C_m value of 0.6 and a C_b factor of 1.67 are used in strength checks. The brace slenderness ratio is determined using an effective length factor (K) equal to unity.

After determining the lightest brace section that satisfies the strength provision and is capable of remaining elastic under the amplified link forces, the final step is to check the beam outside of the link. This element is one of the most crucial elements of an EBF because it is subjected to high axial compressive forces and bending moments. In the present study, it is assumed that the beam outside of the link is acting compositely with a concrete deck. The concrete deck prevents any kind of lateral torsional instability of the beam outside of the link. Although instability types of failure modes are prevented, the beam outside of the link can still plastify due to high axial force and bending moment. In order to ensure elastic behavior during

seismic actions, the beam outside of the link is checked using the beam-column limit states of AISC 360-05 (2005) that were applied to the brace section. At this point it is observed that some beams do not satisfy the AISC 360-05 (2005) provisions. Designers can overcome this problem by introducing cover plates to the beam outside of the link to reinforce this element. However, using cover plates can be costly and is not desired in many cases. Another option is to use a stiffer brace section that attracts more bending moment and results in reduced beam end moments. This often times results in an increase in the brace member weight. In the present study neither of these options was deemed viable and to be able to make fair comparisons between the designs the cases that do not satisfy the strength limit states are extracted from the library of sub-assemblages.

After applying the design procedure, details of which are explained in this section, a library of sub-assemblages is formed to be used in the design of EBFs. In general the weight of each sub-assemblage is calculated and the sub-assemblages are sorted from the lightest to the heaviest. The trial and error procedure adopted in the design of EBFs selects among these sub-assemblages based on the forces and link rotation constraints.

2.2.2. Design Algorithm

The following steps are undertaken for the design of EBFs:

Step 1: For a given story height, bay width and link length the program forms a library of sub-assemblages which consists of wide flange link/beam sections and their corresponding wide flange diagonal brace sections. The sub-assemblage weights are computed and they are sorted from the lightest to the heaviest.

Step 2: Seismic design forces (F_x) according to ASCE 7-10 (2010) are computed using equivalent lateral force procedure and the approximate fundamental period of vibration (T_a). After determining the seismic forces, the link design shears (V) are calculated. These shears can be determined independent of the link length, bracing configuration, section properties or any elastic analysis (Becker and Ishler, 1996). By considering the free body diagram of an EBF with equal story height shown in Figure 2.2 and assuming that the flexural stiffness of columns is negligible the following link shear forces are determined:

$$\begin{aligned}
 V(n_s) &= \frac{F_x(n_s)h_s}{L} && \text{For } i = n_s \\
 V(i) &= \frac{F_x(i)h_s}{L} + V(i+1) && \text{For } 1 \leq i < n_s
 \end{aligned}
 \tag{2.16}$$

where n_s = number of stories, $F_x(i)$ = seismic design force at the i^{th} story, $V(i)$ = link design shear at the i^{th} story.

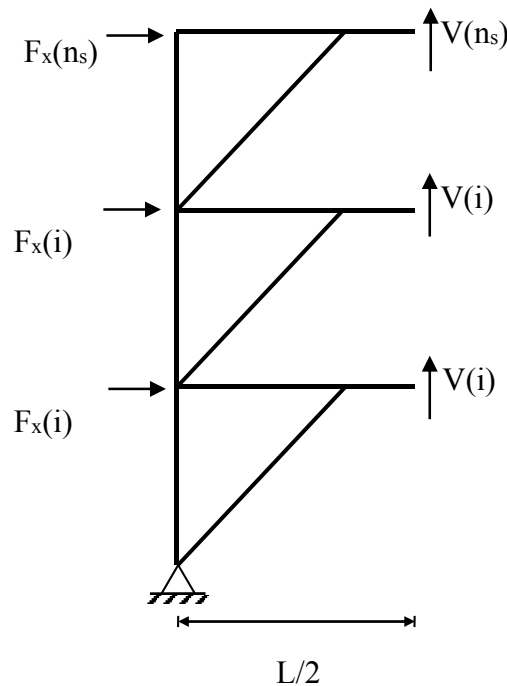


Figure 2.2 Free body diagram of lateral forces and link force distribution

Step 3: Based on the design link shear force at the first story the lightest sub-assembly that has a link shear strength greater than the link design shear is selected. This sub-assembly is used for all the stories resulting in the same type of link/beam and diagonal brace sections at all stories.

Step 4: The columns of the framing are designed based on capacity design principles. In finding out the required strength of the columns the forces generated by 1.1 times the expected nominal shear strength ($R_y V_n$) of all links above the level under consideration and the loads due to gravity are considered. Similarly the amplified seismic forces are also considered in the design of these members. The columns are selected from W14 shapes and considered to have a steel grade of A992 with a yield strength of 345 MPa.

Step 5: The selected member sizes are input into the analysis routine and the fundamental period of vibration (T) of the resulting frame is determined. Because ASCE 7-10 (2010) permits the use of elongated periods, the seismic design forces are updated based on the new fundamental period. After updating the seismic forces, Steps 2, 3, and 4 are repeated until initial and final periods converge or the computed period is greater than the upper limit on periods ($C_u T_a$).

Step 6: The story drift and link rotation angle limits are checked. By making use of the structural analysis code FedeesLab the lateral drifts are calculated and link rotations limits are obtained using the lateral drift values. While calculating the lateral drifts the seismic forces computed using the actual fundamental period (T) of the EBF is used without any upper bound. If all limit states are satisfied then the program proceeds according to Step 8 and conducting Step 7 is not necessary.

Step 7: When drift and/or link rotation limits are not satisfied the members of the framing are redesigned. This is an iterative procedure and utilizes the library of sub-assemblies. From this library the next heaviest sub-assembly that satisfies the strength requirements are selected and the columns are redesigned based on this new

link/beam and brace member sizes. The procedure is continued until all the strength, deflection and link rotation angle provisions are satisfied.

Step 8: At the beginning of this step the lightest uniform frame design alternative is reached. This is a design that uses the same size link/beam and brace sections at all stories. In this alternative the upper stories are deliberately over-designed but the resulting frame presents a lower bound in terms of weight when identical link/beam and brace sections are used at all stories. In this step the member sizes of the upper stories are reduced by making use of an iterative procedure. The second story and the stories above this story are considered. A lighter sub-assembly from the library is selected for these stories. During the selection, the index of the sub-assembly is reduced by one indicating a slightly lighter alternative when compared with the sub-assembly used in the previous step. The columns of the framing are redesigned based on the changes in member sizes of the second story and above. The strength, deflection and link rotation limitations are checked by making use of the updated periods according to the new member sizes. The procedure is repeated until the lightest sub-assembly is found for the stories under consideration. In some cases no lighter sub-assembly can be found and the member sizes are not changed in this case.

Step 9: Step 8 is repeated by considering successively 3rd, 4th, ..., nth stories and the ones above. The final member sizes are considered as the optimum solution for the designed EBF.

2.3. VERIFICATION OF THE DEVELOPED PROGRAM

Data from two independent research teams was used to assess the outputs of the developed program. Both of the reference studies provide EBF design of various buildings having regular floor plans at all stories. Equivalent lateral force procedure

was used in the design of EBFs in these references. Identical floor plans and mass properties were considered in the present study and some of the selected frames were re-designed using the computer program developed as part of this thesis. In the reference studies the researchers designed the brace members using HSS sections. The computer program was modified to be capable of selecting HSS sections for brace members.

The first data set belongs to a study by Özhendekci and Özhendekci (2008). These researchers designed EBFs with various floor plans, heights, bay widths and e/L ratios. All structures were assumed to be located in Los Angeles with a local site class D. The 2005 version of ASCE7 and AISC360-05 (2005) were utilized in the design of EBFs. The frames were designed using W shape links/beams, HSS type braces and W14 columns. Four of the cases reported by Özhendekci and Özhendekci (2008) namely, S-9-800-7-90, S-9-800-7-120, I-9-450-8-150, I-9-450-8-180 were re-designed. The resulting member sizes for these 9-story frames are given in Table 2.1 through Table 2.4. In addition, the resulting frame weights are also indicated in these tables. The comparisons indicate that the designs obtained using the developed program give lighter and more uniform solutions in general. The use of uniform frame design concept results in link/beam members that gradually reduce from bottom to top stories. Designs by Özhendekci and Özhendekci (2008) are based on a different principle where sizes of members in a particular story are increased to stiffen that region to meet the drift limits. Therefore, the sizes of links can vary considerably over the height resulting in sizeable members at upper stories. For example in frame S-9-800-7-120 (Table 2.2), the first story utilizes a W14x145 link section and the link section in the second and third stories is W18x86. While the weight of the link section reduces in second, third and fourth stories, an increase in the section size is observed in the fifth story where a W12x120 section is used. This example demonstrates that if individual member sizes are modified to meet the design requirements then the resulting solutions may have sizeable sections in upper stories. One other observation related with frame S-9-800-7-120 (Table 2.2) is the selected member sizes using the developed computer program. The link sections

tend to increase from W16x40 to W12x45 at the fifth story resulting in an increase in the weight of the link. While the link weight increases the weight of the brace section decreases. The fourth and fifth stories utilize HSS 10x10x0.375 (weight=47.90 pounds per foot) and HSS 7x7x0.5 (weight=42.05 pounds per foot) sections, respectively. It is observed that some of the selected column sections at upper stories are larger than the sections used by Özhendekci and Özhendekci (2008). This is attributable to the capacity design requirements for these members. The forces on the columns are directly influenced by the maximum amount of axial force that can be produced by yielded and strain hardened links. As different link sections are selected for upper stories this results in a change in the selection of column sections. This example demonstrates that considering the link/beam and brace as a sub-assembly results in framings that are overall lighter.

Table 2.1 Comparisons of Developed Program Output with Data Published by Özhendekci and Özhendekci (2008) (Frame ID : S-9-800-7-90)

		Frame ID		S-9-800-7-90		
		Total weight (kN)				
		Özhendekci	Present Study			
L (m)	e/L	248.24	176.45			
Link Sections		Brace Sections		Column Sections		
Story Nr.	Özhendekci	Present Study	Özhendekci	Present Study	Özhendekci	Present Study
1	W12x120	W16X40	HSS12x12x0.5	HSS7X7X0.5	W14x211	W14X145
2	W12x120	W16X40	HSS16x16x0.375	HSS7X7X0.5	W14x176	W14X132
3	W18x65	W16X40	HSS12x12x0.5	HSS7X7X1/2	W14x145	W14X132
4	W18x65	W16X40	HSS12x12x0.5	HSS7X7X0.5	W14x120	W14X132
5	W16x77	W16X40	HSS10x10x0.625	HSS7X7X0.5	W14x109	W14X132
6	W10x100	W16X40	HSS10x10x0.625	HSS7X7X0.5	W14x82	W14X68
7	W14x68	W16X40	HSS10x10x0.5	HSS7X7X0.5	W14x61	W14X68
8	W12x50	W16X31	HSS10x10x0.375	HSS7X7X0.5	W14x43	W14X48
9	W8x40	W14X26	HSS10x10x0.25	HSS8X8X0.375	W14x30	W14X38

Table 2.2 Comparisons of Developed Program Output with Data Published by Özhendekci and Özhendekci (2008) (Frame ID : S-9-800-7-120)

		Frame ID		S-9-800-7-120		
		Total weight (kN)				
L (m)	e/L	Özhendekci	Present Study			
7	0.17	277.78	172.18			
Story Nr.	Link Sections		Brace Sections		Column Sections	
	Özhendekci	Present Study	Özhendekci	Present Study	Özhendekci	Present Study
1	W14x145	W16X40	HSS12x12x0.625	HSS10X10X0.375	W14x233	W14X145
2	W18x86	W16X40	HSS12x12x0.625	HSS10X10X0.375	W14x193	W14X132
3	W18x86	W16X40	HSS12x12x0.625	HSS10X10X0.375	W14x159	W14X132
4	W16x89	W16X40	HSS12x12x0.625	HSS10X10X0.375	W14x132	W14X132
5	W12x120	W12X45	HSS16x16x0.375	HSS7X7X0.5	W14x109	W14X74
6	W12x106	W10X45	HSS14x14x0.375	HSS8X8X0.375	W14x109	W14X68
7	W14x74	W10X45	HSS10x10x0.625	HSS8X8X0.375	W14x61	W14X48
8	W12x50	W14X38	HSS12x12x0.3125	HSS9X9X0.375	W14x43	W14X38
9	W12x50	W8X40	HSS12x12x0.3125	HSS8X8X0.375	W14x30	W14X38

Table 2.3 Comparisons of Developed Program Output with Data Published by Özhendekci and Özhendekci (2008) (Frame ID : I-9-450-8-150)

		Frame ID		I-9-450-8-150		
		Total weight (kN)				
L (m)	e/L	Özhendekci	Present Study			
8	0.19	214.56	183.92			
Story Nr.	Link Sections		Brace Sections		Column Sections	
	Özhendekci	Present Study	Özhendekci	Present Study	Özhendekci	Present Study
1	W8x67	W16X40	HSS12x12x0.625	HSS10X10X0.375	W14x132	W14X132
2	W12x50	W16X40	HSS12x12x0.625	HSS10X10X0.375	W14x109	W14X132
3	W8x67	W16X40	HSS12x12x0.625	HSS10X10X0.375	W14x109	W14X132
4	W8x67	W16X40	HSS12x12x0.625	HSS10X10X0.375	W14x109	W14X132
5	W12x45	W16X40	HSS12x12x0.5	HSS10X10X0.375	W14x68	W14X82
6	W8x58	W16X40	HSS16x16x0.3125	HSS10X10X0.375	W14x61	W14X68
7	W8x48	W16X40	HSS14x14x0.3125	HSS10X10X0.375	W14x43	W14X53
8	W8x40	W14X38	HSS12x12x0.3125	HSS10X10X0.375	W14x34	W14X48
9	W8x40	W12X35	HSS12x12x0.3125	HSS7X7X0.5	W14x30	W14X38

Table 2.4 Comparisons of Developed Program Output with Data Published by Özhendekci and Özhendekci (2008) (Frame ID : I-9-450-8-180)

		Frame ID		I-9-450-8-180		
		Total weight (kN)				
		Özhendekci	Present Study			
L (m)	e/L	Özhendekci	Present Study			
8	0.23	228.77	223.38			
Story Nr.	Link Sections		Brace Sections		Column Sections	
	Özhendekci	Present Study	Özhendekci	Present Study	Özhendekci	Present Study
1	W10x77	W10X68	HSS14x14x0.625	HSS10X10X0.5	W14x132	W14X132
2	W10x77	W10X68	HSS14x14x0.625	HSS10X10X0.5	W14x120	W14X132
3	W14x53	W10X68	HSS12x12x0.625	HSS10X10X0.5	W14x109	W14X132
4	W10x68	W10X68	HSS16x16x0.375	HSS10X10X0.5	W14x109	W14X132
5	W10x48	W10X68	HSS12x12x0.5	HSS10X10X0.5	W14x74	W14X82
6	W12x50	W10X68	HSS16x16x0.3125	HSS10X10X0.5	W14x61	W14X68
7	W12x45	W10X68	HSS12x12x0.5	HSS10X10X0.5	W14x48	W14X53
8	W8x48	W12X50	HSS10x10x0.625	HSS10X10X0.375	W14x34	W14X48
9	W8x48	W12X50	HSS10x10x0.5	HSS10X10X0.375	W14x30	W14X38

The second data set belongs to a design aid prepared by Becker and Ishler (1996). This aid exemplifies the design of a 7 story EBF proportioned based on Uniform Building Code (UBC-94, 1994). The earthquake loading provisions of UBC-94 are quite different when compared with the provisions of ASCE7-10 (2010). In order to make a fair comparison, a spectrum matching procedure was applied to determine the design spectral acceleration at short periods (S_{DS}) and at 1 sec (S_{DI}). The ordinates of the original design spectrum derived using UBC-94 provisions were considered and the values of S_{DS} and S_{DI} were calculated to be equal to 1.1g and 0.6g, respectively. Based on these equivalent design acceleration parameters the frame was re-designed. The comparisons of member sizes are given in Table 2.5 along with a comparison of frame weights. The results indicate that the developed program provides an acceptable solution with a lighter frame weight compared to the earlier design. It is worthwhile to mention that some of the differences can be attributed to the changes in EBF design rules over the years. For example response

modification factors in earlier design specifications were lower than the one presently used.

The comparisons provide a verification of the developed program. The algorithm adopted during the formulation of EBF design has the potential to offer cost effective design solutions.

Table 2.5 Comparisons of Developed Program Output with Data Published by Becker and Ishler (1996)

		Frame ID		Becker and Ishler			
		Total Weight (kN)					
		L (m)	e/L	Becker and Ishler	Present Study		
		6.09	0.15	158.73	126.94		
		Link Sections		Brace Sections		Column Sections	
Story Nr.	Becker and Ishler	Present Study	Becker and Ishler	Present Study	Becker and Ishler	Present Study	
1	W14x68	W18X40	HSS10x10x0.5	HSS9X9X0.375	W14x159	W14X145	
2	W14x68	W18X40	HSS10x10x0.5	HSS9X9X0.375	W14x159	W14X132	
3	W14x68	W18X40	HSS10x10x0.375	HSS9X9X0.375	W14x109	W14X132	
4	W14x68	W16X40	HSS10x10x0.375	HSS8x8x0.375	W14x109	W14X82	
5	W12x50	W14x38	HSS8x8x0.375	HSS8x8x0.375	W14x68	W14X68	
6	W12x50	W12x45	HSS8x8x0.375	HSS8X8X0.3125	W14x68	W14X48	
7	W12x50	W10x30	HSS8x8x0.375	HSS8X8X0.3125	W14x68	W14X38	

CHAPTER 3

FUNDAMENTAL PERIODS OF STEEL ECCENTRICALLY BRACED FRAMES

3.1. BACKGROUND

The fundamental period of vibration is one of the key properties of a structure that is directly used in seismic design utilizing the equivalent lateral force procedure. In general, any properly substantiated analysis that takes into account the structural properties and deformational characteristics can be used to determine the fundamental period.

The use of computed periods differs from one specification to the other. In Eurocode 8 (2004) the computed period can be used to determine the level of base shear force used for strength and serviceability limit states. In other words, the strength of elements and the lateral drifts are checked for a base shear force determined using the computed period. North American based specifications recognize the difference between apparent periods and computed periods. In general, the apparent periods of structures obtained using field measurements are shorter than the computed periods. This is a result of inaccuracies in structural modeling. Nonstructural components which contribute to lateral stiffness are usually ignored in models used to determine

the fundamental period. In ASCE7-10 (2010) two different fundamental periods are used in seismic design; one for conducting strength checks and the other one used for checking the drift limits. Restrictions are imposed on the period value used for strength design in order to safeguard against unreasonable assumptions in the substantiated analysis, which may lead to longer periods and unconservative base shear values (Goel and Chopra, 1997). In general, the computed period, T , shall not exceed the product of the coefficient for upper limit on calculated period (C_u) and the approximate fundamental period, T_a . The C_u coefficients depend on the seismic hazard and vary between 1.4 and 1.7. While an upper limit is placed on the fundamental period, it is permitted to determine the elastic drifts using seismic forces based on computed fundamental period of the structure without the upper limit ($C_u T_a$).

The approximate fundamental period, T_a , is usually expressed in terms of empirical formulas which have been calibrated using the measured period of actual structures (apparent periods) during earthquakes (Goel and Chopra, 1998; ATC3-06, 1978; UBC-88, 1988). Empirical formulas are quite useful at the preliminary design stage because these are based on gross geometrical properties such as the height of structure. In other words, the sizes of members and mass properties do not have to be known in advance to determine the fundamental period. On the other hand, these equations have been calibrated to provide a lower bound estimate and lead to relatively accurate results for structures located in high seismic regions. However, the predictions can be overly conservative for structures located in low seismic regions. In general, structures located in low seismic regions have longer periods than structures located in high seismic regions. For the same geometry and mass properties, structures located in high seismic regions are stiffer compared with the structures located in low seismic regions because of the increased amount of seismic forces.

As mentioned in the second chapter, in ASCE7-10 (2010) the following formula is recommended to estimate the fundamental period of steel eccentrically braced frames (EBFs):

$$T_a = 0.0731 h_n^{0.75} \quad (3.1)$$

where h_n = height of the building, in meters, from the foundation.

The current approximate period formula for EBFs first appeared in UBC-88 (1988) and has not been calibrated since then. In a recent study, Kwon and Kim (2010) compared the measured periods of 8 EBFs with the formula given in Equation (3.1). Owing to the limited number of data points, it was difficult to properly evaluate the code formula. It was found out that Equation (3.1) describes the relationship between building height and apparent building period. However, more data points are required to properly evaluate the formula for high-rise buildings.

A study by Tremblay (2005) on periods of concentrically braced frames (CBFs) revealed that empirical equations can lead to overly conservative estimates. It is expected that the same level of conservatism can be valid for EBFs because EBF is a hybrid system that resembles the behavior of CBFs and moment resisting frames (MRFs). Accurate determination of fundamental period is essential for weight optimized design of EBFs. Link rotation limits imposed during EBF design provides stringent drift limits which usually govern the design of members. In such a case allowing for periods determined from a rational analysis without an upper bound can lead to more economical designs. Clause 12.8.6.2 of ASCE7-10 (2010) permits direct use of the computed period in calculating drifts without the upper limit ($C_u T_a$).

All of the concerns listed above present the need to reevaluate fundamental periods of EBFs. Pursuant to this goal, a hand method has been formulated which can be used to estimate the computed fundamental periods of vibration of building structures in general and steel eccentrically braced frames (EBFs) in particular. A parametric study has been conducted to produce design data which is used to support

the proposed formulation. The hand method is further refined to develop new period-height relationships. In this research study the importance of using computed periods is demonstrated by making use of an example EBF. The derivation of the hand method and the details of the parametric study are given next. Lastly the development of new period height relationships is explained and the findings are compared with apparent building periods.

3.2. IMPACT OF USING COMPUTED PERIODS

In this section, benefits of using computed period as opposed to using approximate period are demonstrated through an example problem. A regular office building having a floor plan shown in Figure 3.1 was considered. The floor plan has side dimensions 30 m by 30 m resulting in a footprint of 900 m². In each of the principal loading direction there are two braced bays which result in a braced bay tributary area of 450 m².

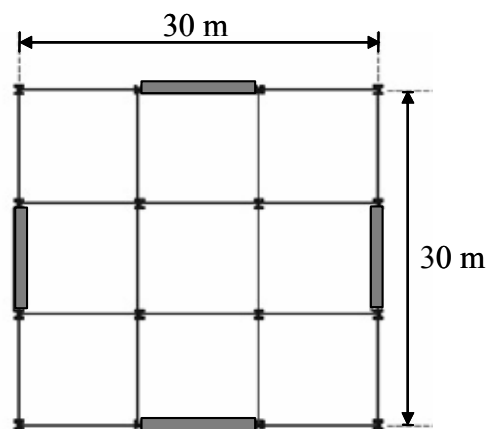


Figure 3.1 Floor plan used in the parametric study

A typical elevation view of a plane EBF which is given in Figure 3.2 was considered. As shown in this figure it was assumed that the gravity framing is attached to the braced bay by simple shear connections. Therefore, eccentrically braced framing is used for resisting the seismic forces and the gravity framing is utilized for resisting forces due to gravity. This assumption simplified the analysis model considerably enabling to model the plane braced bay only. It should be noted that the lateral resistance is provided by the eccentrically braced bay and structural periods computed based on the two dimensional model shown in Figure 3.2 is representative of the three dimensional structure. Only one type of steel, A992, with a yield strength of 345 MPa was considered for all members of the steel framing.

During the EBF design the seismic forces were calculated using the provisions of ASCE7-10 (2010). In sizing the steel members, provisions of the AISC Specification for Structural Steel Buildings (AISC-360, 2005 and AISC Seismic Provisions for Structural Steel Buildings, AISC-341, 2005) were used. It is worthwhile to note that the 2010 version of the AISC specifications became available at the time of writing and the 2010 provisions do not result in substantial changes to the 2005 provisions. Story dead and live loads were assumed to be 5 kN/m² and 2 kN/m², respectively. A redundancy factor of unity was considered. The structure was assumed to be Risk Category 2 structure with an importance factor of 1.0. The designs are formed with the implementation of design program detailed in Chapter 2.

The developed program calculates the initial period of the structure using Equation (3.1). With this initial period, the seismic base shear is computed and lateral loads are determined using the equivalent lateral force method. The program selects proper link sections based on the link force at every story. The braces and columns are sized based on capacity design principles. Links, beams and braces are selected among American wide flange sections (W shapes) while columns are selected from W14 sections. The selection of member sizes is based on the minimum weight principle.

Several design iterations are conducted to arrive at a final design. When a set of link, brace and column sections are selected, the program calculates the fundamental period of the structure using an eigenvalue analysis. The seismic forces are updated according to the period obtained from an eigenvalue analysis. It is allowed to use elongated periods according to the ASCE7-10 (2010) provisions. The upper limit on periods ($C_u T_a$) is utilized in calculating base shear forces but the period without an upper bound is used in checking lateral drifts and link rotation angles. The iterations are continued until the selected member sizes satisfy all limit states under lateral forces computed using the actual period from an eigenvalue analysis.

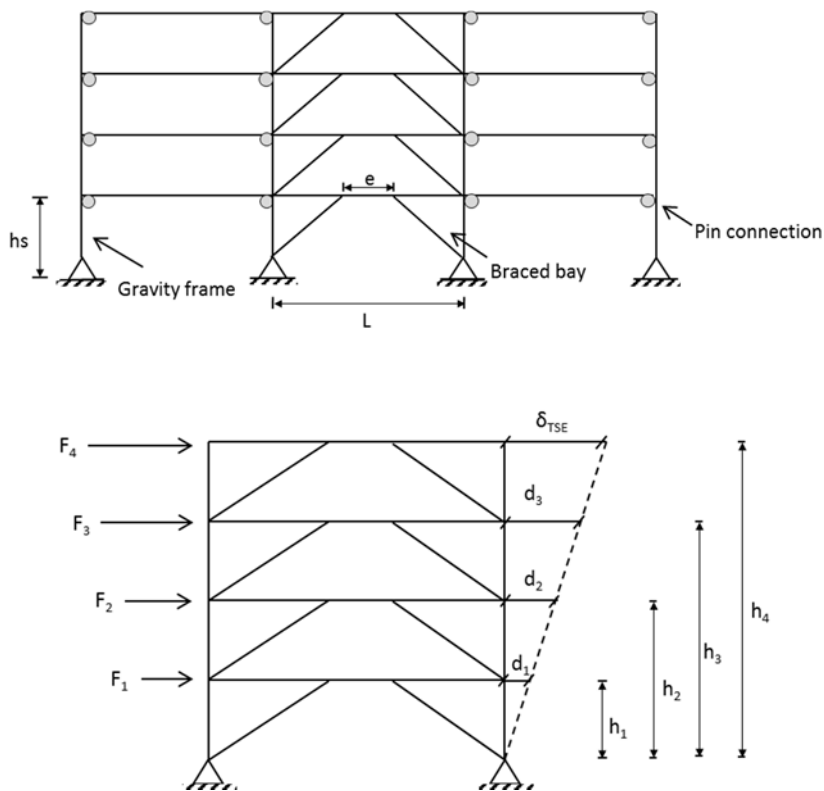


Figure 3.2 Typical elevation view of a plane EBF and illustration of linear displaced shape

It should be recognized that the resulting member sections are dependent on the type of optimization utilized during EBF design. The details of the developed program and the optimization process are given in Kuşyılmaz and Topkaya (2013) and Chapter 2. Furthermore, the designs obtained using the developed program are compared with designs presented by Özhendekci and Özhendekci (2008). For the four EBFs that were compared, it was found out that the design optimization used by the developed program results in on average 21% lower frame weights and on average 27% longer fundamental periods.

The example EBF is a 15 story building located in Western Tennessee. The story height was constant for all stories and considered as 4 m. The link length to bay width ratio (e/L) is 0.15, and the braced bay width (L) is 8 meters. According to ASCE7-10 (2010) the seismic hazard can be represented by two mapped acceleration parameters. These are S_s and S_l which are the 5 percent damped, risk adjusted maximum considered earthquake (MCE_R) spectral accelerations at a short period of 0.2 sec and at a period of 1 sec, respectively. It was assumed that the building is located on Site Class D type soil. The MCE_R spectral accelerations (S_s and S_l), the design spectral acceleration in the short period range (S_{DS}) and design spectral acceleration at a period of 1 sec (S_{DI}) are indicated in Table 3.1.

The EBF was first designed by making use of the computed periods and the resulting member sizes are given in Table 3.1. The design starts with an initial guess for fundamental period equal to 1.575 sec according to Equation (3.1). After having several iterations the final design converges to a fundamental period of 3.40 s. The seismic response coefficient (C_s) is 0.0410 for strength design indicating that the lateral forces are 4.1% of the vertical forces. The upper bound on period ($C_u T_a = 1.4 \times 1.575 = 2.205$ s) should be used to determine C_s but in this case the C_s value is governed by the minimum design base shear provisions of ASCE7-10 (2010) which is equal to $0.044 S_{DS}$ and results in $C_s = 0.041$. Because no upper bound or minimum base shear provisions (Clauses 12.8.6.1 and 12.8.6.2 of ASCE7-10 (2010)) exist for drift checks the computed period is directly used in determining the

C_s value for drift limitations. In this case the C_s value turns out to be equal to 0.0152. It should be noted that the lateral drifts and the link rotation angles which are calculated using lateral drifts according to AISC341-05 (2005) were determined using a C_s equal to 0.0152. The weight of the EBF is equal to 550.2 kN when the computed period is used in the design process.

For comparison purposes the very same design was repeated without updating the value of the fundamental period. In other words, a period value equal to 1.575 s was utilized for strength and drift checks which result in a C_s value equal to 0.041 for both limit states. The resulting member sizes are given in Table 3.1. The weight of the EBF is equal to 959.6 kN which is 74% higher than the value for the previous design. The weight, which is a direct indication of the cost of framing, increased by a significant amount when the computed period was not used in design.

This example demonstrates the impact of using different period values in the design process. To come up with weight-optimized and cost-effective solutions, it is desirable to use the computed value of the fundamental period in design calculations. A typical design starts with an initial guess on the fundamental period using Equation (3.1). After the member sizes are determined on the basis of lateral forces calculated using the approximate period, a more accurate estimate of the period can be found by making use of any substantiated analysis. The lateral forces are updated by making use of this new period value and the member sizes are changed to meet the demands due to the updated forces. In general, this procedure requires designing the lateral load resisting system twice resulting in an increase in the design time and effort.

The increase in the design time is not pronounced in cases where special design software which can automate the member selection can be used. EBFs are less frequently used when compared with MRFs and CBFs. Therefore, most of the tools available to design engineers do not have options to automate EBF designs and engineers often have to manually input trial sections and iterate until all design requirements are met. This is particularly onerous for EBF design because selecting

link sections based solely on the strength requirement often times does not give a satisfactory solution. Sizing of the link sections are generally governed by stringent link rotation angle limits. In addition, the columns, the braces, and the beam outside of the link must be checked under the forces generated by the yielded and strain hardened link due to the capacity design requirements. In general, updating only the link section sizes is not sufficient in cases where the link rotation angle limits are not met. A change in the link section size directly impacts the forces generated in the other members of an EBF resulting in changes to the sizes of these members too.

Due to the complexities in design of EBFs some engineers may opt to design the framing once rather than twice by using the approximate period to calculate the amount of lateral forces for strength and displacement checks. In this case, however, the design does not benefit from the fact that the computed period is different from the approximate period. In other words, the structure has to be designed for higher levels of lateral force which in turn increases the member sizes and cost of framing.

A method has been developed as a part of this study to estimate the computed periods of EBFs with higher accuracy. The following section presents a general formulation that can be used to predict the computed periods of structures in general and EBFs in particular.

Table 3.1 Comparative Designs of an Example EBF

Location		Western Tennessee						
N		15						
e/L		0.15						
L (m)		8						
S ₁		0.38						
S _s		1.4						
S _{d1}		0.41						
S _{ds}		0.93						
Design Type		Design based on T _{computed}			Design based on T _{approximate}			
T _{final} (sec)		3.40			2.46			
C _s (drift)		0.0152			0.0410			
C _s (strength)		0.0410			0.0410			
Link Section	Story Nr.		Story Nr.		Story Nr.		Story Nr.	
	1	W18X50	9	W18X40	1	W27X94	9	W24X84
	2	W18X50	10	W18X40	2	W27X94	10	W24X84
	3	W18X50	11	W14x38	3	W27X94	11	W24X84
	4	W18X50	12	W12x45	4	W27X94	12	W24X84
	5	W18X50	13	W12x45	5	W27X94	13	W24X84
	6	W18X50	14	W8X40	6	W27X94	14	W24X84
	7	W18X40	15	W8X40	7	W27X94	15	W24X84
	8	W18X40			8	W27X94		
Brace Section	Story Nr.		Story Nr.		Story Nr.		Story Nr.	
	1	W10X68	9	W14X68	1	W12X106	9	W12X96
	2	W10X68	10	W14X68	2	W12X106	10	W12X96
	3	W10X68	11	W8X67	3	W12X106	11	W12X96
	4	W10X68	12	W8X58	4	W12X106	12	W12X96
	5	W10X68	13	W8X58	5	W12X106	13	W12X96
	6	W10X68	14	W8X48	6	W12X106	14	W12X96
	7	W14X68	15	W8X48	7	W12X106	15	W12X96
	8	W14X68			8	W12X106		
Column Section	Story Nr.		Story Nr.		Story Nr.		Story Nr.	
	1	W14X370	9	W14X145	1	W14X605	9	W14X283
	2	W14X342	10	W14X132	2	W14X550	10	W14X233
	3	W14X311	11	W14X132	3	W14X550	11	W14X193
	4	W14X283	12	W14X74	4	W14X500	12	W14X159
	5	W14X257	13	W14X68	5	W14X426	13	W14X132
	6	W14X233	14	W14X48	6	W14X398	14	W14X132
	7	W14X193	15	W14X38	7	W14X342	15	W14X68
	8	W14X159			8	W14X311		
Total weight (kN)		550.2			959.6			

3.3. DEVELOPMENT OF A METHOD TO DETERMINE FUNDAMENTAL PERIODS

The proposed method is based on estimating the stiffness properties of structures which essentially depend on many parameters. This property is represented by the elastic displacement at the roof of the structure (δ_{TSE} as shown in Figure 3.2) computed under design seismic forces which are determined using the computed fundamental period of the structure. The elastic roof displacement is converted into roof drift ratio and subsequently used in the formulation. The elastic roof displacement values are dependent on the structural system and should be determined from design data. The roof drift ratios are obtained using a parametric study details of which are explained in the following sections. A similar method was formulated for concentrically braced frames designed according to European norms by Günaydın and Topkaya (2013).

The present method is applicable to regular structures having the same mass properties at all floors. In general, this assumption is valid for most of the residential and office type buildings. Although the roof level may contain lower amounts of mass this does not lead to significant errors. The story height is considered to be constant. While the height of the first story can be greater than the height of other stories, it is considered that using equal height assumption does not lead to significant errors. Verification of the method using structures with a lower story mass at the roof and having different first story height will be given in the later sections. It is assumed that the displacements of the stories vary linearly over the height of the structure as shown in Figure 3.2.

According to the Rayleigh's method the fundamental period of a structure can be determined as follows:

$$T = 2\pi \sqrt{\frac{\sum_{i=1}^N m_i d_i^2}{\sum_{i=1}^N F_i d_i}} \quad (3.2)$$

where m_i = mass of i^{th} story which is assumed to be equal to m for all stories, F_i = lateral force at level i , d_i = displacement at the i^{th} story, N = number of stories.

The amount of lateral force at each story can be determined as follows according to the equivalent lateral force procedure given in ASCE7-10 (2010):

$$F_i = \frac{m_i h_i^k}{\sum_{j=1}^N m_j h_j^k} C_s W \quad (3.3)$$

where W = the effective seismic weight, h_i = height from the base to level i , k = exponent related to the structure period as follows: for structures having a period of 0.5 s or less, $k=1$, for structures having a period of 2.5 s or more, $k=2$, for structures having a period between 0.5 s and 2.5 s, k shall be 2 or shall be determined by linear interpolation.

According to the aforementioned linear variation of displacements assumption, the displacement at each story can be expressed as follows:

$$d_i = RD_R h_i \quad (3.4)$$

where RD_R = roof drift ratio

With the equal story height assumption the height from the base level can be expressed as follows:

$$h_i = h_s i \quad (3.5)$$

where h_s = height of one story.

Inserting Equations (3.3), (3.4), (3.5) into Equation (3.2) yields:

$$T = 2\pi \sqrt{\frac{m R D_R h_s \sum_{i=1}^N i^2 \sum_{i=1}^N i^k}{C_s W \sum_{i=1}^N i^{k+1}}} \quad (3.6)$$

Equation (3.6) presents an estimate of the fundamental period as a function of several quantities including the k factor, which also depends on the fundamental period itself. To come up with a simplified equation that does not require an iterative solution, the use of different k values between 1 and 2 were studied during the development of this method. Finally, it was decided to use $k=2$, and the quality of the estimates under this assumption will be presented in the following sections. Equation (3.6) simplifies to the following expression by using $k=2$:

$$T = 2\pi \sqrt{\frac{m R D_R h_s \left(\sum_{i=1}^N i^2 \right)^2}{C_s W \sum_{i=1}^N i^3}} \quad (3.7)$$

For the case with equal story mass, the effective seismic weight can be determined as follows:

$$W = N m g \quad (3.8)$$

The summation terms in Equation (3.7) can be written in terms of the number of stories as follows:

$$\sum_{i=1}^N i^2 = \frac{N(N+1)(2N+1)}{6} \quad (3.9)$$

$$\sum_{i=1}^N i^3 = \left(\frac{N(N+1)}{2} \right)^2 \quad (3.10)$$

Inserting Equations (3.8), (3.9), (3.10) into Equation (3.7) yields:

$$T = \frac{2\pi}{3} \sqrt{\frac{Q}{C_s}} \quad \text{where} \quad Q = \frac{h_s (2N+1)^2}{N g} R D_R \quad (3.11)$$

Equation (3.11) provides a simple method to estimate the fundamental period and it depends on the seismic response coefficient (C_s). According to ASCE7-10 (2010) the seismic response coefficient is divided into various regions. For the structures studied herein three regimes should be considered. These are the constant spectral acceleration region, the descending branch and the minimum base shear region. It should be noted that the most of the minimum base shear provisions are not applicable to drift checks but there is only one that is required when $S_I \geq 0.6g$. The corresponding seismic response coefficients can be represented as follows:

$$C_{s1} = \frac{S_{DS}}{\left(\frac{R}{I_e}\right)} \quad C_{s2} = \frac{S_{D1}}{T \left(\frac{R}{I_e}\right)} \quad \text{for } S_1 \geq 0.6g \quad C_{s3} = \frac{0.5S_1}{\left(\frac{R}{I_e}\right)} \quad (3.12)$$

where R = the response modification factor, I_e = the importance factor.

In Equation (3.12), C_{s1} represents the constant acceleration region, C_{s2} represents the descending branch, and C_{s3} represents the minimum base shear region.

Inserting Equation (3.12) into Equation (3.11) yields the following simplified equations to find out the fundamental period.

$$T = \frac{4\pi^2}{9} \left(\frac{R}{I_e}\right) \frac{Q}{S_{D1}} \quad T_{\min} = \frac{2\pi}{3} \sqrt{\frac{R}{I_e}} \sqrt{\frac{Q}{S_{DS}}} \quad \text{for } S_1 \geq 0.6g \quad T_{\max} = \frac{2\pi}{3\sqrt{0.5}} \sqrt{\frac{R}{I_e}} \sqrt{\frac{Q}{S_1}} \quad (3.13)$$

where T_{\min} = minimum period, T_{\max} = maximum period.

The method requires calculating the fundamental period using the first equation and then comparing it against the minimum and maximum values of fundamental period. If the estimated period is less than the minimum one then the minimum should be

used. Similarly for cases where $S_1 \geq 0.6g$ the maximum value should be used in cases where the estimate is greater than the maximum.

Equation (3.13) simplifies into the following form for EBFs of normal importance ($I_e = 1$) designed according to the recommended value of $R = 8$:

$$T = \frac{35.1 Q}{S_{D1}} \quad T > \frac{5.92 \sqrt{Q}}{\sqrt{S_{DS}}} \quad \text{for } S_1 \geq 0.6g \quad T < \frac{8.38 \sqrt{Q}}{\sqrt{S_1}} \quad (3.14)$$

It is worthwhile to note that the values of S_{D1} , S_{DS} , and S_1 should be normalized by the gravitational acceleration (g) and subsequently used in Equation (3.14).

Equation (3.14) requires roof drift ratio (RD_R) to be known in advance. The roof drift ratio can be estimated by obtaining design data. A parametric study has been performed on EBFs to collect information on RD_R . The following section outlines the findings of the parametric study.

3.4. A PARAMETRIC STUDY ON PERIOD ESTIMATION OF EBFs

Regular office buildings with various geometric properties were designed for locations with differing seismic hazard. All structures had similar details (floor plan, grade of steel, dead and live load intensity, soil conditions, etc.) that were used for the example EBF studied earlier in this chapter.

Number of stories, link length to bay width (e/L) ratio, and braced bay width (L) were considered as the prime variables. Number of stories varied from 3 to 15, link length to bay width ratio varied as 0.1, 0.15, 0.2, 0.25, and 0.3. Bay widths of 8m, 10m, 12m, 14m were considered. These variables resulted in 260 design cases.

Different geographical locations were considered in order to take into account the seismic hazard. A total of 16 locations in the United States with diverse seismic hazards were taken into consideration. Depending on their S_s and S_l values, 16 geographical locations which are detailed in Table 3.2 were considered in this study. The 2002 version of the USGS maps were used to find the spectral accelerations. EBFs are usually designed in high and moderate seismic regions due to their superior ductility and energy dissipation capacity. The commentary to the NEHRP Recommended Provisions for Seismic Regulations for New Buildings and Other Structures (FEMA 450) (2003) defines regions based on mapped spectral acceleration values S_s and S_l . The provisions recommend that the spectral acceleration values must be adjusted for specific site conditions. In other words, the recommendations are based on S_{MS} and S_{MI} which are the spectral response acceleration parameters at short periods and at a period for 1 sec adjusted for site class effects. According FEMA 450 provisions regions with $0.25g < S_{MS} < 1.5g$ and $0.1g < S_{MI} < 0.6g$ are classified as regions with low and moderate to high seismicity. As mentioned before the structures in the parametric study were assumed to be located on Soil Class D. The S_{MS} and S_{MI} values corresponding to Soil D are also given in Table 3.2. As shown in this table, six of the locations represent low and moderate to high seismic regions and the rest of the locations represent high seismic regions. Wind design criteria was ignored based on the assumption that the locations represent high and moderate seismicity where seismic design governs over wind design for members of EBFs. A total of 4160 designs were conducted by considering the aforementioned parameters.

The RD_R values under seismic forces used for checking drift and link rotation limits were collected as a result of the parametric study. The type of the link used in EBF design has a direct influence on the global elastic stiffness and consequently fundamental periods of frames. When shear-yielding links are used the frame behavior resembles behavior of a concentrically braced frame whereas when flexural yielding links are used the frame behavior resembles behavior of a moment resisting frame. A model based on deformation pattern of EBFs was developed to predict the

RD_R values. During the design stage the link rotation angle (γ) is checked using a rigid plastic deformation mechanism as shown in Figure 3.3. For the commonest EBF configuration where the link is a horizontal framing member located between braces as shown in Figure 3.3, the relationship between the lateral displacements and the link rotation angle can be expressed as follows:

$$\frac{\Delta}{h_s} = \gamma \frac{e}{L} \quad (3.15)$$

where Δ = lateral displacement of a story, γ = link rotation angle.

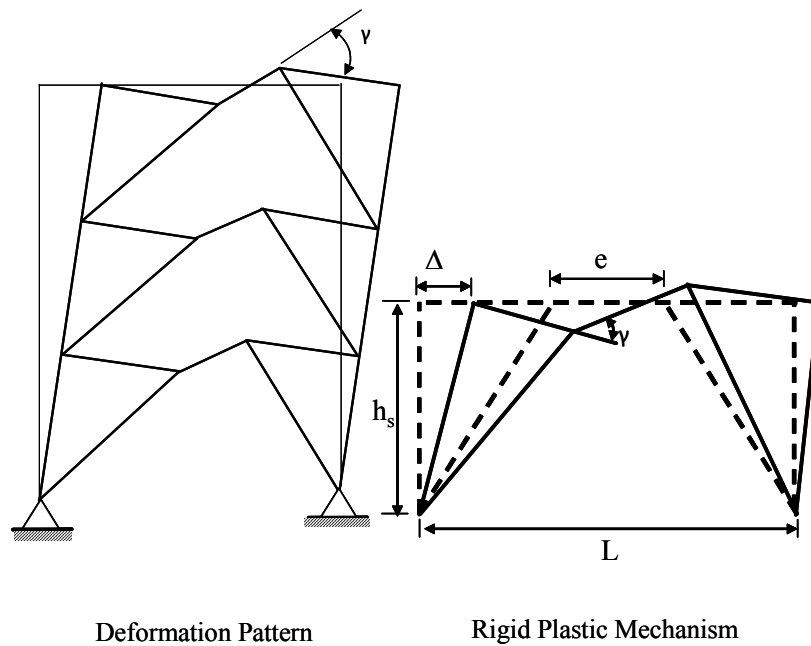


Figure 3.3 Typical deformation pattern of an EBF

Table 3.2 Spectral Ground Motion Parameters S_s and S_1 for 16 Regions in USA

Location	Latitude (degrees)	Longitude (degrees)	S_s (g)	S_1 (g)	S_{MS} (g)	S_{M1} (g)
High Seismic						
San Francisco, CA	37.46	-122.25	2.222	1.020	2.222	1.53
Kern County, California, CA	34.57	-119.00	2.030	0.830	2.030	1.245
Los Angeles, CA	34.03	-118.14	2.030	0.695	2.030	1.043
Long Beach, CA	33.08	-118.04	1.890	0.778	1.890	1.167
Northridge, Los Angeles, CA	34.12	-118.32	1.794	0.600	1.794	0.900
Carbondale, Southern Illinois, IL	37.46	-89.11	1.620	0.518	1.620	0.777
San Jose, CA	37.20	-121.53	1.500	0.600	1.500	0.900
Western Tennessee, TN	35.70	-89.23	1.398	0.378	1.398	0.621
Seattle, WA	47.37	-122.28	1.288	0.438	1.288	0.684
San Diego, CA	32.42	-117.09	1.198	0.478	1.223	0.728
Low and Moderate to High Seismic						
Memphis, TN	35.08	-90.02	1.200	0.334	1.224	0.578
N. Charleston, SC	32.53	-80.08	1.083	0.270	1.155	0.502
Western Kentucky, KY	36.58	-88.37	1.017	0.274	1.112	0.507
Georgetown, SC	33.50	-79.17	0.892	0.259	1.020	0.487
Southern Idaho, ID	44.23	-113.51	0.823	0.287	0.964	0.524
Portland, OR	45.31	-122.40	0.762	0.273	0.911	0.506

The relationship given in Equation (3.15) indicates that the roof drift ratios are related with the link rotation angle (γ) and the link length to bay width ratio (e/L). The link rotation angle is limited by the design specifications and its allowable value is dependent on the normalized link length (e_N) defined as follows:

$$e_N = \frac{e}{\left(\frac{M_p}{V_p} \right)} \quad (3.16)$$

where M_p = plastic flexural strength of the link and V_p = plastic shear strength of the link.

According to the AISC Seismic Provisions for Structural Steel Buildings (AISC-341, 2005) the following limits are defined for the link rotation angle:

$$\begin{aligned}
\gamma &= 0.08 && \text{for } e_N \leq 1.6 \\
\gamma &= 0.02 && \text{for } e_N \geq 2.6 \\
\gamma &= 0.08 - (e_N - 1.6) \times 0.06 && \text{for } 1.6 < e_N < 2.6
\end{aligned} \tag{3.17}$$

While the value of link length to bay width ratio (e/L) is known at the design stage, it is difficult to determine the value of normalized link length (e_N). In fact the normalized link length is not a constant and changes at every story depending on the link member size. In general, there is a direct relationship with the link length to bay width ratio (e/L) and the normalized link length (e_N). For the designs obtained during the parametric study the normalized link length (e_N) values of the resulting link sections were collected at every story. Later, e_N values were averaged over the height of an EBF to come up with a representative normalized link length. Variation of normalized link length as a function of the link length to bay width ratio is given in Figure 3.4. The best fit line to the data points is also shown in this figure. It is evident from Figure 3.4 that the normalized link length increases as e/L increases. This means that for low e/L values such as 0.1 the resulting links qualify as shear links while for high e/L values such as 0.3 the resulting links qualify as flexural yielding links. Representing the normalized link length with only the e/L results in a significant amount of scatter because other factors such as seismic hazard, bay width, and total height also influence the design.

The data set was separated into two according to the seismic hazard classification of the Commentary to FEMA 450 (2003). The roof drift values (RD_R) are plotted against $\gamma \times \frac{e}{L}$ in Figure 3.5 for the two seismic hazard categories. It is evident from Figure 3.5 that the product of the link rotation angle and the link length to bay width ratio provides a good measure of the roof drift ratio. In general, the roof drift ratio increases linearly with $\gamma \times \frac{e}{L}$. The best fit lines to the data points can be used to arrive at the relationships for the roof drift ratio given in Equation (3.18). Coefficient of determination (R^2) values for these regression lines are 0.9 and 0.85 for high seismic and low and moderate to high seismic regions, respectively.

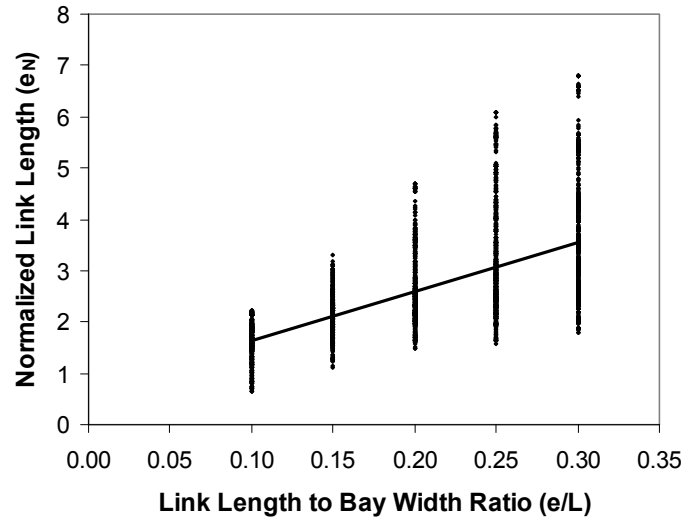


Figure 3.4 Normalized link length versus link length to bay width ratio

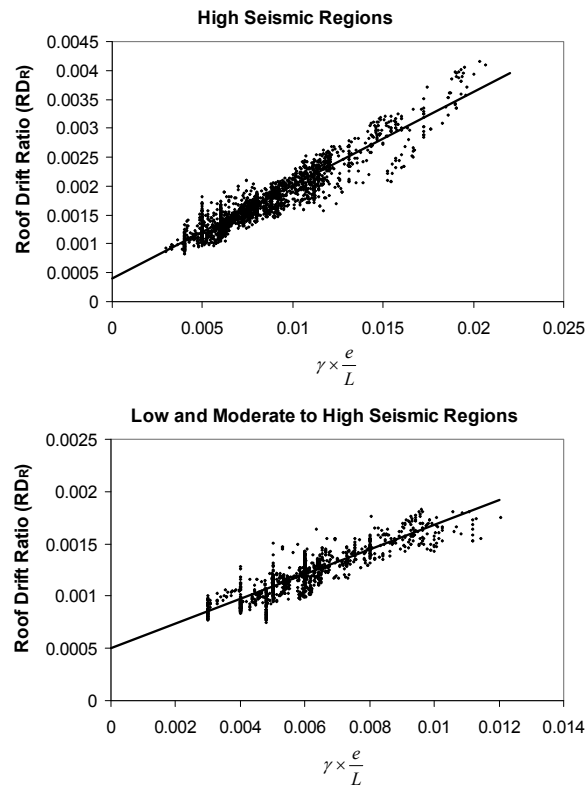


Figure 3.5 Variation of roof drift ratio with the product of link rotation angle and link length to bay width ratio

$$RD_R = 0.1616 \left(\gamma \times \frac{e}{L} \right) + 0.0004 \quad \text{for high seismic regions} \quad (3.18)$$

$$RD_R = 0.1183 \left(\gamma \times \frac{e}{L} \right) + 0.0005 \quad \text{for low and moderate to high seismic regions}$$

The link rotation angle determined using Equation (3.17) can be directly used in Equation (3.18) to estimate the roof drift ratio for EBFs. However, the use of Equation (3.17) requires prior knowledge of the normalized link length (e_N) during the design stage. Engineers can estimate the normalized link length by experience and considering the link length to bay width ratio. In the present work a regression analysis was performed to provide equations that can be used to predict the normalized link length (e_N). As shown in Figure 3.4 the e_N values significantly depend on the e/L value with considerable scatter. To represent the data more efficiently the data points were divided according to the seismic hazard level and according to the e/L ratio. For each set it was assumed that the S_{DI} , S_{DS} , bay width and height are the potential variables that influence the response. Preliminary regression analyses revealed that S_{DI} and S_{DS} are related and adding both of these variables makes the prediction equations more complicated without increasing significantly the accuracy of the predictions. Therefore, it was decided to conduct regression analysis of each group of data by considering S_{DI} , bay width and height as the prime variables. A regression model given as follows was adopted:

$$e_N = C_1 \times S_{DI}^{C_2} \times L^{C_3} \times h_n^{C_4} \quad (3.19)$$

where C_1, C_2, C_3, C_4 = coefficients obtained from regression analysis.

For each group of data the coefficients were determined and the coefficients C_2, C_3 , and C_4 which were obtained for different e/L ratios were averaged to reduce the number of equations. Furthermore, a linear equation was developed to represent coefficient C_1 as a function of e/L . The resulting prediction equations for the two seismic regions can be given as follows:

$$e_N = \left[2.27 \left(\frac{e}{L} \right) + 0.27 \right] \times \left[S_{D1}^{-0.3826} \times L^{0.669} \times h_n^{-0.1828} \right] \text{ for high seismic regions} \quad (3.20)$$

$$e_N = \left[1.87 \left(\frac{e}{L} \right) + 0.09 \right] \times \left[S_{D1}^{-0.545} \times L^{0.8314} \times h_n^{-0.1984} \right] \text{ for low and moderate to high seismic regions}$$

It should be noted that the bay width and height should be in meter units in Equation (3.20). A comparison of the calculated e_N values and predicted e_N values are given in Figure 3.6.

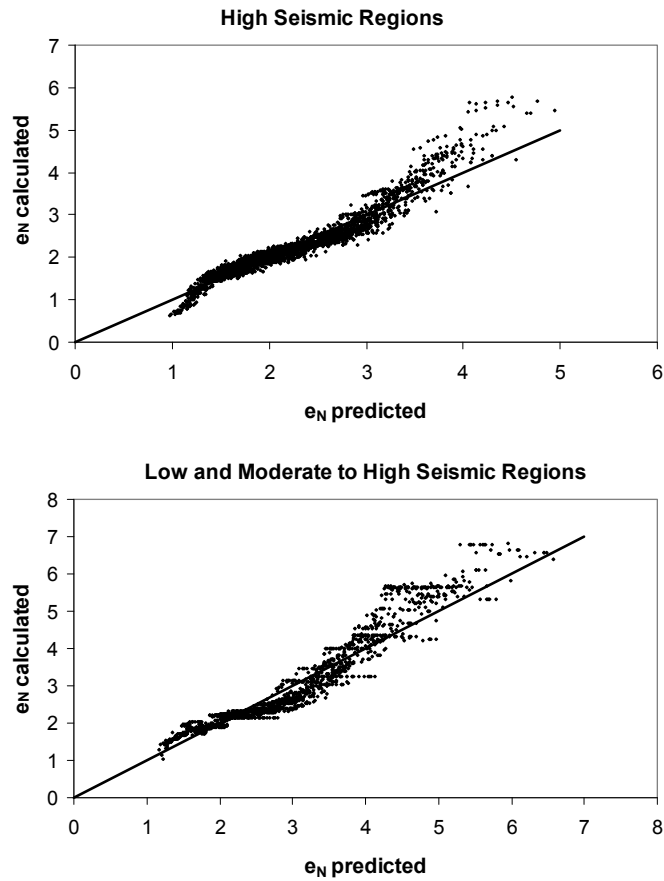


Figure 3.6 Comparison of calculated and predicted normalized link lengths

3.4.1. Verification of the Method Using Actual Top Story Drift Ratios

The proposed method for estimating fundamental periods is based on a number of assumptions. The quality of the predictions offered by this method was first assessed using the computed RD_R values. These values are the ones that directly come from the design of EBFs that were conducted as a part of the parametric study. Statistical measures of the estimates are given in Table 3.3. According to the statistical measures the proposed method has the potential to predict the fundamental periods with accuracy provided that the RD_R values are accurately known. The ratios of the actual period to estimated period have an average close to unity and the standard deviation is close to 0.06. These comparisons indicate that the $k=2$ assumption used in the derivation of the method is sufficient.

Table 3.3 Statistical Analysis of the Ratios of Computed Period to Estimated Period

	Ratio of Computed Period to Estimated Period						
	All Regions	High Seismic	Low and Moderate to High Seismic	High Seismic	Low and Moderate to High Seismic	High Seismic	High Seismic
	Calculated RD_R	RD_R from Equation (3.18)	RD_R from Equation (3.18)	Equation (3.1)	Equation (3.1)	Published Data Proposed Method	Published Data Equation (3.1)
Mean	1.03	1.05	1.04	1.47	1.86	0.98	1.35
Median	1.03	1.02	1.02	1.45	1.83	0.98	1.30
Standard Deviation	0.06	0.15	0.14	0.32	0.32	0.21	0.19
Maximum	1.22	1.83	1.58	2.49	2.93	1.50	2.06
Minimum	0.87	0.65	0.71	0.76	1.22	0.64	1.13

3.4.2. Evaluation of the Method Using Estimated Roof Drift Ratios

The proposed method was evaluated by making use of the estimated roof drift ratios. The RD_R values were computed according to Equation (3.18) and used in predicting the fundamental period according to the proposed method. The comparisons of the estimated period and computed period are given in Figure 3.7. The statistical analysis of the ratios of computed period to estimated period is given in Table 3.3. The results given in Figure 3.7 and Table 3.3 indicate that the proposed method is capable of estimating the fundamental periods with reasonable accuracy. The mean of the ratios is close to unity and the standard deviation value is close to 0.15 for both seismicity regions.

The estimations offered by Equation (3.1) were also studied for comparison purposes. The comparisons of computed periods and the estimated periods from Equation (3.1) are given in Figure 3.8 and the related statistics are given in Table 3.3. When Equation (3.1) is used the mean of the ratios reaches to 1.47 and the standard deviation is 0.32 for high seismic regions indicating large scatter in data points. For low and moderate to high seismic regions the mean of the ratios is 1.86 indicating that Equation (3.1) provides more conservative estimates of the fundamental period as expected. Compared with the estimations offered by the empirical lower bound relationship, the proposed method significantly improves the predictions. The mean and standard deviation of the estimates are reduced when the proposed method is used. In addition, a significant reduction in the maximum of the ratios is observed while there is no change in the minimum of ratios.

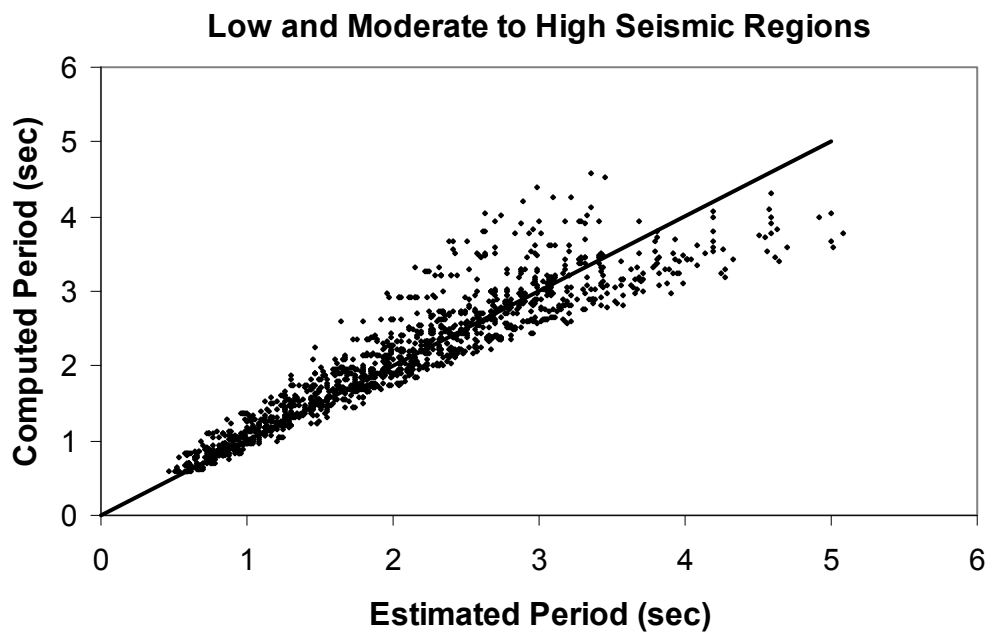
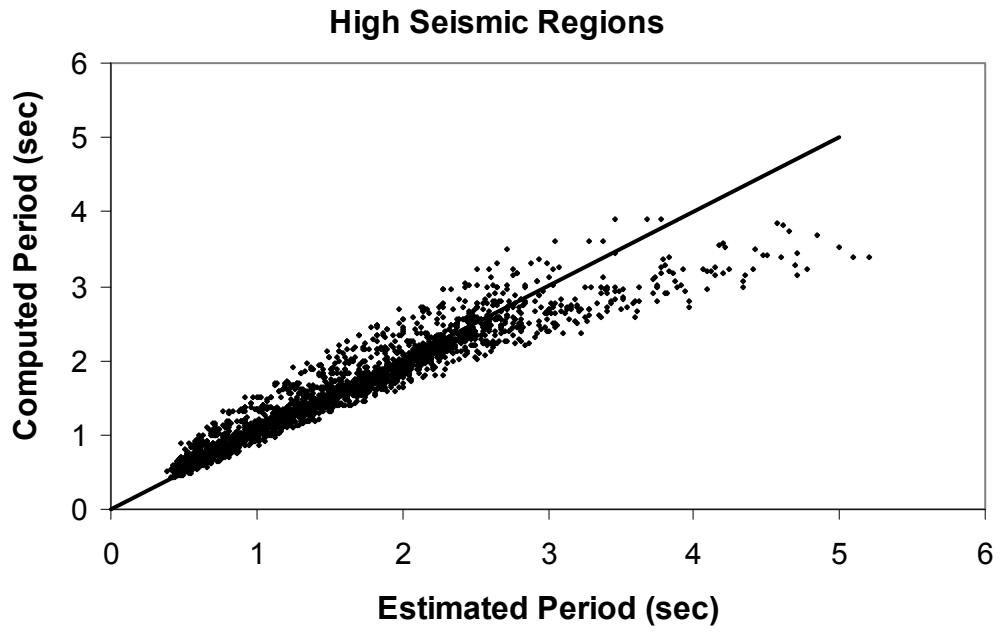


Figure 3.7 Comparison of computed and estimated periods using the proposed method

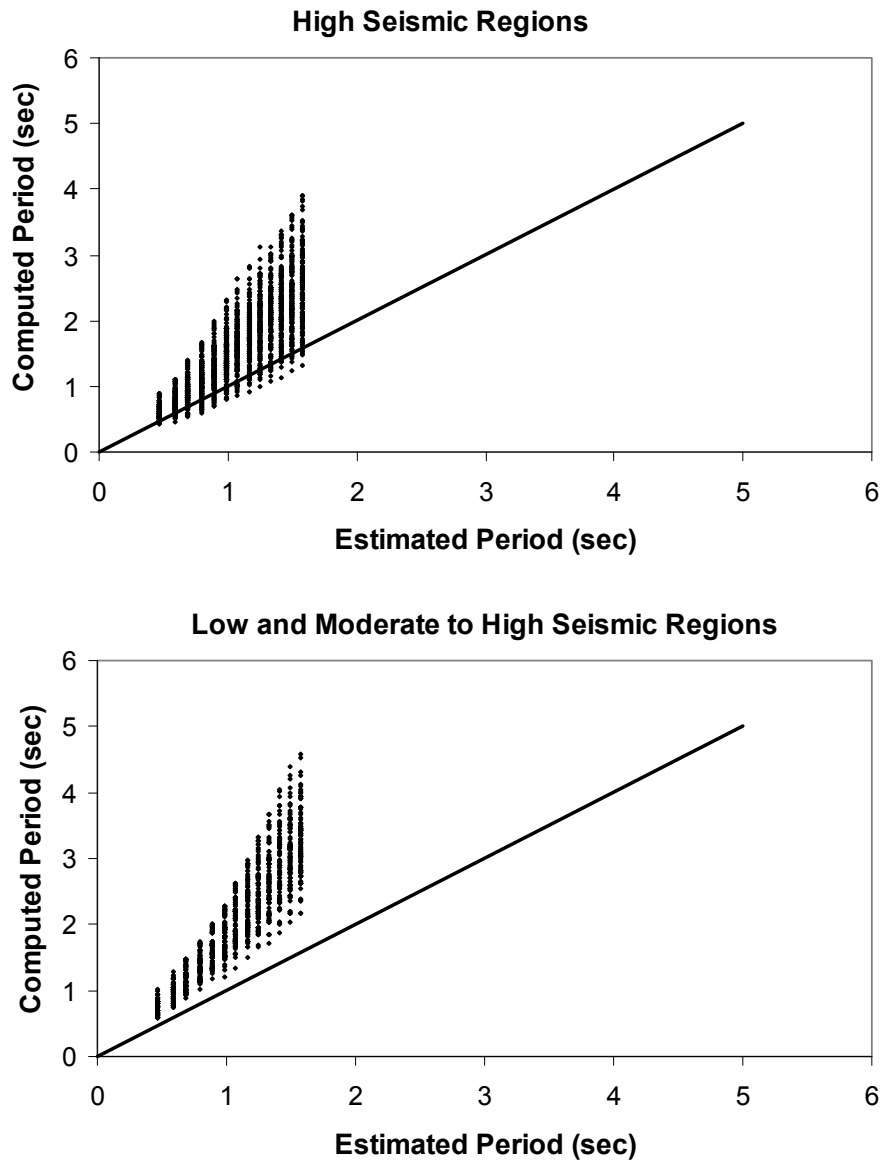


Figure 3.8 Comparison of computed and estimated periods using Equation (3.1)

3.4.3. Verification of the Method Using Data Published in Literature

In general, the final designs are dependent on the designer as there is no universally accepted way of designing EBFs. Similarly the current study is based on designs

conducted in accordance with ASCE7-10 (2010), AISC 360-05 (2005), and AISC 341-05 (2005) specifications and the estimations are expected to be better when the proposed equations are applied to designs based on these specifications. Equation (3.14) requires spectral acceleration parameters that are defined in ASCE 7-10 (2010) but this equation can be modified to produce solutions for EBFs designed using specifications other than ASCE 7-10 (2010). In this section the method is verified using data from two independent research teams.

The first set of data belongs to a study conducted by Özhendekci and Özhendekci (2008). The primary focus of the study was to investigate the effects of frame geometry on the weight and inelastic behavior of EBFs. A total of 360 EBFs were designed as a part of this study and properties of 45 frames are reported. The study considered 3 different floor plans and structures with number of stories varying between 3 and 9. All structures were assumed to be located in Los Angeles with a local site class D. The S_s and S_I values were considered to be 1.5g and 0.6g, respectively. The braced bay widths changed between 7 and 10 meters. The frames have e/L ratios of 0.09, 0.13, 0.17, 0.23, 0.24, 0.28, and 0.32. The story height is 3.5 meters for all stories. A lower roof mass compared to the mass of other floors was considered. The designs were based on the 2005 version of ASCE7, 1999 version of AISC-360 and 2005 version of AISC-341. The fundamental periods of vibration were not reported alongside the member properties. Therefore, these frames were independently modeled to obtain actual fundamental periods of the resulting designs.

The second set of data belongs to a study conducted by Rossi and Lombardo (2007). The focus of the study was to investigate the link overstrength factor on the seismic behavior of eccentrically braced frames. A total of 16 EBFs were designed having e/L ratios in the range of 0.1 and 0.3. The 1993 version of Eurocode 8 was employed in the design of EBFs. The buildings have a square floor plan having side lengths of 24 m. A braced bay width of 8 m was considered. All stories have a height of 3.3 m. The design peak ground acceleration was considered to be equal to 0.35g and soft soil condition was assumed. The response spectrum given in Eurocode 8 is quite

different compared to the one defined by ASCE7-10. Therefore, a spectrum matching procedure was applied to determine S_{DS} and S_{DI} . The ordinates of the original design spectrum derived using Eurocode 8 provisions were considered and the values of S_{DS} and S_{DI} were calculated to be equal to $0.8g$ and $0.7g$, respectively. The value of S_{DI} was amplified by $3/2=1.5$ to arrive at the value of S_I which is $1.05g$.

The comparisons of computed periods and estimated periods are given in

Figure 3.9. The related statistics are given in Table 3.3 alongside the statistics related to estimates using Equation (3.1). The comparisons indicate that the proposed expression is capable of accurately finding the fundamental period of EBFs designed by other research teams. It is worthwhile to mention that differences can arise due to the variations in the nature of the design specifications. For example the minimum design base shear approaches are different in Eurocodes when compared with US provisions.

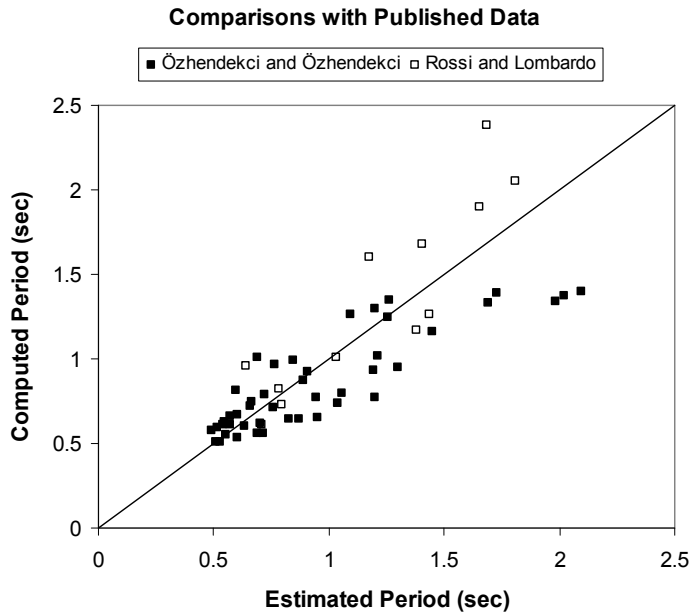


Figure 3.9 Comparison of computed and estimated periods for published data

3.5. DEVELOPMENT OF NEW PERIOD-HEIGHT RELATIONSHIPS AND THEIR VERIFICATION WITH APPARENT PERIODS

The proposed method to estimate calculated periods of EBFs can be extended to develop simple period-height relationships. To come up with simplified relationships the auxiliary term (Q) can be simplified as follows:

$$Q = \frac{h_s (2N + 1)^2}{N g} RD_R \approx \frac{4 h_n}{g} RD_R \quad (3.21)$$

The distribution of roof drift values for two different seismic hazard categories are given in Figure 3.10. For the high seismic regions, the RD_R values have a mean of 0.0017 and a standard deviation of 0.0005. For low and moderate to high seismic regions the RD_R values have a mean of 0.0012 and a standard deviation of 0.0002. These values indicate that majority of the roof drift ratios cluster around the mean value and adopting the mean value provides a convenient estimate. Using the mean values for the roof drift ratio and utilizing Equations (3.14) and (3.21) the following simplified relationships can be found:

$$T = \frac{0.024}{S_{D1}} h_n \quad T > \frac{0.156}{\sqrt{S_{DS}}} \sqrt{h_n} \quad \text{for } S_1 \geq 0.6g \quad T < \frac{0.22}{\sqrt{S_1}} \sqrt{h_n} \quad \text{for high seismic regions} \quad (3.22)$$

$$T = \frac{0.017}{S_{D1}} h_n \quad T > \frac{0.131}{\sqrt{S_{DS}}} \sqrt{h_n} \quad \text{for low and moderate to high seismic regions}$$

The accuracy of the proposed relationships was evaluated by making use of apparent periods of actual buildings. Unfortunately there are few structures that were monitored in the past and these belong to high seismic regions. The California Strong Motion Instrumentation Program (CSMIP) developed by the California Geological Survey (CGS) has instrumented 4 buildings in California that utilize EBFs as lateral load resisting systems. The measurements by CGS have been processed by Kwon and Kim (2010) to obtain apparent building periods. For each

building two apparent periods for any given earthquake excitation can be calculated depending on the direction of loading. In general, all 4 buildings utilize EBFs as a lateral load resisting system in both longitudinal and transverse directions. In this study the average of the apparent periods in two principal directions as reported by Kwon and Kim (2010) are considered. The properties of these 4 buildings are given in Table 3.4. The values of S_s and S_l were extracted using the 2002 version of the USGS maps. Based on the reported site geology it was assumed that all structures are located on Soil Class D. The S_{DS} and S_{DI} values were calculated based on this assumption and are given in Table 3.4. It is observed that the building ensemble consists of two hospitals and a school building. The importance factor for hospitals and school buildings were considered to be equal to 1.5 and 1.25, respectively. These importance factors were utilized to amplify S_l , S_{DS} , and S_{DI} values which are used in Equation (3.22). A comparison of the estimated periods from Equation (3.22) and apparent periods are given in Table 3.4. The comparisons reveal that the proposed relationship accurately represents the apparent periods of EBF buildings. However, more measurements are needed to verify the accuracy of the developed period-height relationship. Similarly measurements of structures located in low and moderate to high seismic regions are needed to verify the accuracy of the proposed formula for these regions.

Table 3.4 Properties of Instrumented EBF Buildings

Station	Instrumented Stations			
	03603	57594	58496	58593
Location	San Diego	San Jose	Berkeley	Stanford
Description	19 story commercial building	5 story hospital	2 story hospital	3 story school building
Latitude	32.7186	37.328	37.8548	37.7318
Longitude	-117.161	-121.938	-122.257	-122.172
Design Date	1980	1979	1984	1984
Height (m)	80.8	25.8	7.7	17.4
Site Geology	Very soft rock	Deep alluvium	Alluvium	Deep alluvium
S _s	1.572	1.5	1.927	1.929
S ₁	0.615	0.6	0.741	0.815
S _{DS}	1.048	1	1.285	1.286
S _{D1}	0.615	0.6	0.741	0.815
Apparent Period (sec)	2.69	0.59	0.34	0.58
Estimated Period (Eqn (3.22) (sec)	2.52	0.69	0.31	0.51
Apparent/ Estimated Period Ratio	1.07	0.86	1.09	1.13

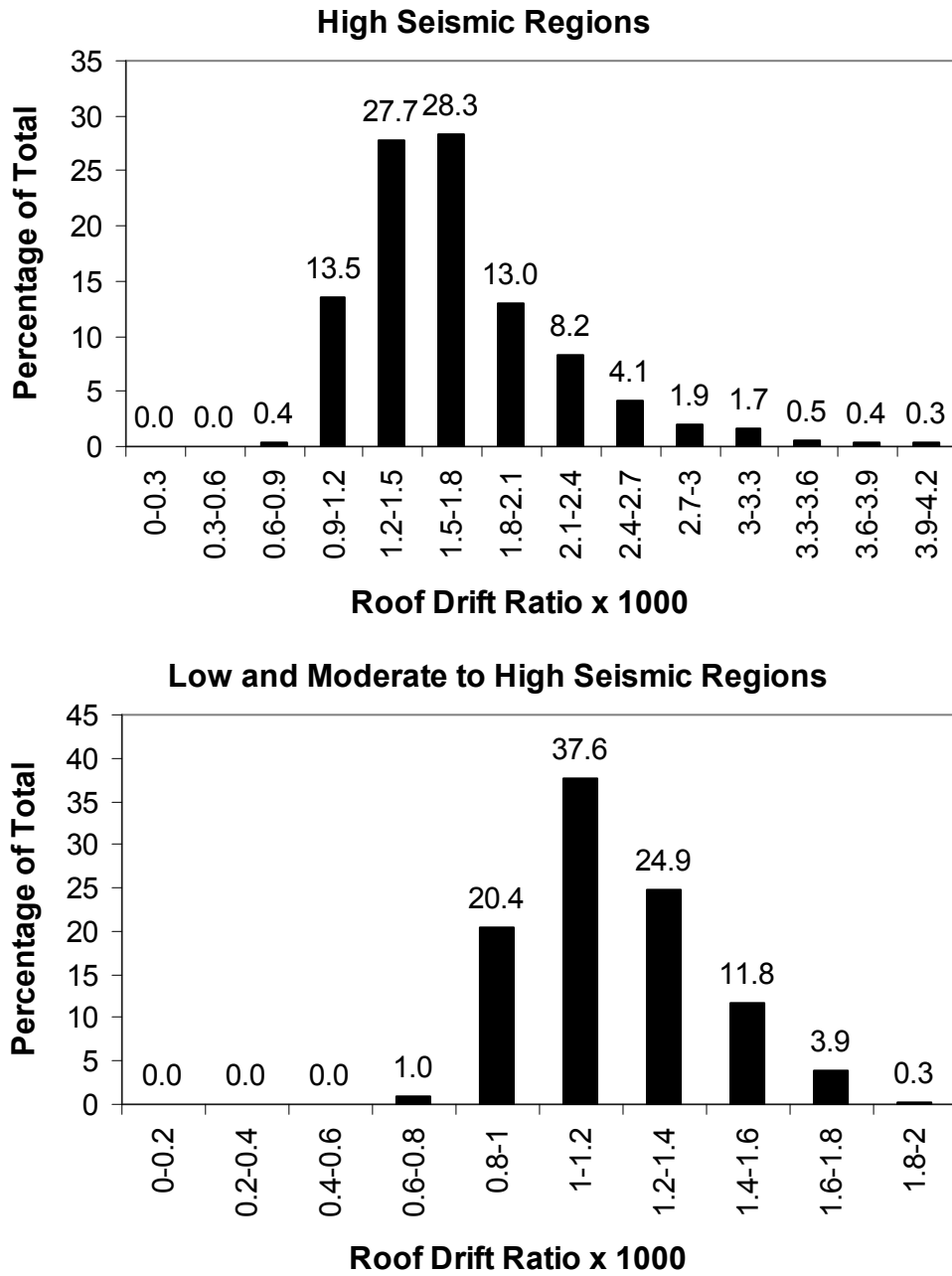


Figure 3.10 Histograms for roof drift ratio by proposed method in this thesis

CHAPTER 4

DESIGN OVERSTRENGTH OF STEEL ECCENTRICALLY BRACED FRAMES

4.1. BACKGROUND

The response modification factors are utilized to achieve economical designs for seismic resistance. The explicit formulation of these factors was proposed by Uang (1991). In this formulation a typical global structural response shown in Figure 4.1 is considered. According to Uang (1991) the following relationships hold:

$$\mu_s = \frac{\Delta_{\max}}{\Delta_y} \quad R_\mu = \frac{V_e}{V_y} \quad \Omega_o = \frac{V_y}{V_s} \quad R = \frac{V_e}{V_s} = R_\mu \Omega_o \quad C_d = \frac{\Delta_{\max}}{\Delta_s} = \mu_s \Omega_o \quad (4.1)$$

where, V_e = the ultimate elastic base shear, V_s = the base shear at the first significant yield, V_y = the base shear at the structural collapse level, Δ_s = the drift at the first significant yield, Δ_y = the drift at the structural collapse level, Δ_{\max} = the maximum amount of drift, μ_s = the ductility factor, Ω_o = the structural overstrength factor, R_μ = the ductility reduction factor, R = the response modification factor, and C_d = the displacement amplification factor.

A huge body of knowledge exists on the steel eccentrically braced frames (EBFs) that are used for seismic resistance. (Engelhardt and Popov, 1989; Roeder and

Popov, 1978; Hjelmstad and Popov, 1984; Ricles and Popov, 1994; Okazaki, 2005; Rossi and Lombardo, 2007; Özhendekci and Özhendekci, 2008; Koboevic and Redwood, 1997; Popov and Engelhardt, 1988; Hjelmstad and Lee, 1989; Ghobarah and Ramadan, 1991) While many experimental and analytical studies were conducted on EBF systems, the response modification (R), the overstrength (Ω_o), and the displacement amplification (C_d) factors presented in design specifications mostly depend on engineering judgment and on some observations during past earthquakes. The specification on Minimum Design Loads for Buildings and Other Structures (ASCE7-10, 2010) recommends a value of 8 for R , 2 for Ω_o , and 4 for C_d factors for steel eccentrically braced frames which are not a part of a dual system. This study has been conducted to evaluate, using analytical methods, the overstrength in these systems that arise during the design of EBF members.

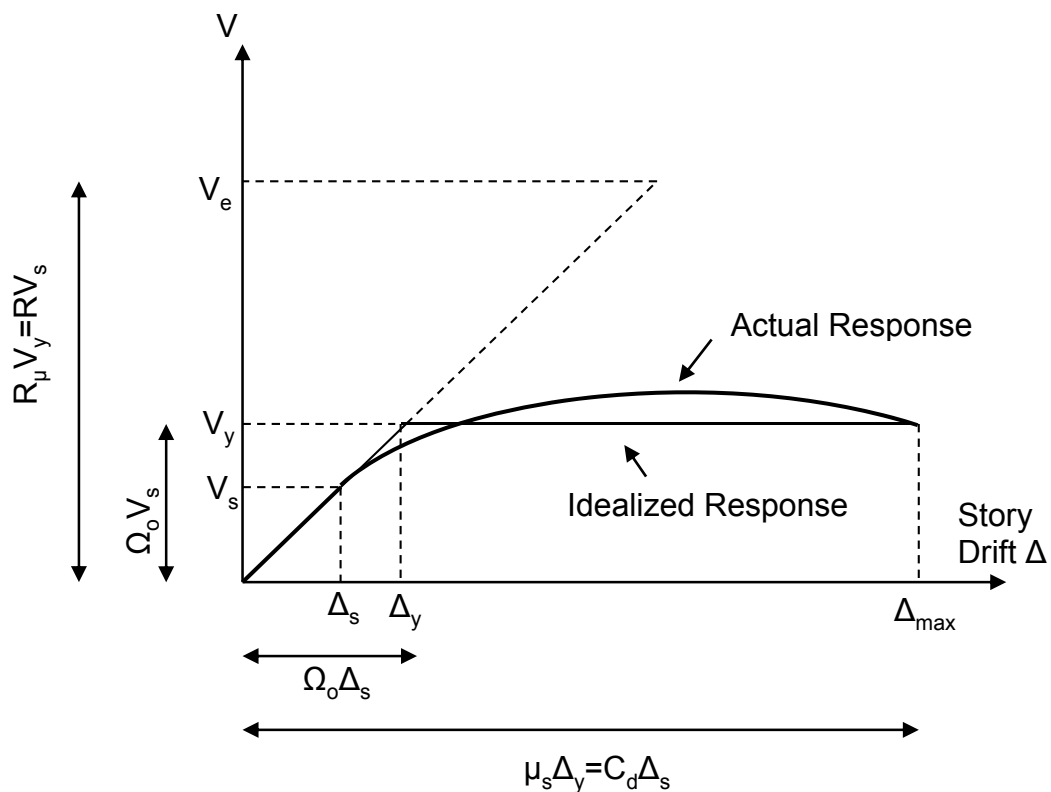


Figure 4.1 General structural response

As explained by Uang (1991) the overstrength of a structural system is influenced by many factors. The structural overstrength depends on internal force redistribution, presence of higher material strength, strain hardening, strain rate effects, deflection constraints on system performance, member oversize, minimum requirements, use of multiple load combinations, presence of nonstructural elements, variation of lateral load profiles and so on. In general the following relationship can be used to arrive at the structural overstrength:

$$\Omega_0 = \Omega_d \Omega_m \quad (4.2)$$

where Ω_d = structural overstrength that arises due to the design of members and redundancy of framing, Ω_m = structural overstrength that arises due to material behavior.

Equation (4.2) aims at grouping the sources of overstrength into two main categories.

The structural overstrength factor can be determined from analytical studies that employ time history analysis of typical EBF systems. This approach requires considering code compliant EBFs which are analyzed using time history records that are compatible with the design response spectrum. The material properties and hardening rules can be adjusted considering typical experimental results of link members. Before embarking on such an analytical study the general trends in overstrength due to the design of these systems must be known in advance. The stringent link rotation and lateral drift limits applicable to these systems result in design overstrength. The value of design overstrength is expected to be influenced by geometrical properties and seismic hazard level.

The present study aims at evaluating the design overstrength of typical EBF systems. A parametric study has been conducted to evaluate the dependency of design overstrength on the geometrical properties and the seismic hazard level. The details of the parametric study together with its results are presented herein. The designs are performed utilizing the computer program for which the details are presented in

preceding chapter. The program is capable of designing EBFs according to the US provisions and is based on the minimum frame weight principle.

4.2. A PARAMETRIC STUDY ON DESIGN OVERSTRENGTH OF EBFs

4.2.1. Details of Parametric Study

A parametric study was conducted to evaluate the design overstrength of EBFs. The primary aim of the parametric study is to understand the influence of geometrical properties and seismic hazard level on the design overstrength. For this purpose typical office buildings with a regular floor plan were designed. All buildings were assumed to have a floor plan shown in Figure 4.2. As shown in this figure the floor plan has 30 m side lengths resulting in a floor area of 900 m². In each principal direction, there are two exterior braced bays which result in a braced bay tributary area (total floor area divided by the number of braced bays) of 450 m². It was assumed that the gravity framing is attached to the braced bay by making use of simple connections. In other words the lateral loads were assumed to be carried by the eccentrically braced bays and the remaining beams and columns are used to carry gravity loads. All structures were assumed to be Risk Category 2 with an importance factor equal to unity. For all structures story dead and live loads were assumed to be 5 kN/m² and 2 kN/m², respectively. A redundancy factor of unity was considered in all designs.

In terms of the geometrical properties, the number of stories, link length to bay width ratio (e/L), and bay width (L) were considered as the prime variables. Number of stories varied from 3 to 15, link length to bay width ratio varied as 0.1, 0.15, 0.2, 0.25, and 0.3. Bay widths of 8m, 10m, 12m, 14m were considered. The story height

was constant for all stories and considered as 4 meters. Only one type of steel, A992, with a yield strength of 345 MPa was considered for all members of the steel framing. These variables resulted in 260 design cases.

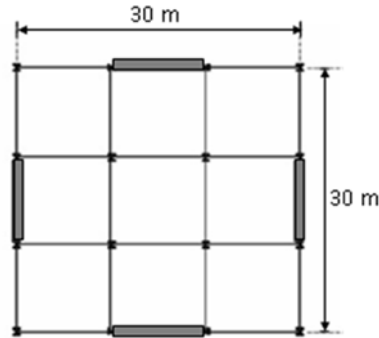


Figure 4.2 Floor plan used in parametric study

Different geographical locations and site classes were considered in order to take into account the seismic hazard. A total of 16 provinces in the United States with diverse seismic hazards were taken into consideration. The seismic hazard can be represented by two mapped acceleration parameters. These are S_s and S_l which are the 5 percent damped, risk adjusted maximum considered earthquake (MCE_R) spectral accelerations at a short period of 0.2 sec and at a period of 1 sec, respectively. EBF systems are more suitable for regions with high and moderate seismicity and less suitable for low seismic regions. Depending on their S_s and S_l values, 16 geographical locations which are detailed in Table 3.2 were considered in this study. These geographical locations represent high and moderate seismic regions. Four site classes named as A, B, C, and D according to ASCE7-10 (2010) were taken into account. A total of 16640 designs were conducted by considering the aforementioned parameters. For each EBF a design overstrength factor (Ω_d) was computed as follows:

$$\Omega_d = \frac{\sum_{i=1}^N V_n(i)}{\sum_{i=1}^N V(i)} \quad (4.3)$$

where, N = number of stories.

Equation (4.3) was derived based on the premise that the lateral load profile does not change during loading history and consequently the link shear, $V(i)$, which is calculated using the code based lateral load profile remains the same. The summation term in the denominator represents the total required shear strength of the links under code specified lateral forces. It was further assumed that a collapse mechanism forms when links at all stories reach to their nominal capacity, $V_n(i)$. Therefore, the term in the numerator represents the maximum amount of resistance provided by the links when all links form plastic hinges due to either bending or shear. It is worthwhile to mention that the design overstrength factor represents over-sizing of members to meet the link rotation angle limits and deflection constraints, and internal force redistribution. This factor does not represent the overstrength due to strain hardening of the links or higher material strength. The influence of these additional sources of overstrength will be discussed separately. It should also be mentioned that the nominal shear strength of the links is used in Equation (4.3) rather than the design shear strength. In other words, the resistance factor of Φ which is equal to 0.9 is not used in calculating $V_n(i)$.

The overstrength was calculated by making use of Equation (4.3) as it provides a simple and effective way of predicting the overstrength of an EBF. The free body diagram given in Figure 2.2 can be considered to derive Equation (4.3). By taking moments with respect to the pin support at the bottom it can be observed that the lateral forces are directly related to the sum of the shears that are developed at the links. This in turn means that any increase in the sum of link shears result in a similar increase in the lateral load carrying capacity. A similar approach is also adopted in the design of special truss moment frames (Goel and Itani, 1994). Inelastic static

(pushover) analyses were conducted to verify the accuracy of Equation (4.3). The EBFs exemplified in Table 2.1 through Table 2.4 was analyzed using pushover analysis to determine the level of overstrength. The frames were modeled using the FedeasLab program. The columns, beams outside of the links, and the braces were modeled using nonlinear beam column elements. The links were modeled using a special finite element developed by Saritas and Filippou (2009) for shear yielding metallic elements. The details for the verification studies of this numerical model will be presented in following chapter. All frames were subjected to the ASCE7-10 (2010) lateral load profile and the loading was increased until the load versus top story displacement response reaches to a plateau. The pushover curves for the four EBFs are given in Figure 4.3. The design base shear values are also indicated using dashed lines in this figure. The values of the link shear and nominal shear strength are given in Table 4.1 alongside with the design base shear and the maximum base shear attained during the pushover analysis. The results indicate that the overstrength values for frames S-9-800-7-90, S-9-800-7-120, I-9-450-8-150, and I-9-450-8-180 calculated according to Equation (4.3) are 1.58, 1.39, 2.87, and 2.84, respectively. The overstrength values for frames S-9-800-7-90, S-9-800-7-120, I-9-450-8-150, and I-9-450-8-180 obtained using pushover analysis are 1.45, 1.29, 2.68, and 2.57, respectively. Comparisons indicate that Equation (4.3) provides an accurate way of calculating the overstrength. The differences are generally less than 10 percent for the cases studied herein and are due to the differences between the code specified link shear capacities and the capacities calculated using the FedeasLab (2001) program. It is worthwhile to note that elastic perfectly plastic material response was utilized in these pushover analyses to eliminate the effect of strain hardening in links.

Table 4.1 Summary of Pushover Analysis Results

Story Nr.	S-9-800-7-90		S-9-800-7-120		I-9-450-8-150		I-9-450-8-180	
	V (kN)	V _n (kN)	V (kN)	V _n (kN)	V (kN)	V _n (kN)	V (kN)	V _n (kN)
1	495.9	610.1	495.9	610.1	244.1	549.9	244.1	535.4
2	490.8	610.1	490.8	610.1	241.6	549.9	241.6	535.4
3	477.1	610.1	477.1	610.1	234.8	549.9	234.8	535.4
4	452.7	610.1	452.7	610.1	222.8	549.9	222.8	535.4
5	415.8	610.1	415.8	489.5	204.7	549.9	204.7	535.4
6	365.1	610.1	365.1	414.0	179.7	549.9	179.7	535.4
7	299.2	610.1	299.2	414.0	147.3	549.9	147.3	535.4
8	217.1	551.2	217.1	540.7	106.8	463.2	106.8	451.3
9	117.7	444.4	117.7	342.5	57.9	385.7	57.9	451.3
Sum	3331.3	5266.4	3331.3	4640.8	1639.6	4697.9	1639.6	4650.6
Ω_d	1.58		1.39		2.87		2.84	
Pushover Analysis								
V _{design}	991.8		991.8		557.9		557.9	
V _{max}	1435.9		1282.1		1494.5		1435.6	
Ω	1.45		1.29		2.68		2.57	

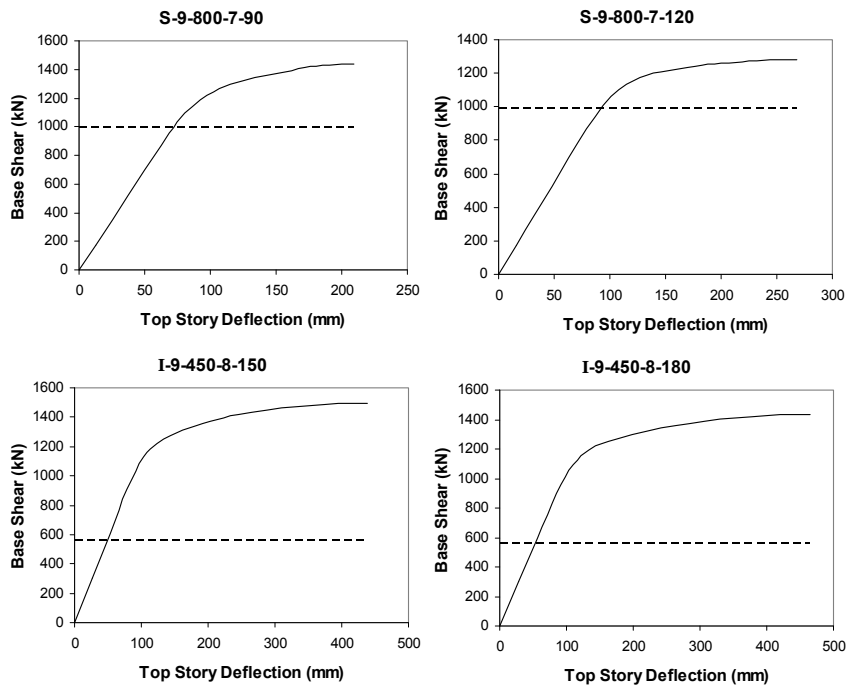


Figure 4.3 Pushover analysis of representative frames

4.2.2. Results of the Parametric Study

The values obtained for the design overstrength factor were first evaluated as a whole followed by a more detailed analysis on the influence of geometrical properties and seismic hazard level. The statistical analysis of the data is presented in Table 4.2 where the average, standard deviation, maximum and minimum values are reported. The overstrength values were grouped into bins to observe its variation and are plotted in Figure 4.4. The results indicate that the design overstrength (Ω_d) has an average of 2.36 for the EBFs considered in this study. This average value which does not include additional overstrength due to material behavior is well over the structural overstrength (Ω_o) value of 2.0 which is recommended by the ASCE7-10 (2010) specification. The standard deviation of the design overstrength reaches to 0.86 indicating a large scatter in data points. Figure 4.4 indicates that 16.7 percent and 26.1 percent of structures designed herein have design overstrength values that are between 1.0-1.5 and 1.5-2.0, respectively. This means that 57.2 percent of structures considered have a design overstrength greater than the codified value of 2.0 even without considering additional overstrength due to material behavior.

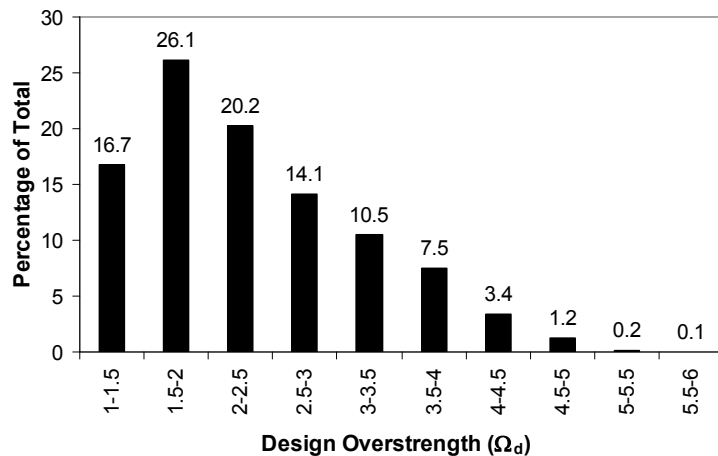


Figure 4.4 Variation of design overstrength for the entire data set

Table 4.2 Statistical Analysis of Design Overstrength Values

	Average	Standard Deviation	Maximum	Minimum
All data	2.36	0.86	6.01	1.16
e/L= 0.1	1.96	0.69	5.26	1.16
e/L=0.15	2.19	0.72	4.76	1.18
e/L= 0.2	2.47	0.92	6.01	1.20
e/L=0.25	2.58	0.89	5.66	1.22
e/L= 0.3	2.57	0.85	5.38	1.20
h _n = 12m	2.59	0.86	5.26	1.16
h _n = 16m	2.52	0.84	5.02	1.18
h _n = 20m	2.47	0.84	4.61	1.17
h _n = 24m	2.42	0.84	4.69	1.21
h _n = 28m	2.39	0.85	4.76	1.22
h _n = 32m	2.35	0.86	4.89	1.22
h _n = 36m	2.33	0.85	5.02	1.22
h _n = 40m	2.33	0.84	5.35	1.21
h _n = 44m	2.30	0.85	5.72	1.17
h _n = 48m	2.26	0.85	5.80	1.18
h _n = 52m	2.23	0.85	6.01	1.19
h _n = 56m	2.22	0.85	5.65	1.18
h _n = 60m	2.21	0.84	5.66	1.19
L = 8m	1.78	0.52	4.46	1.16
L = 10m	2.16	0.64	4.21	1.20
L = 12m	2.57	0.81	5.38	1.23
L = 14m	2.91	0.94	6.01	1.20
S _{D1} ≥ 0.4 g	2.43	0.84	5.07	1.16
0.3 g ≤ S _{D1} < 0.4 g	2.53	0.93	6.01	1.17
0.2 g ≤ S _{D1} < 0.3 g	2.17	0.78	4.76	1.17
0.1 g ≤ S _{D1} < 0.2 g	2.04	0.61	5.26	1.20

4.2.2.1. Influence of Link Length to Bay Width Ratio (e/L) on Design Overstrength

The link length to bay width ratio (e/L) is expected to influence the design overstrength values because behavior of EBFs is dependent on the e/L ratio. As the e/L ratio decreases the EBF behavior resembles behavior of concentrically braced frames (CBFs). On the contrary, as the e/L ratio increases the behavior resembles behavior of moment resisting frames (MRFs). The data points were separated according to the e/L ratio and the variation of design overstrength is given in Figure 4.5 for different e/L ratios. The relevant statistical measures are presented in Table 4.2. The percentage of designs with an overstrength less than 2.0 correspond to 63 percent, 46 percent, 40 percent, 33 percent, 33 percent of data for e/L ratios of 0.1, 0.15, 0.2, 0.25, and 0.3, respectively. The results indicate that EBFs with low e/L ratios tend to have smaller design overstrength values when compared with EBFs with high e/L ratios. This natural because as the e/L ratio increases the frame becomes more flexible and deflection and link rotation constraints on design become much more pronounced. The statistical measures indicate that the average design overstrength increases from 1.96 to 2.57 as the e/L ratio increases from 0.1 to 0.3.

4.2.2.2. Influence of Building Height (h_n) on Design Overstrength

The statistical measures for different building heights (h_n) are given in Table 4.2. These measures indicate that the design overstrength decreases as the height of the structure increases. The average design overstrengths for 12 meter and 60 meter tall structures were found to be equal to 2.59 and 2.21, respectively.

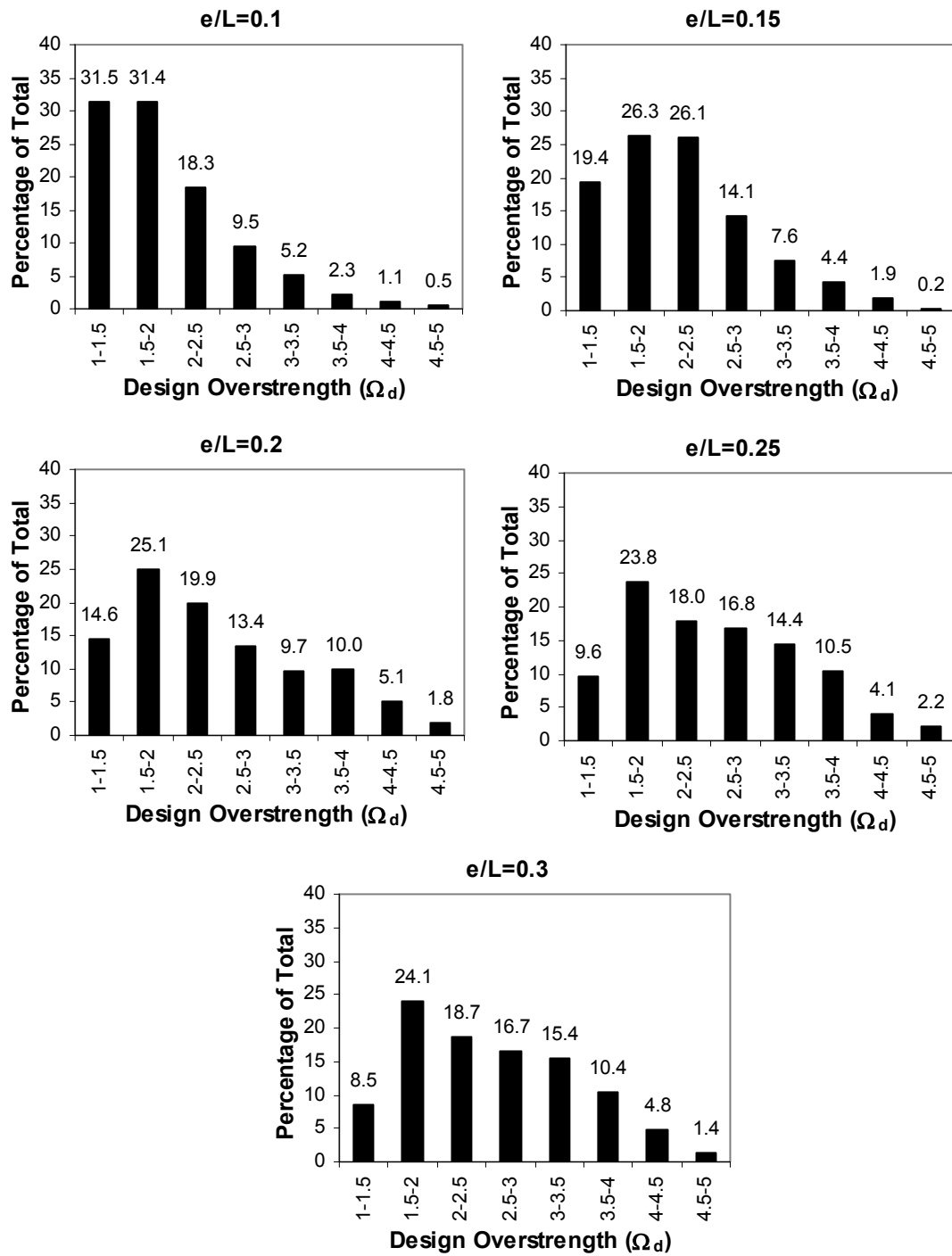


Figure 4.5 Variation of design overstrength for different link length and bay width ratios

4.2.2.3. Influence of Bay Width (L) on Design Overstrength

The data points were separated according to the bay width (L) and the variation of design overstrength is given in Figure 4.6 for different bay widths. The relevant statistical measures are presented in Table 4.2. The results indicate that the design overstrength is significantly influenced by the bay width. The average design overstrength increases from 1.78 to 2.91 as the bay width increases from 8 meters to 14 meters. The percentage of designs with an overstrength less than 2.0 correspond to 75 percent, 47 percent, 29 percent, 20 percent of data for bay widths of 8 m, 10 m, 12 m, and 14 m, respectively.

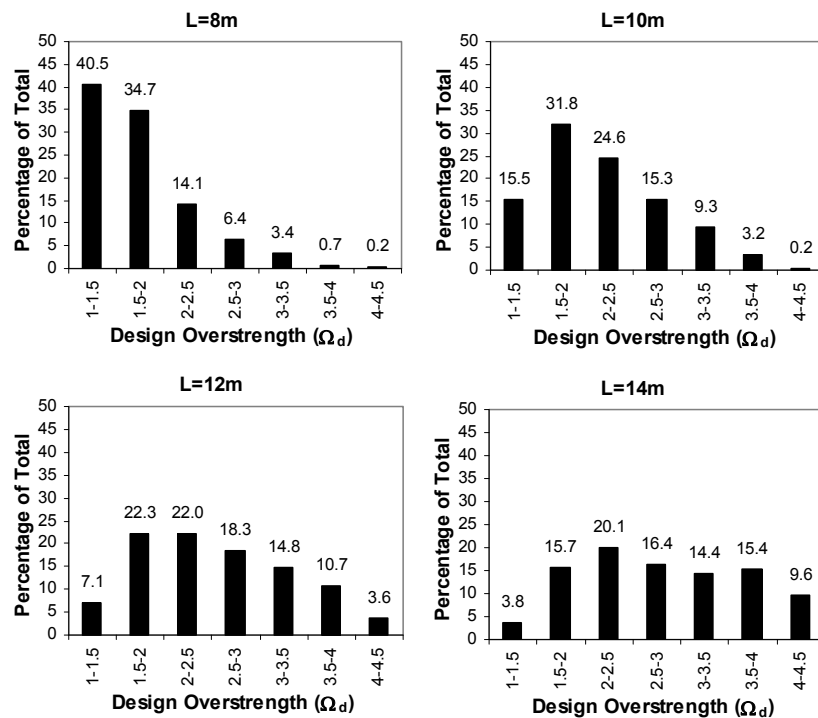


Figure 4.6 Variation of design overstrength for different bay widths

4.2.2.4. Influence of Seismic Hazard Level on Design Overstrength

The design spectral acceleration at 1 sec (S_{DI}) was considered as a parameter to quantify seismic hazard level. The data points were separated into bins according to the S_{DI} value. Variation of design overstrength for different S_{DI} values are given in Figure 4.7 and the statistical measures are presented in Table 4.2. The results indicate that the design overstrength decreases as the seismic hazard level decreases. The average design overstrength values are 2.43 and 2.04 for structures designed with $S_{DI} \geq 0.4g$ and $0.1g \leq S_{DI} < 0.2g$, respectively. While 38 percent of structures designed with $S_{DI} \geq 0.4g$ have a design overstrength less than 2.0, the same measure increases to 56 percent for structures designed with $0.1g \leq S_{DI} < 0.2g$.

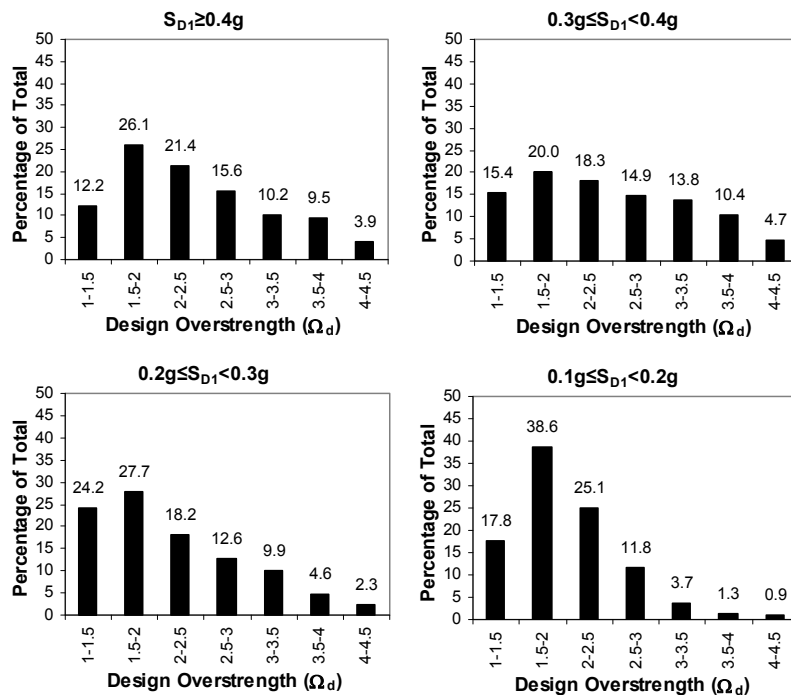


Figure 4.7 Variation of design overstrength for different seismic hazards

4.2.2.5. Evaluation of Structural Overstrength (Ω_o)

The results of the analytical study have been presented by considering the overstrength due to member selection process. As mentioned previously other sources of overstrength which are based on material properties also influence the structural overstrength (Ω_o). As shown in Equation (4.2) the design overstrength values (Ω_d) can be amplified by the overstrength that arises due to material behavior (Ω_m). There are two factors that need to be considered in deriving Ω_m . First of all actual material yield strength can be greater than the design yield strength. The difference is usually represented by the R_y factor as explained earlier in the text. The R_y factors depend on the grade of steel and usually decrease as the yield strength increases. According to AISC341-05 (2005) an R_y factor of 1.1 can be considered for A992 which accounts for an average increase of 10 percent in the yield strength beyond the design yield strength. The second source of overstrength arises due to strain hardening. When the links experience inelastic deformations significant amount of strain hardening occurs that increases the resistance produced by the link members. The amount of strain hardening is usually dependent on the type of the link. Strain hardening is more pronounced for short links that yield in shear compared to long links that yield in bending (Okazaki, 2005). In general the overstrength due to strain hardening is considered to be 25 percent of the actual strength in the AISC341-05 (2005) specification. Therefore, by combining the two sources, the overstrength due to material behavior (Ω_m) can be estimated as $1.1 \times 1.25 = 1.375$. This means that the design overstrength (Ω_d) values can be amplified by 1.375 to arrive at an estimate of the overall structural overstrength (Ω_o).

Using this procedure the average structural overstrength (Ω_o) is obtained as 3.25 for the structures considered herein. This value is well above the codified value of 2.0 indicating that EBFs in general exhibit high overstrength than assumed. The overstrength factor is used in the design of columns where amplified seismic forces are used for the design of these elements. Presence of higher overstrength may have

an adverse effect on the design of these elements because lower amount of axial force is considered in design when the current provisions are used. Considering, however, that capacity design principles are also used in the design of columns, it is anticipated that considering lower overstrength values does not results in significant errors in the design process.

The minimum structural overstrength is on the order of 1.6 for the structures considered herein. This value is lower than the codified value of 2.0 and indicates that some of the EBFs have larger ductility demands than assumed. According to the ASCE7-10 (2010) specification the ductility reduction factor (R_μ) is 4.0 for these systems when an overstrength value of 2.0 is considered. The ductility reduction factor (R_μ) increases to 5.0 (8/1.6) when the overstrength reduces to 1.6. Although low values of overstrength is attributed to many structural geometries, it is particularly pronounced for EBFs having narrow bay widths and low e/L ratios.

CHAPTER 5

DISPLACEMENT AMPLIFICATION FACTORS FOR STEEL ECCENTRICALLY BRACED FRAMES

5.1. BACKGROUND

In general, the link rotation angle (γ_p) is used to describe inelastic deformation of the link. By definition the link rotation angle is the plastic rotation angle between the link and the beam outside of the link as shown in Figure 3.3. Determining the link rotation angle at the design stage presents a variety of challenges. While this variable is adopted in AISC Seismic Provisions 341-02 (2002), 341-05 (2005), 341-10 (2010) and Eurocode 8 (2004), specifications are generally silent in guiding designers on how to determine the link rotation angle. The Commentary to the AISC Seismic Provisions AISC Seismic Provisions 341-02 (2002), 341-05 (2005), 341-10 (2010) has a conservative procedure to determine this quantity. The procedure estimates the link rotation angle by making use of a rigid-plastic deformation mechanism assumption. By adopting the deformation pattern shown in Figure 3.3, the link rotation angle (γ_p) can be expressed as a function of the plastic story drift angle (θ_p). For the commonest EBF configuration where the link is a horizontal framing member located between braces as shown in Figure 3.3, the relationship between these two quantities can be expressed as follows:

$$\gamma_p = \frac{L}{e} \theta_p \quad (5.1)$$

where L is the bay width.

The plastic story drift angle (θ_p) can be calculated by dividing the plastic story drift (Δ_p) by the story height (h_s). It is quite onerous to calculate the plastic story drift at the design stage. Historically two different approaches were recommended. Up until 2010, the Commentary to the AISC Seismic Provisions 341-02 (2002), 341-05 (2005) recommended that the plastic story drift can conservatively be taken equal to the design story drift. With the introduction of the 2010 version, the Commentary to the AISC Seismic Provisions (2010) recommends to calculate the plastic story drift as the difference between the design story drift and the elastic drift.

The seismic forces are reduced by a response modification factor (R) at the design stage while the elastic displacements are amplified by a displacement amplification factor (C_d) to calculate the design story drifts. In general, single degree of freedom models are utilized to derive relationships between the response modification factor and the displacement amplification factor (Newmark and Hall, 1982; Miranda and Bertero, 1994; Miranda, 2001; Miranda and Ruiz-Garcia, 2002).

According to the longstanding equal displacement rule developed by Newmark and Hall (1982), the displacement amplification factor can be considered equal to the response modification factor ($C_d = R$). In other words, the amount of displacement experienced by the inelastic system is equal to the amount of displacement experienced by the same system if it were to remain elastic. The values of R and C_d for a particular structural system are usually developed based on engineering judgment. In Eurocode 8 (2004), for all structural systems, the equal displacement rule is adopted where the displacement amplification factor is taken equal to the response modification factor (behavior factor). In ASCE7-10 (2010), however, the recommended C_d values are generally less than the recommended value for R . The

difference is more pronounced for EBFs where the recommended value of R is 8 and C_d is 4.

In general roof drifts are considered in selection of a C_d factor for a particular lateral load resisting system. When the displacement amplification factors for roof drifts are extended directly to story drifts, the underlying assumption is that inelastic deformation is distributed evenly among the stories. Numerical studies conducted in the past (Uang and Maarouf, 1994; Medina and Krawinkler, 2005) have shown that appropriate displacement amplification factors for predicting maximum story drifts are greater than those for predicting roof drifts due to the formation of weak stories.

The provisions for the link rotation angle are determined in relation to the displacement amplification factor. Depending on the normalized link length, the link rotation angle limit varies between 0.02 and 0.08 radians according to the AISC Seismic Provisions 341-02 (2002), 341-05 (2005), 341-10 (2010). The 1997 version of the Commentary to the AISC Specification (1997) makes it clear that the selection of 0.08 for shear yielding links and 0.02 for flexural yielding links is based on a C_d factor which results in design story drifts which are reasonable, though not necessarily maximum, estimates of the total building drift under the design earthquake. These limits were selected from test results to provide a modest reserve rotational capability to accommodate frame deformations beyond those corresponding to the C_d value. For example, the ASCE Standard on Seismic Rehabilitation of Existing Buildings ASCE41-06 (2007) recommends link rotation angle limits of 0.11 and 0.14 radians for shear yielding links evaluated under life safety and collapse prevention criteria, respectively.

Recent test results, however, have shown the great complexity of the link behavior. Experiments conducted by Okazaki et al. (2005) revealed that the link rotation capacity depends on the loading protocol. The shear links tested under the loading protocol given in the 2002 version of the AISC Specification (2002) failed to meet the 0.08 radian criterion. On the other hand, shear links tested under the loading

protocol given in 2005 version of the AISC Specification (2005) failed at link rotation angles between 0.11 and 0.12 radians.

Based on the above discussion it is clear that displacement amplification and link rotation angle provisions are interrelated. The limits on the link rotation angle can be determined more precisely if the link rotation angle can be estimated with more confidence. In a recent study, Richards and Thompson (2009) explored the accuracy of predicting EBF inelastic drifts and link rotations through amplification of elastic deformations. The study revealed that the current value of C_d is too low to accurately estimate drifts in low rise buildings. Link rotations are underestimated because the inelastic drifts are underestimated. Mid to high-rise EBFs were found to experience much lower story drifts and link rotations than predicted by amplified elastic analysis. Calibrated C_d factors were proposed but the researchers pointed out that the study is inadequate to recommend factors for general design.

A study has been undertaken to evaluate the recommendation given by ASCE7-10 (2010) for the displacement amplification factor and the recommended procedure in the Commentary to AISC Seismic Provisions (2005) to calculate link rotation angles. Pursuant to this goal, 72 EBFs were analyzed using time history analysis and link rotation angles and displacement amplifications were evaluated. As a part of this study recommendations were developed for calculating link rotation angles and displacement amplifications more accurately. The evaluations and recommendations are presented herein.

5.2. VERIFICATION OF NUMERICAL MODELS

The computational framework, FedeesLab, developed by Filippou (2001) was used for numerical analysis. A special finite element developed by Saritas and Filippou (2009) for metallic shear yielding elements is readily available in the FedeesLab

routines. Saritas and Filippou (2009) verified the accuracy of this finite element formulation by considering shear yielding links tested by three independent research teams (Hjelmstad and Popov, 1983; Kasai and Popov, 1986; McDaniel et al., 2003). Before embarking on the numerical studies, the accuracy of this element was verified considering experiments on intermediate and moment links as well as an experiment on a full scale EBF structure.

The component level verification study considered the work of Okazaki (2004) and Okazaki et al. (2006) as a benchmark. These researchers recently investigated link-to-column attachment details using a test setup shown in Figure 5.1. Among the twelve specimens tested three of them named as NAS, NAI, and NAM were considered herein. The normalized link lengths ($e/(M_p/V_p)$) for NAS, NAI, and NAM specimens are 1.1, 2.2, and 3.3, respectively indicating that the NAS specimen is a shear yielding link, NAI specimen is an intermediate link, and the NAM specimen is a moment yielding link. Comparison of experimental results and numerical simulations for these three specimens are given in Figure 5.2. The results indicate that the finite element developed by Saritas and Filippou (2009) is capable of accurately simulating behavior of short, intermediate, and moment links.

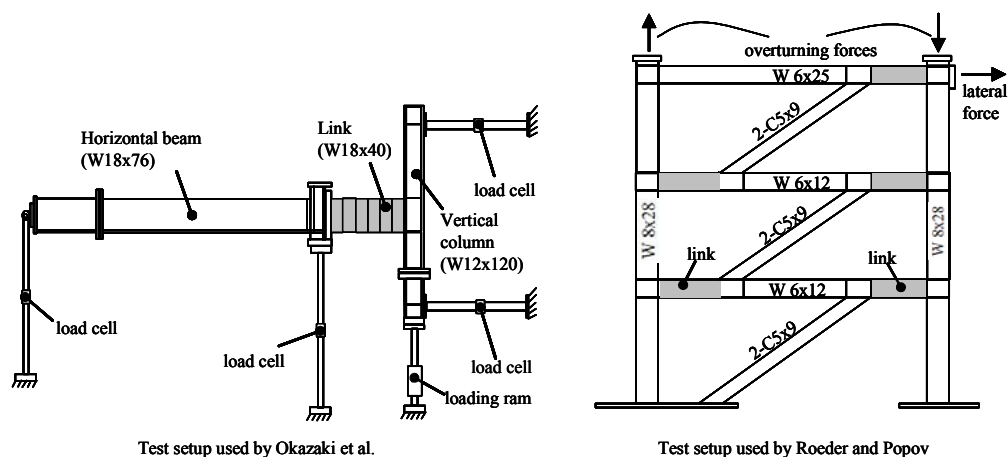


Figure 5.1 Test setups used in the studies of Okazaki et al. (2006) and Roeder & Popov (1978)

The structure level verification study considered one-third scale frame specimen (Frame 1 shown in Figure 5.1) tested by Roeder and Popov (1978) as a benchmark. In the experiment lateral loading was applied to the third story and deflections of all three stories were monitored. Comparisons of experimental and numerical simulations for Test Frame 1 are given in Figure 5.2 for all three stories. The results indicate that the general frame response can be captured by the numerical models.

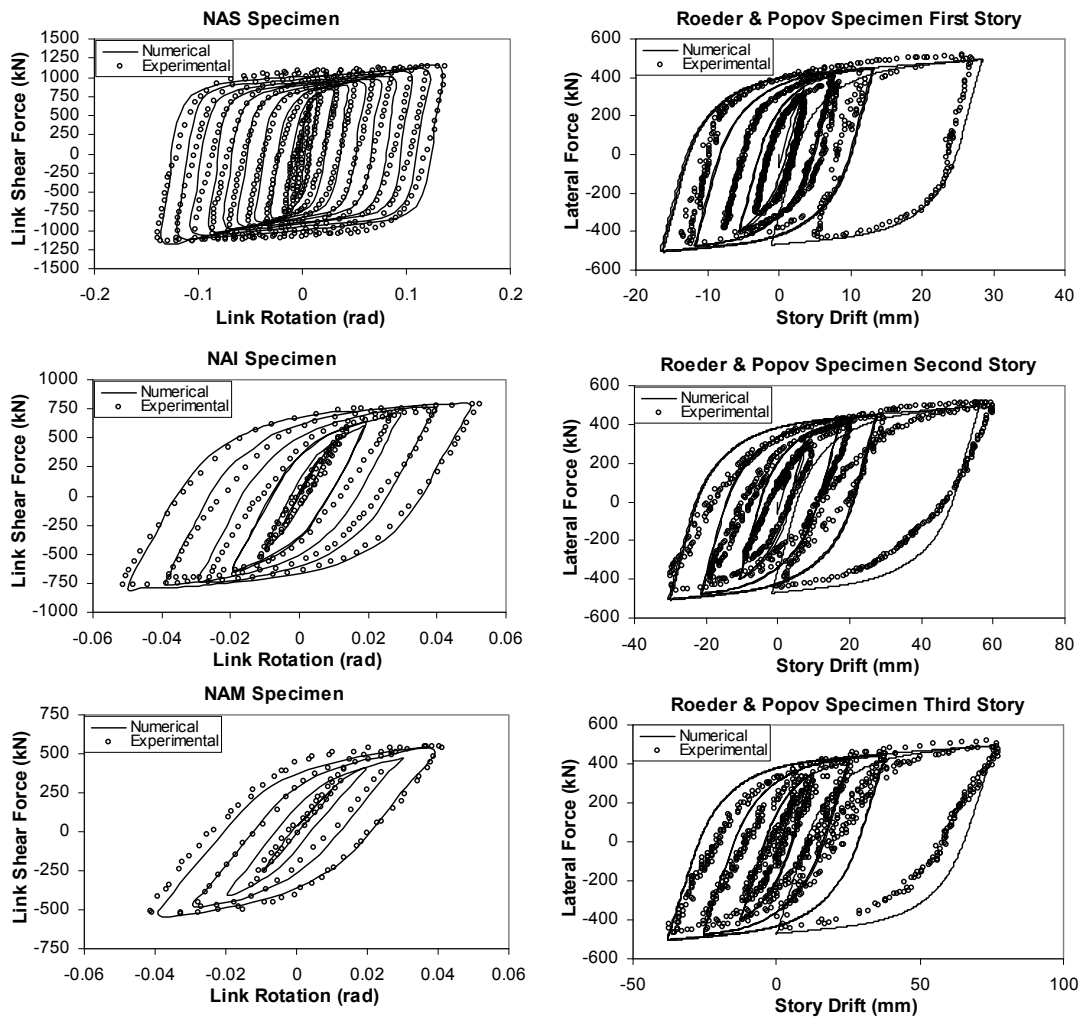


Figure 5.2 Comparison of numerical simulations with experimental results

5.3. A PARAMETRIC STUDY ON DISPLACEMENT FACTORS OF EBFs

5.3.1. Details of Parametric Study

The link length to bay width ratio (e/L), the bay width (L), the number of stories, and the seismic hazard level were considered as the prime variables. Typical three dimensional EBFs regular in plan and elevation were considered. Story height was kept constant at 4 m for all stories. All structures had a square floor plan with side dimensions of 30 m which is shown in Figure 4.2. The structural system consists of a gravity frame and EBFs used for resisting lateral loads. Two EBFs are provided at the perimeter frames in each principal loading direction resulting in a braced bay tributary area (floor plan area divided by the number of braced bays) of 450 m².

Three, 6, 9, and 12 story EBFs were considered. Link length to bay width ratios (e/L) of 0.1, 0.2, and 0.3 were taken into account. Braced bay widths (L) of 8 m, 11 m, and 14 m were considered. Two locations that represent high and moderate seismic regions were selected in order to take into account the seismic hazard level. The selection was based on the guidelines developed as a part of the SAC project (FEMA-355c, 2000; Somerville et al., 1997). The structures were considered to be located in Los Angeles (LA) and Seattle (SE) which represents high seismic and moderate seismic regions, respectively. Combination of all these variables resulted in a total of 72 EBFs. For all structures a story dead load intensity of 5 kN/m² and a live load intensity of 2 kN/m² were considered. Three main specifications namely, Minimum Design Loads for Buildings and Other Structures (ASCE7-10, 2010; Specification for Structural Steel Buildings, AISC 360, 2005 and Seismic Provisions for Structural Steel Buildings, AISC 341, 2005) were considered during the design of a typical EBF. The floor plan given in *Figure 4.2* considerably simplifies the design of the structure. It was sufficient to design one of the perimeter EBFs because

lateral and gravity loads are carried by different framings and the floor plan is symmetrical. Therefore, plane EBFs with various geometric properties were designed to study the behavior of lateral load resisting system. It was assumed that lateral-torsional buckling of beams outside of the links is prevented because these members act compositely with a concrete slab which satisfy continuous beam bracing provisions of AISC360 (2005).

The recommendations of the 2005 version of the Commentary to the AISC Seismic Provisions (2005) were followed for the calculation of link rotation angle. As mentioned before this version of AISC341 provides a conservative approach by taking the plastic story drift as the design story drift. In other words, the link rotation angles calculated by this procedure correspond to total link rotation angles (γ_{total}) rather than plastic link rotation angles (γ_p). It is customary to use such an approach as demonstrated by well-known design guides (AISC 327-05, 2005). The differences between the plastic link rotation angle and total link rotation angle depend on the link length and the flexibility of the members that the link frames in. In general, the differences are quite small for shear yielding links but can be large for flexural yielding links. The total link rotation angle is used throughout this study unless specified otherwise. In other words, both the design and the calculated values from time history analyses represent total link rotation angles.

It is worthwhile to note that the recommended procedure in 2010 version of the Commentary to the AISC Seismic Provisions (2010) was not utilized for the following reason. This procedure requires subtracting the elastic drift from the design story drift which in turn results in an effective C_d factor between 2.0 and 3.0 depending on the assumed value of overstrength. Preliminary analyses revealed that using a reduced C_d factor results in greater discrepancies between the calculated link rotation angles and the ones used in design. More detailed discussions on this issue will be presented in the following sections.

The design, 5 percent damped, spectral response acceleration parameters at short periods (S_{Ds}) were considered to be 1.07 and 0.71 for Los Angeles (LA) and Seattle

(SE), respectively. The design, 5 percent damped, spectral response acceleration parameters at a period of 1 sec (S_{DI}) were considered to be 0.68 and 0.39 for Los Angeles (LA) and Seattle (SE), respectively.

Designs were obtained by making use of the computer program that was developed as a part of this study and detailed in Chapter 2. Equivalent lateral force procedure was adopted for seismic design of framing. The response factors recommended in ASCE7-10 (2010) ($R = 8$ and $C_d = 4$) were directly used in design. Minimum frame weight principle was utilized to come up with optimized EBFs. American wide flange sections with a steel grade of A992 which has a yield strength of 345 MPa were considered in the design of all members. The selection of columns was restricted to W14 sections. It is worthwhile to mention that two different design base shear values were used for each EBF. According to ASCE7-10 (2010) the upper limit on the fundamental period was considered in calculating the design base shear which was used in strength design. For checking story drifts and link rotation angles, the fundamental period from eigenvalue analysis was directly used without considering an upper bound. The eigenvalue analysis results revealed that the fundamental period of EBFs differ between 0.46 sec and 2.33 sec for structures located in Los Angeles and between 0.58 sec and 3.33 sec for structures located in Seattle. A representative design for a 9 story structure with a bay width of 14 m and an e/L ratio of 0.1 which is located in Los Angeles is given in Table 5.1.

A suite of earthquake records for each location was selected to be used in time history analysis. The ground motion records used in the SAC Project (FEMA-355c, 2000; Somerville et al., 1997) was considered. The ground motions with a probability of exceedance of 10 percent in 50 years were used in order to be compatible with the design spectrum. Ten records were selected for each region. Particularly, ground motions designated as LA01, LA02, LA07, LA08, LA09, LA13, LA14, LA17, LA18, LA19 were selected for Los Angeles (FEMA-355c (2000)). Similarly, ground motions designated as SE03, SE04, SE05, SE06, SE08, SE09, SE10, SE12, SE13, SE14 were selected for Seattle (FEMA-355c (2000)).

Comparisons of the design response spectrum with the mean spectrum obtained using the selected earthquake records are given in Figure 5.3.

Table 5.1 Member sizes of the Example EBF

	Story	Ca=4 design	Ca=8 design	Ca variable (Eqn (5.2))	Proposed design (Method 1)	Proposed design (Method 2)
Link sections	1	W10X68	W27X129	W21X111	W14X74	W14X68
	2	W10X68	W27X129	W18X106	W14X68	W14X68
	3	W10X68	W27X129	W18X97	W14X68	W10X68
	4	W10X68	W27X129	W18X86	W14X68	W10X68
	5	W10X68	W24X146	W18X86	W10X68	W14X53
	6	W10X68	W24X146	W14X74	W14X53	W14X48
	7	W14X53	W27X114	W14X68	W14X48	W10X45
	8	W14X48	W24X131	W14X53	W14X48	W10X45
	9	W10X45	W24X131	W10X45	W16X40	W10X45
Brace sections	1	W12X96	W14X211	W14X159	W12X120	W12X106
	2	W12X96	W14X211	W14X159	W12X106	W12X106
	3	W12X96	W14X211	W14X145	W12X106	W12X96
	4	W12X96	W14X211	W14X132	W12X106	W12X96
	5	W12X96	W14X193	W14X132	W12X96	W12X106
	6	W12X96	W14X193	W12X120	W12X106	W12X96
	7	W12X106	W14X211	W12X106	W12X96	W18X86
	8	W12X96	W14X193	W12X106	W12X96	W18X86
	9	W18X86	W14X193	W18X86	W12X96	W18X86
Column sections	1	W14X176	W14X455	W14X257	W14X193	W14X176
	2	W14X145	W14X398	W14X211	W14X159	W14X145
	3	W14X132	W14X370	W14X176	W14X145	W14X132
	4	W14X132	W14X311	W14X145	W14X132	W14X132
	5	W14X132	W14X257	W14X132	W14X132	W14X132
	6	W14X132	W14X211	W14X132	W14X132	W14X82
	7	W14X68	W14X145	W14X68	W14X68	W14X68
	8	W14X53	W14X132	W14X53	W14X68	W14X48
	9	W14X38	W14X68	W14X38	W14X38	W14X38
Fundamental Period (s)		1.43	0.85	1.12	1.34	1.40
Total weight (kN)		419.2	914.2	539.5	436.2	403.4

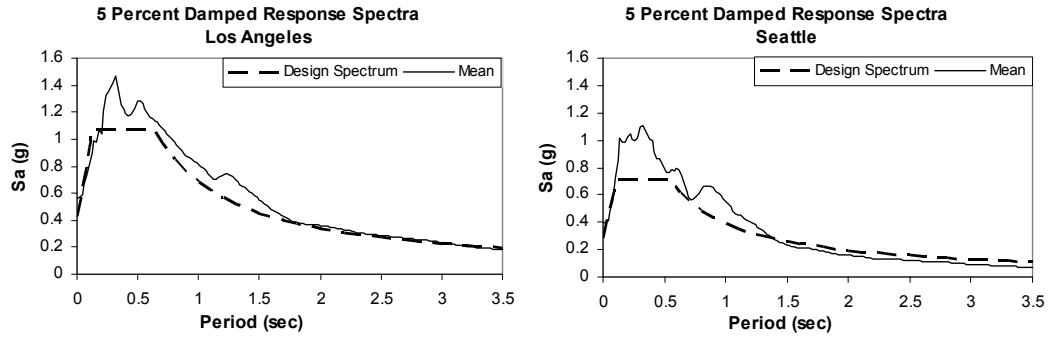


Figure 5.3 Comparison of response spectra

The EBFs were modeled and analyzed using the FedeeasLab computational framework. The links were modeled using the link element developed by Saritas and Filippou (2009) while the columns, the braces and the beam outside of the link were modeled using nonlinear beam elements. Lumped masses were placed at every story. Five percent mass and stiffness proportional Rayleigh damping was used in the analyses. The recommended values of damping vary between 2 to 15 percent for steel structures and they depend on the type of connections and the stress level (Chopra, 1995). The five percent value is selected to be consistent with the design spectrum adopted by the ASCE7-10 (2010) specification. It should be noted that the conclusions of this work is mainly based on inelastic time history analysis results which do not significantly depend on the damping ratio in the vicinity of five percent. Preliminary inelastic analysis of EBFs with two percent and five percent damping ratios indicate that the energy is dissipated mostly by yielding and the difference in lateral displacements between the two cases is negligible.

Elastic time history analyses (ETHA) and inelastic time history analyses (ITHA) were conducted for each ground motion record. A total of 1440 analyses were completed. The primary difference between two types of analysis is that the members are allowed to yield in the ITHA. The primary focus is on the results of the ITHA; however, the results of ETHA analyses are primarily used to assess the

equivalent lateral force procedure. In addition, these results are also used in the theoretical assessment of the displacement amplification factor.

5.3.2. Results of the Parametric Study

The results of the parametric study will be presented in this section. In general, averages of the response quantities, obtained from analyses under 10 ground motion records, were considered for each of the 72 structures. Emphasis was given to lateral displacements and link rotation angles. Representative plots of response quantities are given in Figure 5.4 for the 9 story structure with a bay width of 14 m, an e/L ratio of 0.1, located in Los Angeles and member sizes of which are given in Table 5.1.

The total link rotation angles are examined in Figure 5.4 (a). The results indicate that the calculated link rotation angles are larger than the design link rotation angles for the first three stories. The design link rotation angles for the first three stories are much less compared with the allowable link rotation angles. This is due to the fact that in tall EBF systems the bottom stories are over-designed to meet the link rotation angle limits at upper stories. Even though the links are over-designed and stiffened to have a link rotation angle capacity of 0.08 radians, the calculated link rotation angles in the first two stories exceed the allowable value. The maximum link rotation angle for the first story reached 0.111 radians. It is worthwhile to note that the calculated plastic link rotation angle is only 13.5 percent lower than the total link rotation angle for the first story. This particular structure was also analyzed under 20 ground motion records which have a probability of exceedance of 2 percent in 50 years. These ground motions correspond to the Maximum Considered Earthquake (MCE) for the Los Angeles area and produced as a part of the SAC Project (FEMA-355c, 2000; Somerville et al., 1997). The total link rotation angles under this ground motion set are much larger than the allowable rotations as shown

in Figure 5.4 (a). The maximum link rotation angle reached 0.213 radians which produces a demand much higher than many of the links can sustain.

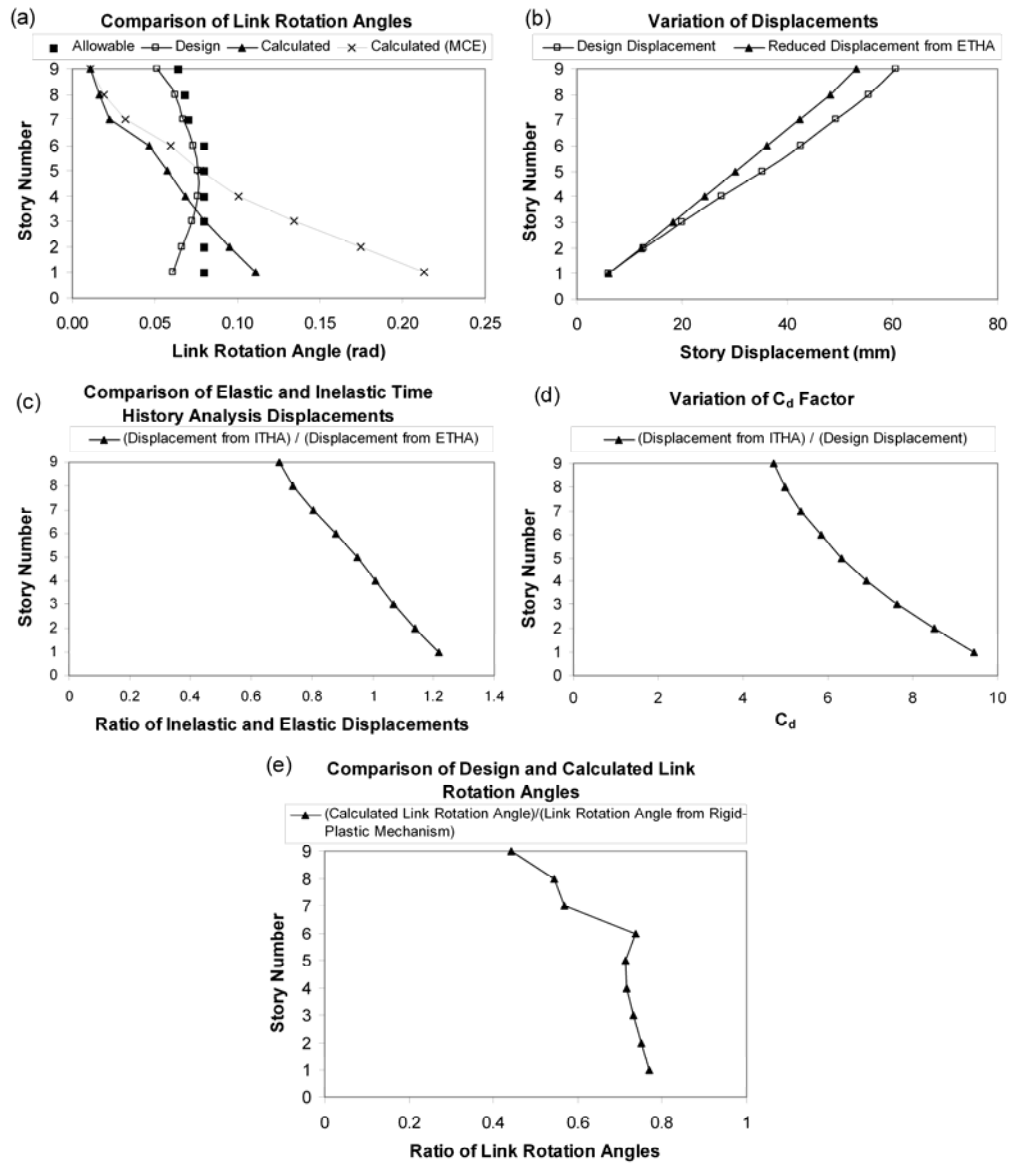


Figure 5.4 Response of a 9 story EBF

A comparison of displacements from ETHA and the design displacements is given in Figure 5.4 (b). A direct comparison of these quantities can only be possible if the elastic displacements are reduced by the calculated R factor. This means that all the story displacements must be divided by the ratio of the average of the maximum base shears computed under 10 ground motions to the design base shear. In the particular case studied here the design base shear was determined as 1290 kN per EBF. The average of the maximum base shears for 10 ground motions was 10043 kN resulting in a calculated R factor of 7.78 for this case. Therefore, the displacements found using elastic time history analysis were divided by 7.78 and compared with the design displacements. It can be observed that the lateral load profile adopted by the ASCE7-10 (2010) specification estimates the displacement of the bottom stories accurately. For top stories, however, it is observed that the reduced displacements from elastic time history analysis are lower than the design displacements indicating that the ASCE7-10 (2010) provides conservative estimates.

The relationship between elastic and inelastic displacements is examined in Figure 5.4 (c) to gain a better insight into the deformation pattern of EBFs. If the equal displacement rule holds then the ratio of displacements from ITHA to the displacements from ETHA should be unity. The results for the case shown in Figure 5.4 (c) indicate that ratios vary between 1.21 and 0.69 from the first to the top story.

The C_d factor is evaluated by making use of story displacements from inelastic time history analyses and the design story displacements in Figure 5.4 (d). By definition this factor is the ratio of the inelastic displacements to the design displacement. The C_d factors for this particular case are observed to vary along the height of the building ranging from 9.44 to 4.71.

The link rotation angle calculation procedure recommended in AISC Seismic Provisions AISC341 (2005) is evaluated by comparing the link rotation angles from inelastic time history analysis with the ones computed using this procedure by making use of lateral displacements obtained from inelastic time history analysis. According to Figure 5.4 (e) the ratios of these two quantities vary along the height

of the structure from 0.77 to 0.44. The ratios are generally less than unity indicating that the procedure given in AISC341 provides conservative estimates of the link rotation angle.

Variation of these response quantities and ratios were computed for all 72 structures. Later, the average of all cases was calculated for any given number of stories. The following sections present detailed evaluation of response parameters.

5.3.2.1. Evaluation of the Displacements from ETHA and ITHA, and Design Displacements

Relationships between displacements from ETHA and ITHA, and design displacements provide an insight into the EBF system behavior and help understand the underlying principles in development of the displacement amplification factor. The ratio of displacement from ITHA to displacement from ETHA should be equal to unity for equal displacement rule to hold. However, the results shown in Figure 5.5(a) indicate that displacements from ITHA exceed displacements from ETHA for the bottom stories. For these stories the ratios increase as the total number of stories increases. The maximum of the ratios reaches to 1.2 at the first story of 12 story EBFs. It is observed that the displacement ratios tend to attenuate at higher floors. The top story displacements from ITHA are between 76 to 80 percent of displacements from ETHA for 6, 9, and 12 story structures. The results clearly indicate the differences in EBF lateral deformations for elastic and inelastic systems.

As mentioned before, displacements from ETHA must be reduced by the calculated R factor to compare them with the design displacements. According to Figure 5.5(b), when reduced displacements from ETHA are compared with the design displacements it can be concluded that the lateral load profile recommended in ASCE7-10 (2010) results in conservative estimates. In other words the design

displacements are greater than the displacements obtained using ETHA. The differences are not pronounced for lower stories but significant differences can be observed at higher floors. The ratios of displacements tend to decrease along the height of the structure reaching to a constant value at the upper three stories. The ratio observed at the top story is dependent on the total number of stories. For example, the displacement ratios for 6 and 12 story EBFs are 0.87 and 0.68, respectively.

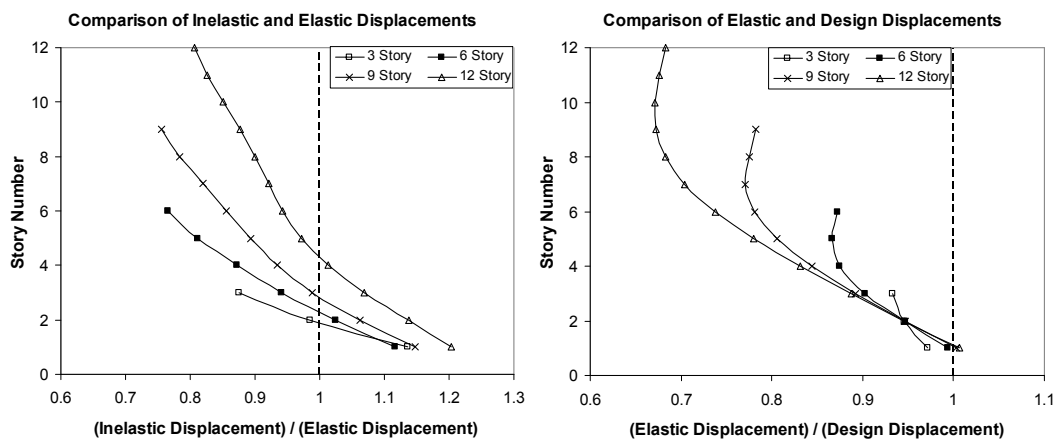


Figure 5.5 Evaluation of inelastic, elastic and design displacements

5.3.2.2. Evaluation of the Displacement Amplification Factor (C_d)

The displacement amplification factor (C_d) can be calculated by considering the ratio displacement from ITHA to the design displacement. The C_d factors are computed for all structures and averaged considering the total number of stories. The variation of C_d factors along the height is given in Figure 5.6(a). It is clear that the C_d factor is not a constant but tends to decrease along the height of a structure. The maximum values of C_d are observed at the bottom story reaching to average values of 9.34,

8.89, 8.45, and 8.40 for 3, 6, 9, and 12 story EBFs. In general, C_d value is expected to be less than or equal to the R factor. As shown in Figure 5.5(a), for the bottom stories, the displacement from ITHA can be 20 percent greater than the displacement from ETHA. This is the prime reason for having C_d factors that exceed the R value of 8.

The variation of C_d shows a similar trend for EBFs with different number of stories. The C_d factor reaches to an average value of 3.91 for 12 story systems which is close to the recommended value of 4.0. The reason for having a C_d value about half the value of the R factor can be attributed to the differences in displacements from ETHA and ITHA, and design displacements. As demonstrated earlier the displacements from ITHA are lower than the displacements from ETHA for upper stories resulting in conservatism. Similarly, the reduced displacements from ETHA are lower than the design displacements resulting in additional conservatism. When combined, these two factors produce C_d values that are much less than the R value for upper stories.

It is clear that the recommended value given in ASCE7-10 (2010) is unconservative for calculating lateral displacements of bottom stories. It is observed that $C_d = 4$ can be utilized to estimate the amount of inelastic displacements at the top story of tall EBFs. In cases where displacements at lower stories are considered, the $C_d = 4$ assumption provides significant underestimations of lateral displacements.

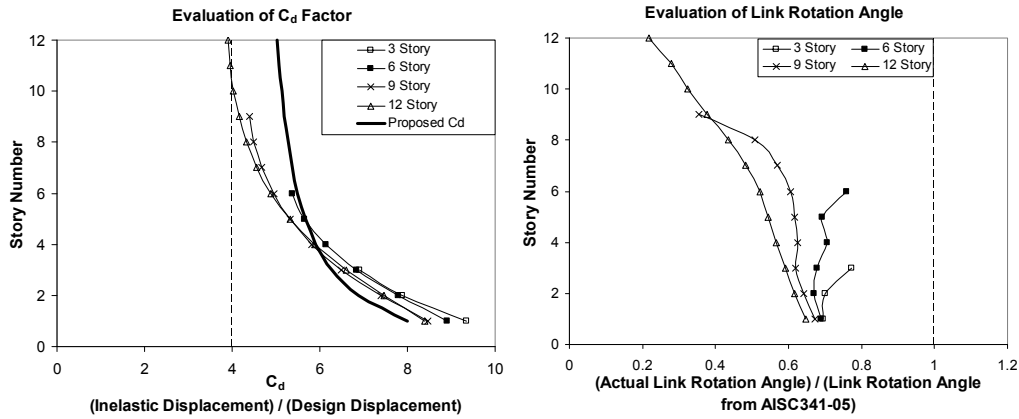


Figure 5.6 Evaluation of the C_d factor and link rotation angle calculation procedure

5.3.2.3. Evaluation of the Link Rotation Angle Calculation Procedure Given in AISC341 (2005)

The procedure given in AISC341 (2005) for calculating total link rotation angles is evaluated in Figure 5.6(b). The link rotation angles were estimated using Equation (5.1) where the lateral displacements were obtained from inelastic time history analysis. These link rotations that were derived using a rigid-plastic mechanism are compared with calculated link rotations observed in inelastic time history analysis. The ratio of the calculated link rotation angle to the one estimated using the AISC341 procedure is presented in Figure 5.6(b). It is evident that the procedure recommended in AISC341 (2005) is conservative. The ratios tend to cluster around 0.7 and vary between 0.77 and 0.21. These ratios indicate that the rigid plastic mechanism offers larger link rotation angles when compared with the calculated ones. As will be demonstrated in the following sections the differences are due to the deformations that take place in the columns, beams outside of the link and braces which are not taken into account by the rigid plastic mechanism.

5.3.2.4. Evaluation of the Link Rotation Angles

The calculated link rotation angles from inelastic time history analysis are compared with the design link rotation angles by taking ratios of these quantities. The EBFs were separated into 4 groups according to the total number of stories. Each group consists of 9 structures located Los Angeles and 9 structures located in Seattle. The results for these 18 structures were averaged and plotted along the height of the structure in Figure 5.7 using filled markers ($C_d = 4$ design). The results indicate that the average link rotation angles in the first two stories significantly exceed the design values. The maximums of the averaged ratios are 1.65, 1.55, 1.42, and 1.36 for 3, 6, 9, and 12 story EBFs, respectively. The ratios tend to attenuate at higher floors. For 12 story EBFs the averaged ratios can be as low as 0.2.

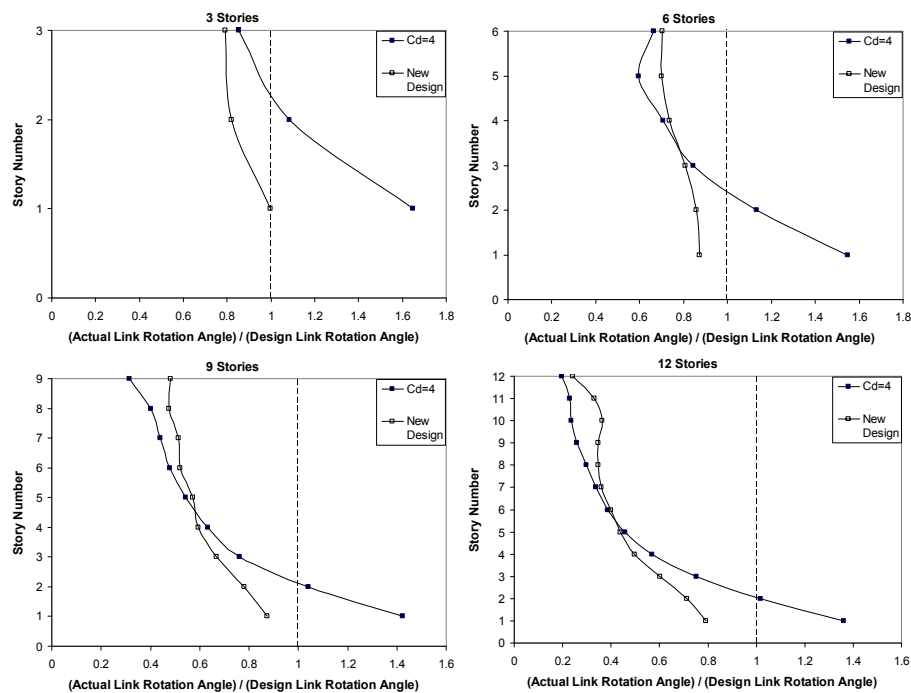


Figure 5.7 Ratio of actual and design link rotation angles

5.4. PROPOSED MODIFICATIONS

The evaluation phase results revealed that the recommended value of C_d in ASCE7-10 (2010) and the link rotation calculation procedure recommended in AISC341-05 (2005) can lead to designs where the link rotation angle can exceed its allowable value. As explained earlier, exceeding the allowable limit does not necessarily mean that the link is not going to function properly. The link rotation angle limits were selected to provide a margin of safety. This safety margin, however, can be exhausted due to the following reasons. The first reason is due to the differences between the calculated link rotation angle from time history analysis and the design link rotation angle. The second reason is due to higher seismic forces that can occur under MCE level ground motions. Due to these reasons it is worthwhile to match the design link rotation angles with the calculated ones.

The differences between the allowable link rotation and the calculated link rotation are more pronounced for low rise EBFs. For high rise EBFs the bottom story links are over-designed to meet the link rotation angle and in turn the drift limits at upper stories. It has long been recognized that links in the first floor usually undergo the largest inelastic deformation (Popov et al., 1989). Therefore, a conservative design for the links in the first two or three floors is recommended by the Commentary to the AISC Seismic Provisions 341-02 (2002), 341-05 (2005), 341-10 (2010) which can be fulfilled by increasing the minimum available shear strength of these links on the order of 10 percent. It is worthwhile to note that the links in the first few stories were indirectly over-designed in the present study in order to satisfy stringent link rotation limits. For example the links in the first four stories of the case exemplified in Table 5.1 had a design over-strength that ranged between 1.50 and 1.64. Although the recommendations of the Commentary have been fulfilled the link rotation angles still exceed the allowable values.

Two modifications to the existing design procedures are developed herein. The first one is a modification of the C_d factor and the second one is a modification of the link rotation angle calculation procedure.

5.4.1. Modification of the C_d Factor

The results shown in Figure 5.6(a) indicate that the displacement amplification factor (C_d) reach to its recommended value of 4.0 at upper stories of 12 story EBFs. For lower stories the C_d value is significantly higher. In general, a constant value is adopted for the displacement amplification factor in the well known design specifications (Eurocode, 2004; ASCE 7-10, 2010). An upper bound for the C_d factor can be taken equal to the displacement amplification factor (R). The results in Figure 5.6(a) reveal that the C_d value can actually exceed the R value of 8 by 16 percent for 3 story EBFs. While C_d factors that are greater than the R factor are observed, it will not be practical to choose a C_d factor greater than 8. The C_d factor can be selected equal to R and this modification may as well be sufficient to solve majority of the issues related with the displacements and link rotation angles. Because the link rotation angles play an important role in the design of EBF systems, changes in the C_d factor significantly influences the design. When tall EBFs are considered, an increase of C_d from 4 to 8 means that the displacements of the upper stories must be reduced to half of its original value to be able to meet the stringent link rotation limits. This in turn means that the entire EBF system must be stiffened to reduce the amount of deflections. An example for the case of a 9 story structure with a bay width of 14 m and an e/L ratio of 0.1 which is located in Los Angeles and designed according to $C_d = 8$ is given in Table 5.1. It is evident that the member sizes of the seismic lateral load resisting system increases significantly. The weight of the framing which is a direct measure of its cost increases from 419.2 kN to 914.2 kN resulting in an increase of 118 percent. All the 72 structures were redesigned using

the $C_d = 8$ assumption. The results indicate that the increase in weights is between 15 to 224 percent with an average of 70 percent.

The costly outcome of using a design with a constant value of C_d motivated the need to derive a relationship that takes into account the variation of the C_d factor along the height of the structure. After having several trials, it was decided to vary the C_d factor between 8 and 5. The following equation which is plotted in Figure 5.6(a) was developed to represent the C_d factor along the height of an EBF:

$$C_{di} = 9.0 - 4.5 \exp\left(\frac{\ln\left(\frac{1}{4.5}\right)}{i}\right) \quad (5.2)$$

where C_{di} is the C_d factor at the i^{th} story, and i is the story number.

The member sizes for the example case studied are given in Table 5.1 for a design based on Equation (5.2). The weight of the framing increases from 419.2 kN to 539.5 kN resulting in an increase of 28 percent which is much less than the increase when $C_d = 8$ is utilized. When all 72 structures were redesigned using the C_d expression given in Equation (5.2), the increase in weights was between zero to 103 percent with an average of 30 percent.

5.4.2. Modifications for the Procedure for Link Rotation Angle Calculation

The primary differences between the calculated and design link rotation angles are due to the neglect of elastic deformations in the rigid plastic mechanism. When an EBF is subjected to lateral forces, lateral displacements occur due to the deformations of its members. It is not only the link but the braces, the beams outside of the link and the columns that undergo elastic deformations under seismic events.

The contribution to lateral displacements caused by the link and other members strictly depend on the level of lateral force. At low lateral force levels, prior to yielding of the links, the deformations of other members contribute to lateral displacements. This observation is demonstrated on the example EBF details of which are given in Table 5.1 ($C_d = 4$ design). The amount elastic lateral displacements under design forces are given in Figure 5.8. In this figure the total displacements obtained under different assumptions are provided. It is evident that when the links are assumed to be rigid the amounts of lateral displacements are almost the same as the ones assuming that the links are flexible. On the other hand, when the columns, or the braces, or the beams are assumed rigid then the displacements significantly reduce, indicating that majority of the elastic displacements is due to the deformation of other members.

When the link yields, however, majority of the lateral displacements are caused by the deformation of the link. It is evident from this discussion that accurate determination of link deformations requires to calculate the lateral displacements caused by the link alone. In other words, the amount of lateral displacements caused by the deformation of other members must be subtracted from the total displacements. A similar approach is recommended in the Commentary to the Canadian Steel Design Standard CAN/CSA S16-01 (2005). It has been recognized that the axial deformation of columns due to overturning effect contributes significantly to interstory drifts in upper stories but does not affect the link rotations. For this reason it is recommended that the overturning effect be eliminated by making the columns axially rigid in elastic analysis. This method does not address the deformations that take place in the beams outside of the link and also the braces. In addition, it increases the design effort by requiring two structural models; one used for strength checks and the other one used for link rotation angle checks. Similarly, Richards and Thompson (2009) proposed to use only the shear component of frame deformations in arriving at the design link rotation angles.

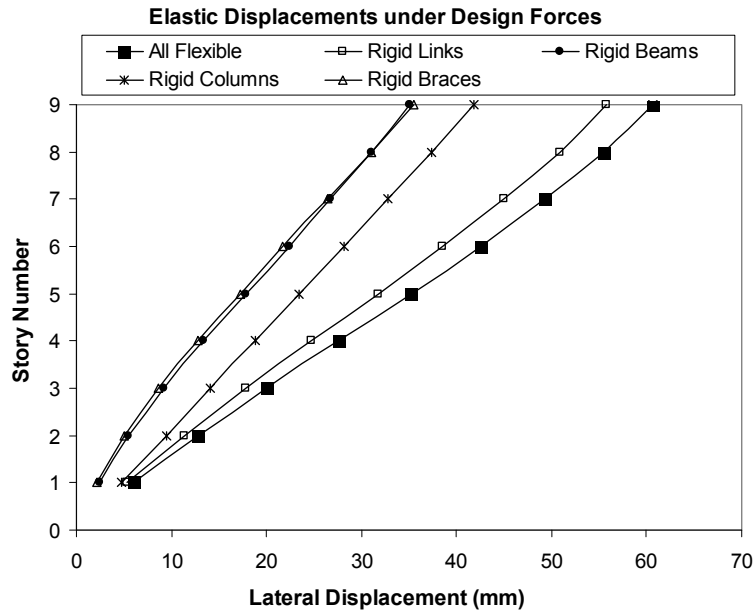


Figure 5.8 Elastic displacements of example EBF using various assumptions

Two methods were developed to modify the rigid plastic mechanism in order to estimate the link rotation angle more accurately. The first method can be used to find out the total link rotation angle while the second method can be utilized to come up with plastic link rotation angle.

The first method is based on subtracting the lateral displacements caused by the deformation of the braces, the beams outside of the link and the columns from the total lateral displacements. Lateral displacements caused by the deformation of the components of an EBF have been studied by Richards (2010). Similar type of analysis was utilized here to arrive at the contributions of each element to the lateral displacements. A proposed form of the modified total link rotation angle (γ_m) is expressed as follows:

$$\gamma_m = \gamma_{total} - \gamma_{da} - \gamma_{dbb} - \gamma_c \quad (5.3)$$

where γ_{total} is the total link rotation angle in unmodified form under the rigid plastic mechanism assumption as explained before, γ_{da} is the link rotation angle caused by lateral displacements which are due to the elastic axial deformations of the braces, γ_{dbs} is the link rotation angle caused by lateral displacements which are due to the flexural deformations of the beams outside of the link and braces, γ_c is the link rotation angle caused by vertical displacements which are due to the elastic axial deformations of the columns.

For any given story (Figure 5.9), the rigid plastic mechanism (Figure 5.1) is first used together with the total displacements and the C_{di} factor and the unmodified form of the total link rotation angle can be calculated as follows:

$$\gamma_{total} = \frac{C_{di} \Delta}{h_s} \frac{L}{e} \quad (5.4)$$

where Δ is the interstory displacement at the story under consideration.

The first modification is due to axial shortening and elongation of brace members (Figure 5.9). The link rotation angle which is caused by the lateral displacements due to the axial deformation of the brace members at the story under consideration can be expressed as follows:

$$\gamma_{da} = \Omega_o \left(\frac{L_{brace}^2}{L_{beam} h_s} \right) \left(\frac{P_d}{EA_d} \right) \frac{L}{e} \quad (5.5)$$

where P_d is the axial force on the brace, E is the elastic modulus of steel brace member, and A_d is the area of the brace member, L_{beam} is the length of the beam outside of the link (Figure 5.9), L_{brace} is the length of the brace (Figure 5.9).

It is worthwhile to mention that the P_d value is always taken positive and in cases where the axial forces in two braces differ, averaging of the two values is recommended.

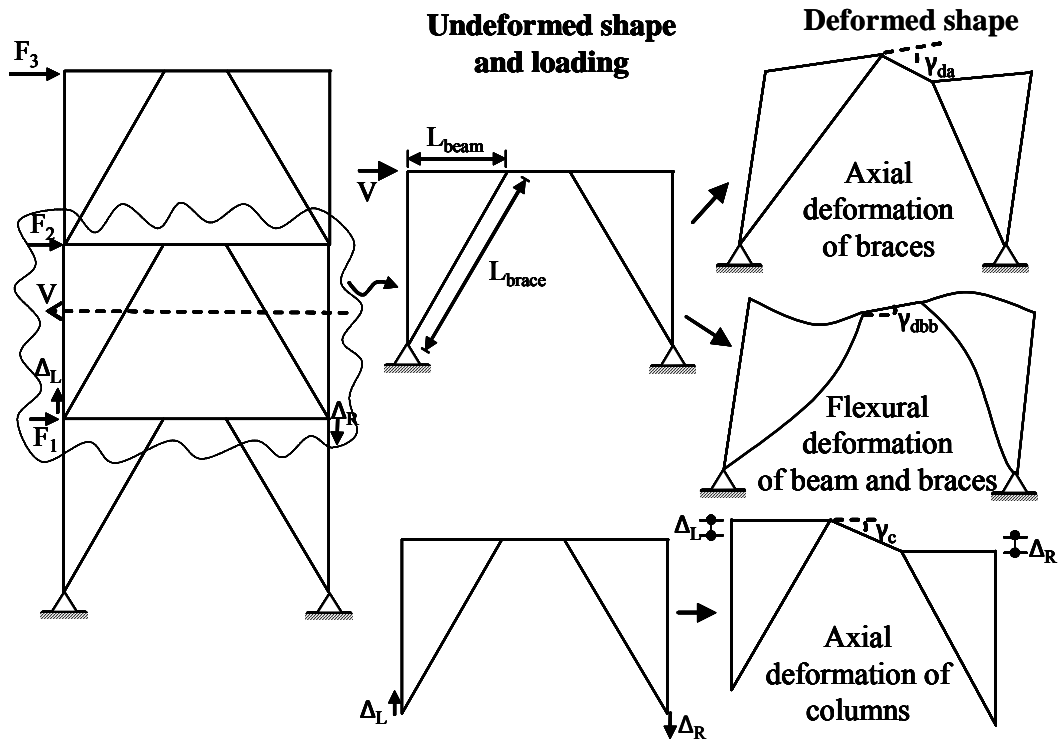


Figure 5.9 Deformation of EBF components

The second modification is due to flexural deformations of the beam outside of the link and the braces. The link rotation angle which is caused by the lateral displacements due to the flexural deformation of the beam outside of the link and braces at the story under consideration can be expressed as follows:

$$\gamma_{dbb} = \Omega_o \frac{V h_s e}{6 E L} \left(\frac{1}{\frac{I_{beam}}{L_{beam}} + \frac{I_{brace}}{L_{brace}}} \right) \quad (5.6)$$

where V is the design shear force at the story under consideration, I_{beam} is the moment of inertia of the beam outside of the link in the plane of the EBF, I_{brace} is the moment of inertia of the beam outside of the link in the plane of the EBF.

The third modification is due to the axial deformations of the columns. A similar modification has been proposed by Özhendekci and Özhendekci (2008) earlier. As shown in Figure 5.9, if the columns below the story under consideration shortens or elongates then the assumption of a supported base in rigid plastic mechanism is violated. When the bottom joints of the columns at any story displace vertically this will result in link rotation angles that must be subtracted from the link rotation angle obtained using a rigid plastic mechanism. According to the deformation pattern shown in Figure 5.9, the contribution of column axial deformations to the link rotation angle can be represented as follows:

$$\gamma_c = \Omega_o \left(\frac{|\Delta_L - \Delta_R|}{e} \right) \quad (5.7)$$

where Δ_L and Δ_R are the vertical deflections of the bottom joints of the left and right column, respectively. Note that the absolute value of the difference in deflections is used in the calculations. While an absolute value is used it is important to distinguish between upward and downward deflections by assigning a set of consistent sign convention. For example positive for upward displacements and negative for downward displacements or vice versa.

It should be recognized that modified link rotations angles are based on subtracting the components due to elastic deformations of members other than the links. Considering the deformations of these members at design level lateral load will result in an underestimation of the level of deformations. As shown in Figure 4.1, a typical EBF will have a reserve strength beyond the first significant yield point. In fact the amount of base shear resistance can increase significantly beyond the design base shear. During a seismic event the members other than the links should remain elastic according to the current design philosophy of AISC 341-02 (2002), 341-05 (2005), 341-10 (2010). This in turn means that these members should also be in the elastic range under the amplified seismic forces. Therefore, the results from an elastic analysis under design forces can easily be amplified to estimate the response

at the structural collapse level (Figure 4.1). The recommended overstrength factor (Ω_o) for EBF systems is equal 2.0 according to ASCE7-10 (2010). The recommended value has been adopted in this study and the displacements and link rotation angles are amplified by this factor as demonstrated in Equations (5.5), (5.6), (5.7)

A verification of the proposed modifications was studied through the example EBF given in Table 5.1 ($C_d=4$ design). The results of inelastic static analysis (pushover analysis) and inelastic time history analysis are given in Figure 5.10(a) and Figure 5.10(b), respectively. In the inelastic static analysis, the EBF was subjected to lateral forces that take the pattern of loading recommended by the ASCE7-10 (2010) specification. The loads were increased until the top story displacement is equal to the average top story displacement obtained using inelastic time history analysis. The displacements of the two analysis were kept close to be able to make a fair comparisons between the results presented in Figure 5.10(a) and Figure 5.10(b). The calculated link rotation angles are shown in filled square markers in Figure 5.10(a). In addition, the link rotations were calculated using the procedure given in AISC341 (2005) by making use of lateral displacements. Similar to what has been demonstrated before the results show that the AISC341 procedure provides overestimates of the link rotations. These link rotation angles were updated by making use of the proposed modifications. Two cases were considered. In the first case the calculated story shears, brace forces and vertical displacements from inelastic static analysis were used and in the second case the elastic analysis results were utilized together with an overstrength factor (Ω_o) of 2.0. The results obtained using displacements and forces from inelastic static analysis are shown in unfilled triangular markers in Figure 5.10(a) and are very close to the calculated link rotations. Similarly, using the proposed modifications (Equations (5.5), (5.6), (5.7) directly by considering an overstrength of 2.0 results in accurate estimates.

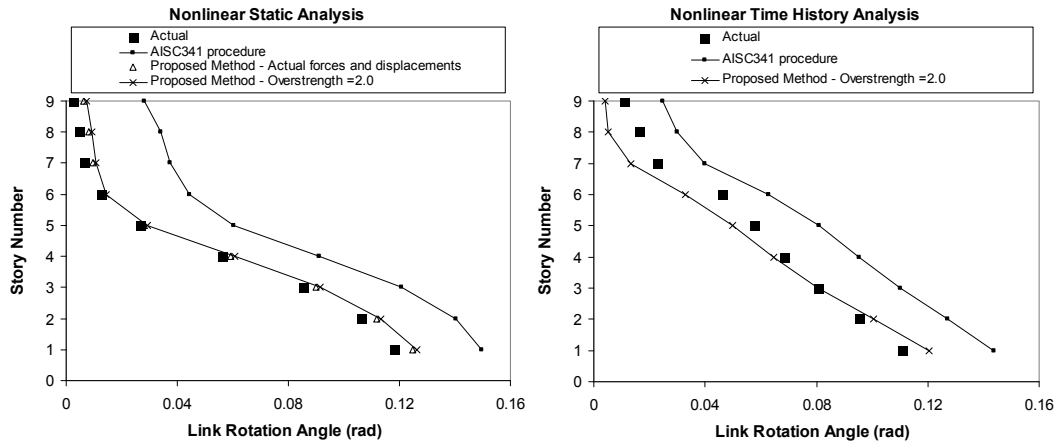


Figure 5.10 Verification of proposed modifications for the example EBF

The inelastic time history analysis also reveals the same conclusions. The procedure offered by AISC341 (2005) provides conservative estimates and the proposed method provides more accurate estimates. The differences between the calculated link rotations and the ones from the proposed method are more pronounced for inelastic time history analysis. This is due to the change in the pattern of inertia forces during the seismic event. While the nonlinear static pushover analysis only adopts a single loading pattern, the nonlinear time history analysis reflects the change in lateral load pattern.

The proposed method was used to redesign the example EBF. The member sizes for this redesigned frame are given in Table 5.1. It should be noted that when the proposed modifications to link rotation angle calculation are applied together with the proposed C_d factor (Equation (5.2)) the weight of the frame changed from 419.2 kN to 436.2 kN resulting in an overall increase of 4 percent. All 72 frames were redesigned and the results indicate that the change in weights is between -18 to 65 percent with an average of 9 percent. The weight comparison shows that the proposed modifications do not result in a significant increase in the cost of framing.

The second method is more practical and directly provides an estimate of the plastic link rotation angle. It builds upon the first method and concurs with the thinking presented in the 2010 version of the Commentary to the AISC Specification (2005). The elastic link rotation angle can be subtracted from the modified total link rotation angle to arrive at the plastic link rotation angle. This can be accomplished by using the rigid plastic mechanism and directly subtracting the elastic lateral displacements from the design displacements which is similar to the recommendations of the Commentary to the AISC Specification (2005). The plastic link rotation angle at any given story can be determined as follows:

$$\gamma_p = \frac{(C_{di} - \Omega_o)\Delta L}{h_s e} \quad (5.8)$$

The member sizes obtained using the second method is given in Table 5.1 for the example frame. When all frames were redesigned using the second method it is observed that both methods provide similar results. The second method results in framings that are on average 5 percent lighter. This is due to the use of plastic rotations as opposed to total rotations.

5.5. VERIFICATION OF PROPOSED MODIFICATIONS

The performance of example frame redesigned according to the proposed modifications is demonstrated in Figure 5.11. Two designs are provided based on two different methods proposed to modify the link rotation angles. The variation of link rotation angles along the height are given in Figure 5.11(a) and Figure 5.11(b) for the example frame designed according to the first and second method, respectively.

When the first method is used, it is evident that total link rotation angles do not exceed their allowable values in any of the stories. Only at the 5th story the total link rotation angle exceeds its design value by 7 percent. It is clear that the application of the proposed modifications result in more uniform total link rotation angles that are close to their design values. In addition, the total link rotation angle demands under MCE level ground motions were observed to decrease. Similar conclusions can be derived for the design based on the second method. According to the results presented in Figure 5.11(b) the calculated plastic link rotation angles do not exceed their allowable values in any of the stories.

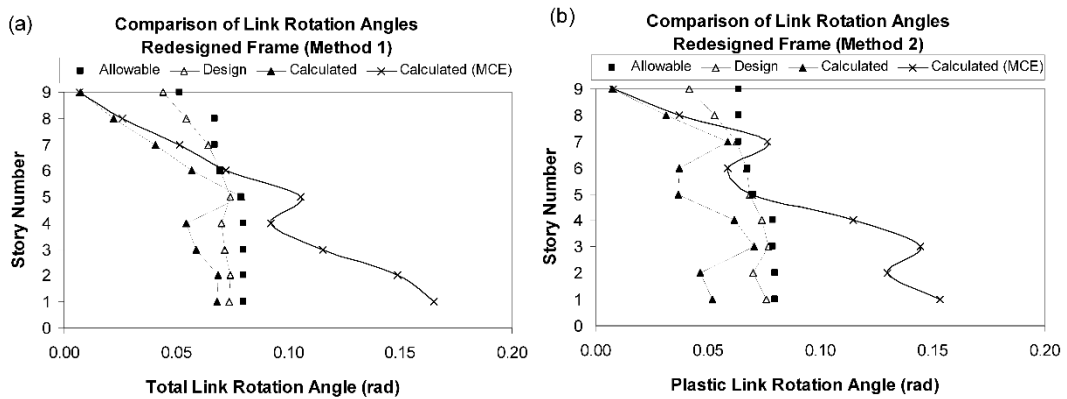


Figure 5.11 Link rotation angles for redesigned EBF

All 72 frames were redesigned in light of the proposed modifications and utilizing the first method in modifying the link rotation angles. All 720 inelastic time history analyses were repeated for this new set of EBFs. The results of these additional analyses are compared in Figure 5.7 with the results of existing designs. It is evident that the proposed modifications result in ratios that are less than unity indicating that the design values are not exceeded at any story. The ratios are more uniform for 3 story structures and tend to be non-uniform as the number of stories increases. This is attributable to the EBF system behavior where majority of the inelastic action is

constrained in the lower stories for tall frames. Therefore, for these frames the differences between design and calculated link rotations are still pronounced for upper stories although improvements over the existing method are observed.

CHAPTER 6

EVALUATION OF SEISMIC RESPONSE FACTORS FOR EBFs USING FEMA P695 METHODOLOGY

6.1. BACKGROUND

Seismic response factors for EBFs are given in Minimum Design Loads for Buildings and Other Structures (2010) referred as ASCE7-10 (2010). The recommended values of the response modification coefficient (R), the system overstrength factor (Ω_o), and the deflection amplification factor (C_d) are 8, 2, and 4, respectively. These factors were developed based on judgment and observations from past earthquakes. The recommendations in ASCE7-10 (2010) are supplemented by the recommendations of the Commentary to AISC341-10 (2010). Analytical studies conducted by Popov et al. (1989) demonstrated that the links in the first floor usually experience the largest inelastic deformation which may result in formation of a soft story. The Commentary to AISC341-10 (2010) recommends a more conservative design for the links in the first two or three floors. Providing links with available shear strength at least 10 percent over the required shear strength is recommended while being silent on providing a more definite recommendation on the required level of increase.

Fractures in links of EBFs were observed after the 2010 and 2011 New Zealand earthquakes (Clifton et al., 2011). This undesired behavior motivated to evaluate the design rules for EBFs and particularly the seismic response factors. Pursuant to this goal, these factors were evaluated in light of the recommendations given in Quantification of Building Seismic Performance Factors (Federal Emergency Management Agency, FEMA P695, 2009). The proposed methodology, hereafter referred as the Methodology, outlined in FEMA P695 (2009) was applied to EBFs to evaluate the seismic response factors. The application of the Methodology, findings, and proposed modifications to seismic response factors are presented herein.

6.2. NON-SIMULATED COLLAPSE CRITERIA

In general, the Methodology requires collapse simulation of archetypes to determine response factors. Non-simulated collapse modes can be indirectly evaluated using limit state checks in cases where it is not possible to directly simulate all significant deterioration modes contributing to collapse behavior. Fracture in the connections or hinge regions of steel moment frame components are given as examples of possible non-simulated collapse modes. A comparison of responses of a reduced beam section beam-to-column connection and a link beam are given in Figure 6.1 and Figure 6.2. The beam-to-column connection behavior belongs to specimen DB4 tested by Engelhardt et al. (1998) and exhibits a reduction in strength after the peak resistance is reached (Figure 6.1). Collapse simulation incorporating such behavior is possible as long as the deterioration is properly modeled. On the other hand, Figure 6.2 shows behavior of 4A-RLP link beam specimen tested by Okazaki et al. (2005). The specimen showed stable resistance up to 0.11 radians of positive plastic rotation. Failure of the specimen was through fracture and occurred before the negative 0.11 radian excursion was completed. As shown in Figure 6.2, the failure

of the link beam is sudden and results in a significant strength deterioration where the resistance immediately ceases to exist. In EBFs sudden fracture of a link results in formation of a soft story. In addition, the force on the fractured link has to be redistributed to all the other links which can potentially cause an overload and fracture in these links too. Because of these reasons non-simulated collapse is adopted in the present study.

As mentioned before, link rotation angle (γ_p) is used as a measure to quantify the deformation capacity of links. Naturally, any non-simulated collapse criterion should adopt link rotation angle as its basis. However, it is challenging to develop such criterion as the failure of a link significantly depends on the loading history. The link experiment given in Figure 6.2 is based on the loading protocol recommended by AISC341-10 (2010). The link failed at a link rotation angle equal to 0.12 radians and this deformation level is above the required value of 0.08. The very same link was subjected to a more severe protocol which is given in the 2002 version of AISC341. Experimental results revealed that the link fractured at a rotation of 0.061 radians and failed to meet the required level of deformation capacity (Okazaki et al., 2005).

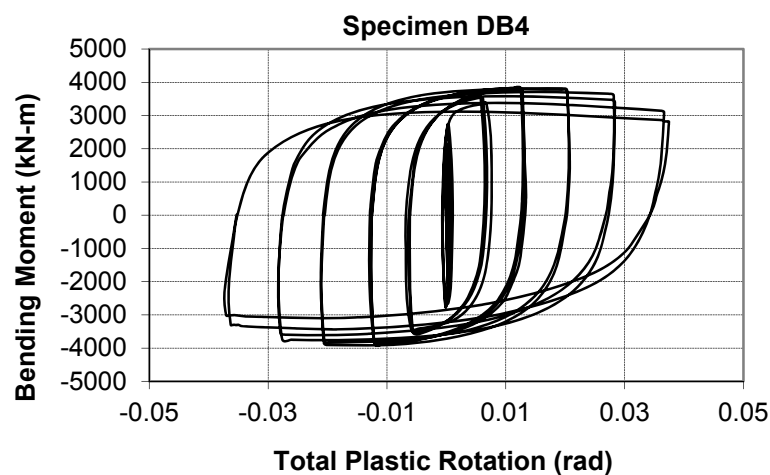


Figure 6.1 Experimental behavior of moment connection (Engelhardt, 1998)

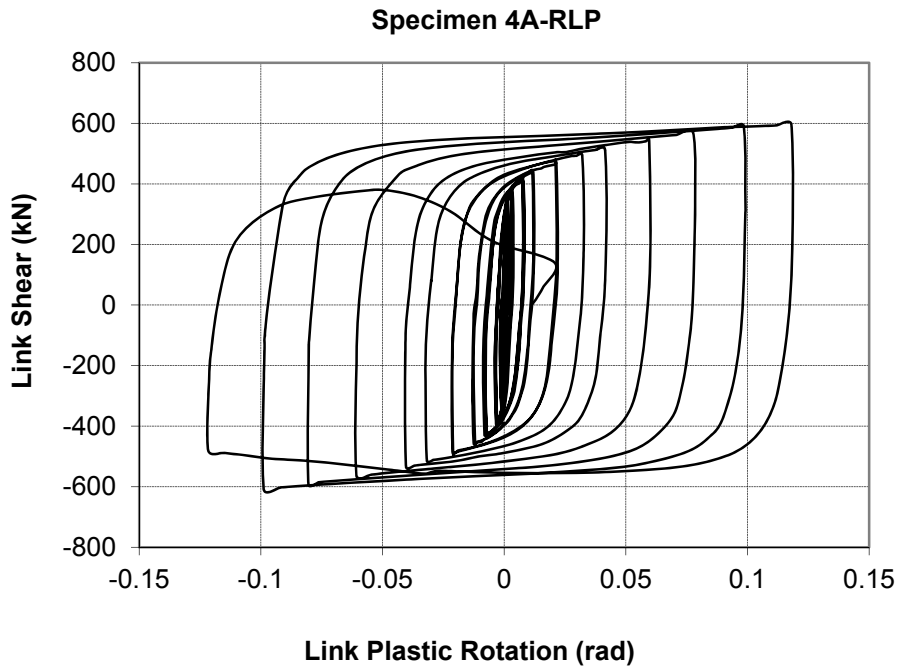


Figure 6.2 Experimental behavior of shear link beam (Okazaki et al., 2005)

A dual criterion is adopted in the present study for non-simulated collapse. These criteria are based on providing limits on the link rotation angle. The first is a limit on the maximum amount of link rotation angle experienced by the link and the second one is a limit on the cumulative link rotation. Providing an upper bound on the link rotation angle requires judgment. It is quite stringent to select the allowable value of link rotation angle as the experimental observations (Figure 6.2) reveal that links can sustain deformations well above the allowable limit. The allowable link rotation can be considered as a lower bound on the maximum link rotation limit. On the other hand, links tested under monotonic loading, where the cumulative rotations are not high, accomplished 0.2 radians of rotation (Malley and Popov, 1984; Kasai and Popov, 1986). Therefore, an upper bound on the maximum link rotation angle can be considered as 0.2 radians. In the present study, the maximum link rotation angle was determined by considering the recommendations of Seismic

Rehabilitation of Existing Buildings (2007) hereafter referred as ASCE41-06 (2007). The limit on link rotation angle is 0.14 radians for shear yielding links ($e/(M_p/V_p) < 1.6$) based on collapse prevention criteria of ASCE41-06 (2007). In the present study any link that experiences link rotation angle beyond 0.14 radians is assumed to trigger collapse.

The second criterion is selected to take into account the loading history. A typical variation of link rotation angle obtained from a time history analysis is given in Figure 6.3. The link experiences a few cycles with large rotation and many cycles with small rotation. The cumulative link rotation must be considered to take into account the variation in loading histories. In this regard, the sum of cycle ranges, which was proposed by Richards and Uang (2006) for link beams, was adopted. Ordered cycles from rainflow counting procedure was used to calculate the sum of cycle ranges. Figure 6.4 shows the ordered cycles from rainflow counting procedure when applied to the time history output shown in Figure 6.3. These cycles are ordered from the largest to the smallest and the magnitudes are determined to produce symmetric cycles. These cycle ranges are summed up to determine the sum of cycle ranges that the link experiences. In the summation process, cycles with a range smaller than 0.0075 are not taken into account because these cycles are not considered damaging (Richards and Uang, 2006). The sum of cycle ranges was considered as a measure of the cumulative link rotation in the present study. A limit on the cumulative link rotation can be developed by considering experimental observations. The study of Okazaki et al. (2005) was considered as a benchmark because this study encompasses behavior of links made of A992 steel which is frequently used in the US. The sums of cycle ranges were calculated for six shear links tested by Okazaki et al. (2005) and were found to be equal to 1.61, 1.77, 1.75, 1.88, 1.55, and 1.92 radians for specimens 4A-RLP, 4C-RLP, 8-RLP, 10-RLP, 11-RLP, and 12-RLP, respectively. The mean and median of the sum of cycle ranges were found to be equal to 1.75 radians and 1.76 radians, respectively. It is worthwhile to note that the target value of the sum of cycle ranges is 1.10 radians according to the recommended loading protocol of AISC341-10 (2010). The

experimental results show that all of the shear links tested by Okazaki et al. (2005) using the AISC341-10 (2005) protocol sustained cumulative rotations well in excess of the target rotation. A cumulative link rotation limit of 1.76 radians was adopted in this study and any link that experiences cumulative link rotations in excess of this value was assumed to trigger collapse.

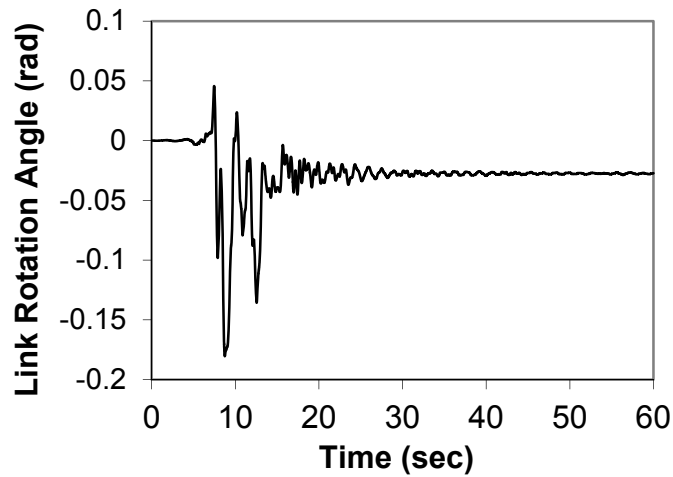


Figure 6.3 Typical time history of link rotation angle

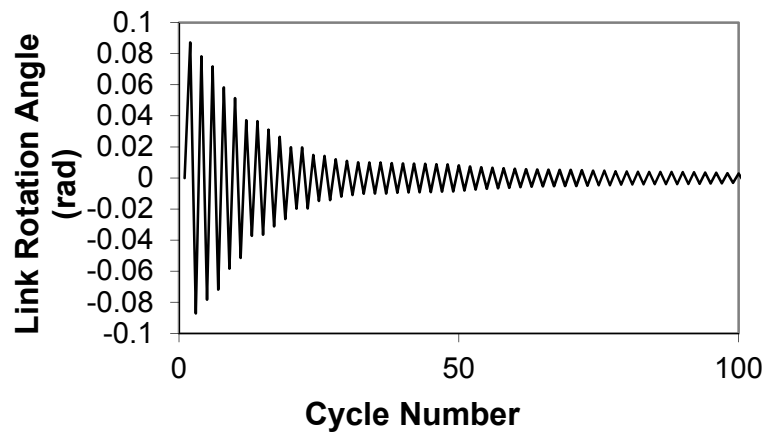


Figure 6.4 Ordered cycles from rainflow counting procedure

6.3. DESCRIPTION OF ARCHETYPES

The Methodology requires developing performance groups which include index archetypes. Performance groups are formed by considering design load variations based on Seismic Design Category, gravity load intensity, design height variations and etc. Acceptance criteria are based on results obtained for performance groups as well as individual archetypes. In general the methodology requires that probability of collapse for Maximum Considered Earthquake (MCE) ground motions is approximately 10%, or less, on average across a performance group and 20%, or less, for each index archetype within a performance group. The probability of collapse is represented by a variable named the Adjusted Collapse Margin Ratio (ACMR).

Only individual archetypes were considered in the present study. In other words, each archetype was evaluated individually without being a part of a performance group. There are several practical reasons behind avoiding performance groups. EBFs are generally used in high and very high seismic areas due to their superior ductility. Therefore, investigating performance groups for different Seismic Design Categories is not practical. Considering only the Seismic Design Category D_{max} with spectral accelerations $S_{MS}=1.5g$ and $S_{M1}=0.9g$ is sufficient for evaluation purposes. In addition, preliminary studies conducted by the authors revealed that EBF designs based on other categories such as D_{min} do not result in problematic cases. Two basic configurations are typically adopted for EBFs in the practice. For the commonest configuration, the link is a horizontal framing member located between braces as shown in Figure 2.1. In the other configuration the link member can be directly connected to a column. However, recent research conducted by Okazaki et al. (2006) revealed that the link to column connection detail can be prone to premature failure. The Commentary to AISC341-10 (2010) recommends avoiding EBF configurations with links attached to columns until further research is available on this issue. Another limitation is based on the behavior of link beams. As reported

by Richards and Uang (2005) majority of the link beams used in practice are shear links. In addition, most of the test data reported to date is on shear yielding links too. Therefore, the present study only concentrated on the performance of EBFs with shear yielding links ($e/(M_p/V_p) < 1.6$).

The archetypes should capture the essence and variability of performance characteristics of the system of interest. The link length to bay width ratio (e/L) and the number of stories were considered as the prime variables while keeping the EBF configuration, type of link, and Seismic Design Category constant. Link length to bay width ratios of 0.1 and 0.15 were considered to cover the practical range of interest for shear yielding links. Number of stories was taken as 3, 6, and 9. A combination of these variable results in six archetypes to be considered in the evaluation process. Naming of the archetypes according to link length to bay width ratio and number of stories is given in Table 6.1.

Table 6.1 Archetype Properties and Scaling Factors

AN	e/L	N_s	Weight (kN)	T	μ_T	β_{RTR}	β_{TOT}	ACMR _{20%}	SSF	Scaling Factor
1	0.10	3	58.76	0.65	5.32	0.400	0.436	1.45	1.29	1.12
2	0.10	6	144.80	1.20	3.57	0.400	0.436	1.45	1.3	1.12
3	0.10	9	251.43	1.83	2.76	0.376	0.414	1.42	1.3	1.09
4	0.15	3	68.18	0.70	4.45	0.400	0.436	1.45	1.26	1.15
5	0.15	6	164.81	1.27	3.84	0.400	0.436	1.45	1.31	1.11
6	0.15	9	277.52	1.95	2.91	0.391	0.428	1.43	1.31	1.09
1R	0.10	3	73.77	0.51	4.15	0.400	0.436	1.45	1.25	1.16
2R	0.10	6	225.73	0.90	2.88	0.388	0.425	1.43	1.26	1.13
3R	0.10	9	432.23	1.32	2.4	0.340	0.382	1.38	1.27	1.09
4R	0.15	3	74.16	0.61	4.84	0.400	0.436	1.45	1.27	1.14
5R	0.15	6	177.07	1.12	3.79	0.400	0.436	1.45	1.31	1.11
6R	0.15	9	346.39	1.59	3.03	0.400	0.436	1.45	1.32	1.10

AN: Archetype number, N_s : Number of story, T: fundamental period of vibration

The floor plan given in Figure 6.5 was considered and the EBFs in the y-direction were designed. The floor plan is identical to the floor plan considered in the study by Richards and Uang (2006). The bay width for EBFs is 9 meters. Preliminary studies conducted by the authors revealed that 9 meter bay width produces more problematic cases when compared with other bay widths such as 6 or 12 meters. The story height is constant for all stories and considered as 4 meters.

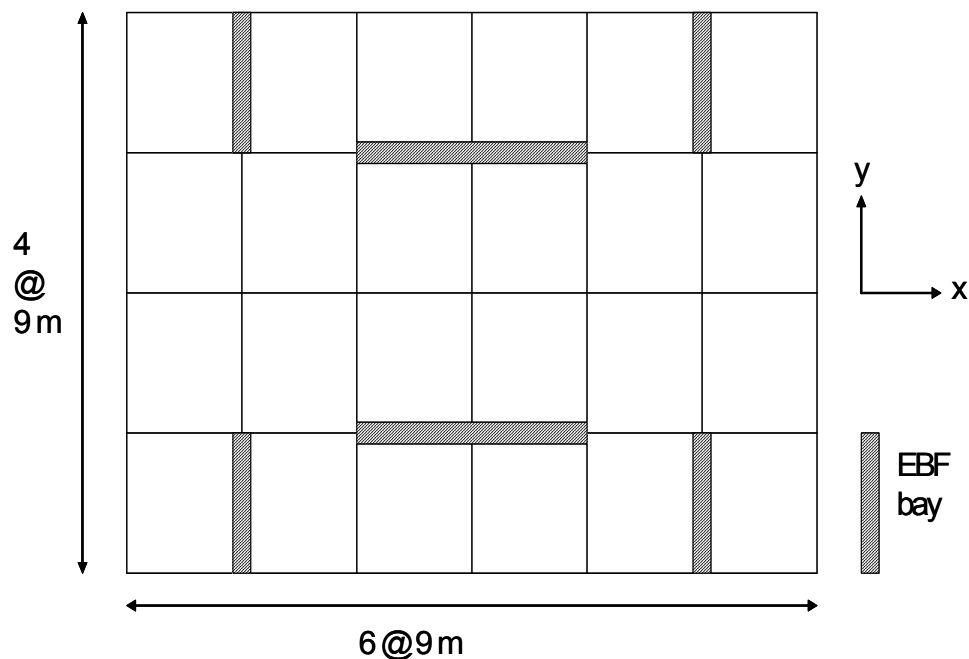


Figure 6.5 Floor plan

EBFs were designed using equivalent lateral force (ELF) procedure presented in ASCE7-10 (2010). In sizing the steel members provisions of the AISC Specification for Structural Steel Buildings (AISC-360, 2010) and AISC Seismic Provisions for Structural Steel Buildings (AISC341-10, 2010) were used. For all structures story dead and live loads were assumed to be 5 kN/m^2 and 2 kN/m^2 , respectively. A redundancy factor of unity was considered in all designs as recommended by the

Methodology. All members of the steel framing were assumed to be from A992 grade steel with a yield strength of 345 MPa. Links, beams and braces are selected among American wide flange sections (W shapes) while columns are selected from W14 sections. Links, braces are changed at every story while the columns change at every three stories. The selection of member sizes is based on the minimum weight principle. The fundamental period was assumed to be equal to 1.4 times the approximate period from ASCE7-10 (2010) as recommended by the Methodology. The details of the design process are given in Chapter 2 and the selected member sizes are given in Table 6.2. It should be reiterated that the selected link sections qualify as shear yielding links. The links in the first three floors were designed shears that are 10 percent more than the design shear. Capacity-demand ratios (link design overstrength) and design link rotations of all links are also given in Table 6.2. In general strength provisions govern the design of the links. Only for the 9 story EBF with $e/L=0.1$ link rotation angle provisions governed the design. The allowable link rotation for all shear links is 0.08 radians.

Table 6.2 Member Sizes of Archetypes and Link Rotation Angles from Design and Analysis

AT	Story	Link	Brace	Column	Link OS	DLRA	MLRA	CLRA
1	1	W14×30	W10×49	W14×68	1.15	0.047	0.21	1.81
	2	W12×30	W10×49	W14×68	1.15	0.047	0.15	1.49
	3	W8×31	W8×40	W14×68	1.30	0.045	0.12	1.74
2	1	W14×38	W10×54	W14×132	1.11	0.046	0.23	1.60
	2	W14×38	W10×54	W14×132	1.15	0.053	0.18	1.17
	3	W14×34	W10×49	W14×132	1.15	0.060	0.14	1.00
	4	W12×30	W10×49	W14×68	1.07	0.061	0.12	1.17
	5	W12×26	W8×48	W14×68	1.26	0.060	0.09	1.15
	6	W8×31	W8×40	W14×68	1.74	0.050	0.06	1.24
3	1	W16×36	W10×60	W14×176	1.10	0.047	0.20	1.33
	2	W16×36	W10×60	W14×176	1.11	0.057	0.18	1.04
	3	W16×36	W10×60	W14×176	1.14	0.065	0.15	0.82
	4	W14×43	W10×49	W14×132	1.04	0.073	0.12	0.78
	5	W14×43	W10×49	W14×132	1.13	0.077	0.08	0.61
	6	W14×43	W10×49	W14×132	1.28	0.077	0.07	0.50
	7	W14×30	W10×49	W14×68	1.42	0.080	0.05	0.57
	8	W12×26	W8×48	W14×68	1.46	0.078	0.06	0.90
	9	W8×31	W8×40	W14×68	2.07	0.069	0.05	0.95
4	1	W12×53	W10×54	W14×68	1.23	0.035	0.15	1.54
	2	W10×49	W10×49	W14×68	1.17	0.040	0.12	1.51
	3	W10×49	W10×49	W14×68	1.92	0.028	0.05	1.01
5	1	W14×61	W10×68	W14×132	1.30	0.030	0.14	0.99
	2	W12×58	W12×58	W14×132	1.11	0.039	0.14	0.98
	3	W12×53	W10×54	W14×132	1.16	0.046	0.12	0.90
	4	W10×49	W10×49	W14×68	1.09	0.050	0.09	1.09
	5	W10×49	W10×49	W14×68	1.45	0.044	0.05	0.89
	6	W10×49	W10×49	W14×68	2.59	0.032	0.03	0.62
6	1	W14×61	W10×68	W14×176	1.17	0.033	0.13	1.05
	2	W14×61	W10×68	W14×176	1.18	0.040	0.11	0.79
	3	W14×61	W10×68	W14×176	1.22	0.046	0.10	0.61
	4	W12×53	W10×54	W14×132	1.02	0.058	0.10	0.72
	5	W12×53	W10×54	W14×132	1.11	0.061	0.08	0.66
	6	W10×49	W10×49	W14×132	1.00	0.068	0.09	0.89
	7	W10×49	W10×49	W14×68	1.22	0.063	0.06	0.80
	8	W10×49	W10×49	W14×68	1.68	0.055	0.03	0.61
	9	W10×49	W10×49	W14×68	3.08	0.045	0.02	0.42

AT: Archetype number, Link OS: Link overstrength, DLRA: Design link rotation angle, MLRA: Median link rotation angle, CLRA: Median cumulative link rotation angle

6.4. MODELING AND ANALYSIS

The computational framework, FedeasLab, developed by Filippou (2001) was used to conduct non-simulated collapse analysis. For the floor plan adopted in this study beam-to-column connections in eccentrically braced bays were considered rigid while connections in the other bays were considered simple. Therefore, eccentrically braced framing is used for resisting the seismic forces and the gravity framing is utilized for resisting forces due to gravity. This assumption simplified the analysis model considerably enabling to model one of the plane braced bays only. A leaner column was also modeled with the braced bay to take into account the P- Δ effects on the gravity columns.

The computational framework, FedeasLab, includes a novel finite element developed by Saritas and Filippou (2009) to model shear yielding metallic elements. The links were modeled by this element while beams, braces and columns were modeled using nonlinear beam elements. The finite element used to model the shear links was verified by Saritas and Filippou (2009) and earlier in this study (see Chapter 5.2) by comparing numerical simulations with experimental results. Two percent mass and stiffness proportional Rayleigh damping was used in time history analyses. Lumped masses were placed at every story.

The Methodology requires non-simulated collapse analysis of archetypes under a set of scaled ground motions. Scaling is performed until 50 percent of the ground motions cause collapse of an archetype. While this approach can be adopted for new structural systems, scaling of all ground motions using a pre-calculated scaling factor is sufficient for evaluation of existing systems. The scale factor is equal to the Adjusted Collapse Margin Ratio (ACMR) which in turn depends on the total system collapse uncertainty (β_{TOT}). Because individual archetypes are considered in this study, the 20 percent probability of collapse was adopted as a criterion for ACMR (i.e. ACMR_{20%}). The total system collapse uncertainty is dependent on four

factors, three of which requires judgment. These factors depend on the knowledge level and modeling capabilities about the system of interest. EBFs have been studied for over 50 years and have been implemented in the practice. In addition, computational models for EBFs were also developed and simulation of EBF behavior can be conducted with confidence. Therefore, high quality level was assigned to design requirements-related collapse uncertainty ($\beta_{DR}=0.1$), test data-related collapse uncertainty ($\beta_{TD}=0.1$), and modeling-related collapse uncertainty ($\beta_{MDL}=0.1$). The fourth factor that needs to be considered is the record-to-record collapse uncertainty (β_{RTR}) which depends on the period based ductility (μ_T). The μ_T values were determined by conducting nonlinear static (pushover) analysis in accordance with ASCE41-06 (2007) and are reported in Table 6.1. The values vary between 2.76 and 5.32 and result in β_{RTR} values that range between 0.376 and 0.4. Resulting β_{TOT} and $ACMR_{20\%}$ are reported alongside Spectral Shape Factors (SSF) for each archetype in Table 6.1.

Time history analyses were conducted for each of the six archetypes using 44 far-field ground motion records described by the Methodology. Response spectra for the 44 ground motions are given in Figure 6.6. The ground motions were scaled twice. First scaling was performed to anchor the far-field record set to MCE spectral demand. An example median spectrum of the record set anchored to MCE response spectra of Seismic Design Category D_{max} at a period of 1 second is given in Figure 6.7. Second scaling was performed to amplify the demand to meet the $ACMR_{20\%}$ value. First scaling was done in accordance with the factors provided by the Methodology whereas second scaling was conducted using the scale factor reported in Table 6.1, which was determined by dividing $ACMR_{20\%}$ by SSF.

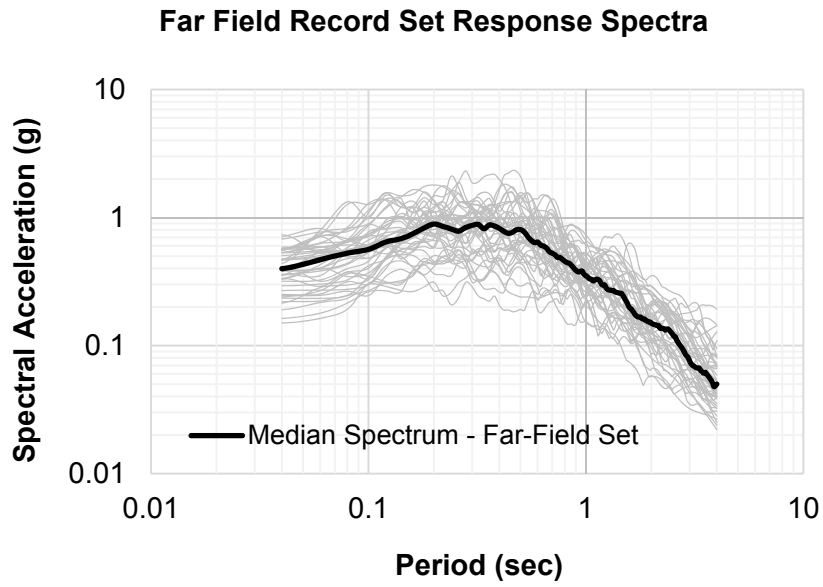


Figure 6.6 Far field record set response spectra

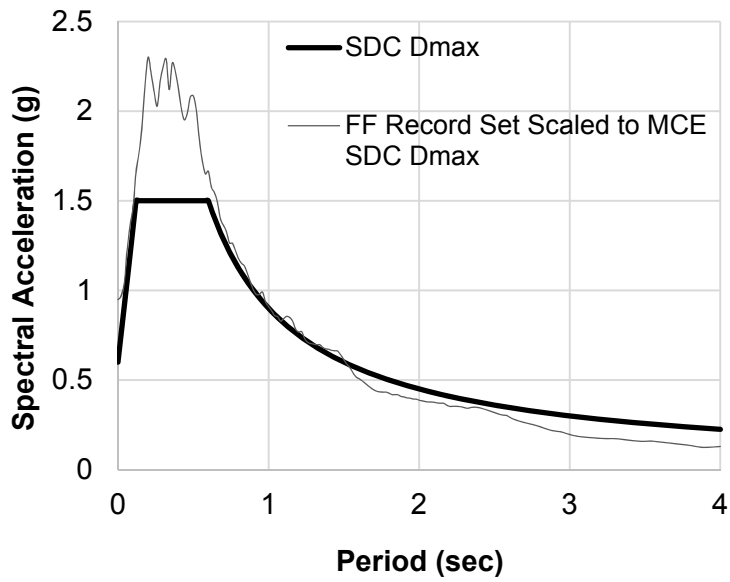


Figure 6.7 Anchored response spectra to SDC D_{max} at 1 second

6.5. EVALUATION OF SEISMIC RESPONSE FACTORS

Maximum link rotation angle and cumulative link rotation angle values were collected for each time history analysis. The median of the values from time history analysis were considered. Variations of maximum link rotation angle along the height of structures are given in Figure 6.8, Figure 6.9 and Figure 6.10 for 3, 6 and 9 story EBFs with $e/L=0.1$, respectively. In these figures the median response from 44 ground motions is given by a black solid curve and the design link rotation angles are indicated by filled markers. Median link rotation angle and median cumulative link rotation angle values are given in Table 6.2 for all archetypes. As shown in Figure 6.8, the median link rotation angle reaches to 0.21, 0.15, and 0.12 radians for the first, second and third story of a 3-story EBF with $e/L=0.1$, respectively. These values indicate that the first two stories experience link rotation angles in excess of the predefined limit of 0.14 radians. Similar conclusions can be drawn for four of the archetypes where the median link rotation angle well exceeds the limit indicating potential fracture in the links of these EBFs. The bottom story link rotation angle reaches to 0.14 radians for the 6-story EBF with $e/L=0.15$ which is right at the limit. Only for the 9-story EBF with $e/L=0.15$ the median link rotation angle is below the limit of 0.14 radians. Cases with $e/L=0.1$ were found to be more problematic when compared to cases with $e/L=0.15$. Maximum link rotation angle variation are given in Figure 6.11, Figure 6.12 and Figure 6.13 for 3, 6 and 9 story EBFs with $e/L=0.15$, respectively. Larger link rotation angle demands form as the link length gets shorter. Lesser amounts of link rotation angles for $e/L=0.15$ can be explained by examining the design link rotation angles. According to Table 6.2, the design link rotation angles for the bottom stories vary between 0.046 and 0.047 radians for $e/L=0.1$ and between 0.030 and 0.035 radians for $e/L=0.15$. As the design link rotation gets lower the rotations experienced by the link during a seismic event reduces. It should be pointed out that a significant difference exists between the design link rotation and the calculated median link rotation.

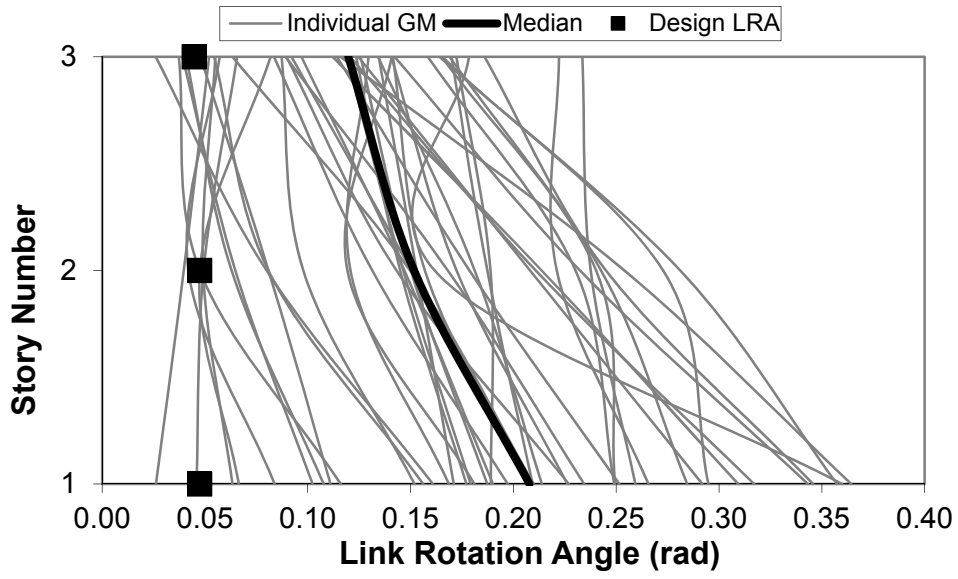


Figure 6.8 Response of 3 story archetype with $e/L=0.1$

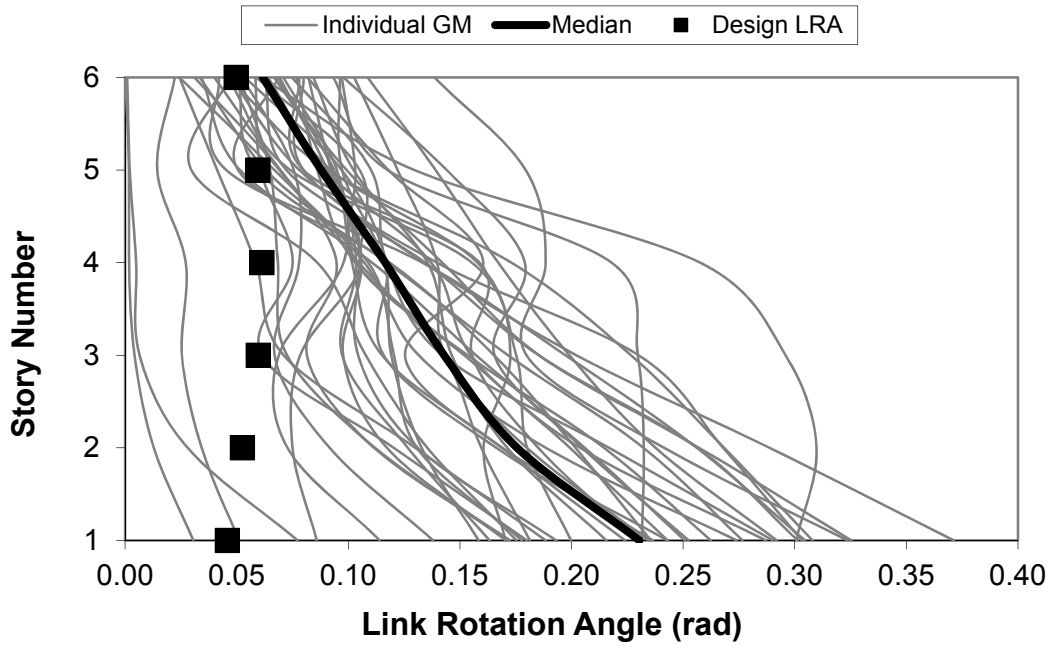


Figure 6.9 Response of 6 story archetype with $e/L=0.1$

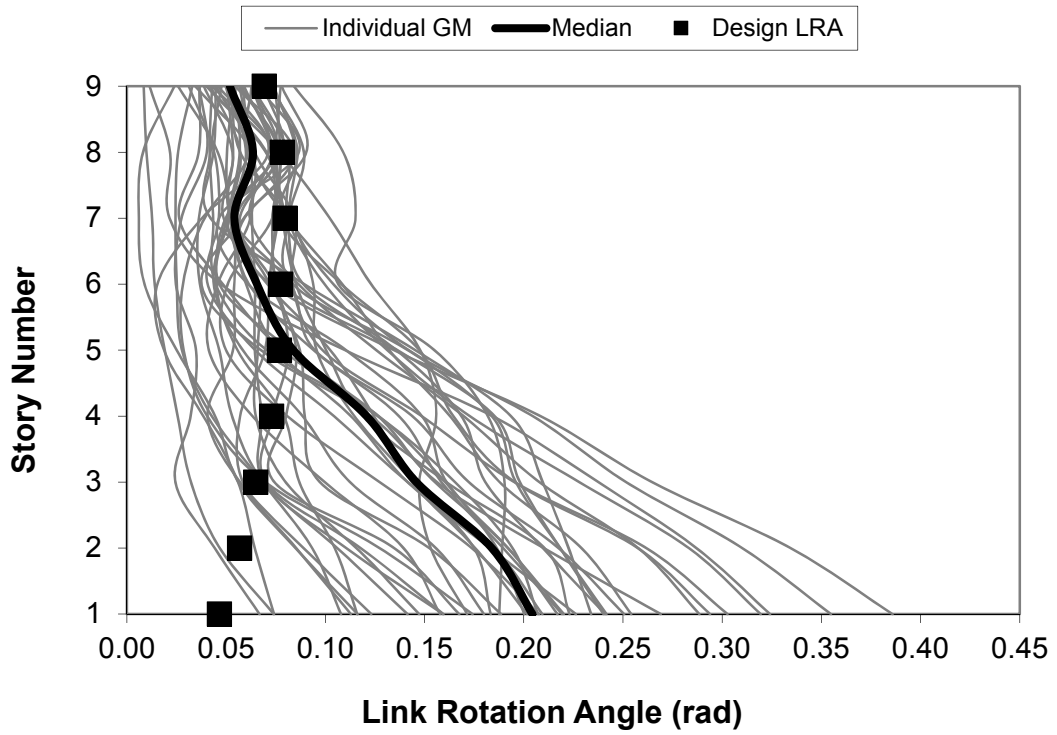


Figure 6.10 Response of 9 story archetype with $e/L=0.1$

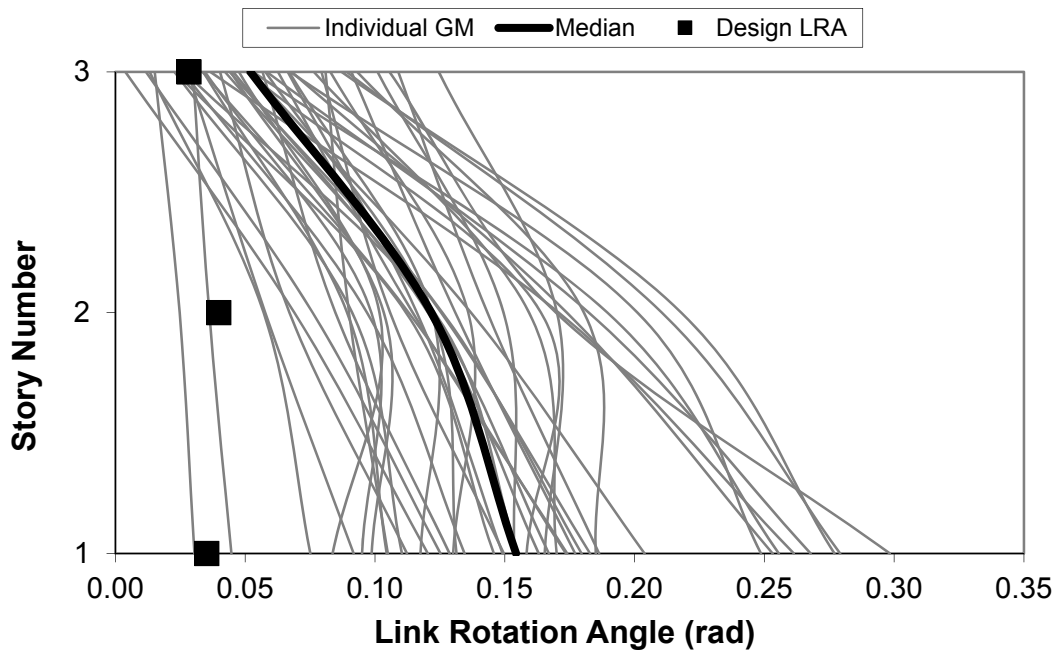


Figure 6.11 Response of 3 story archetype with $e/L=0.15$

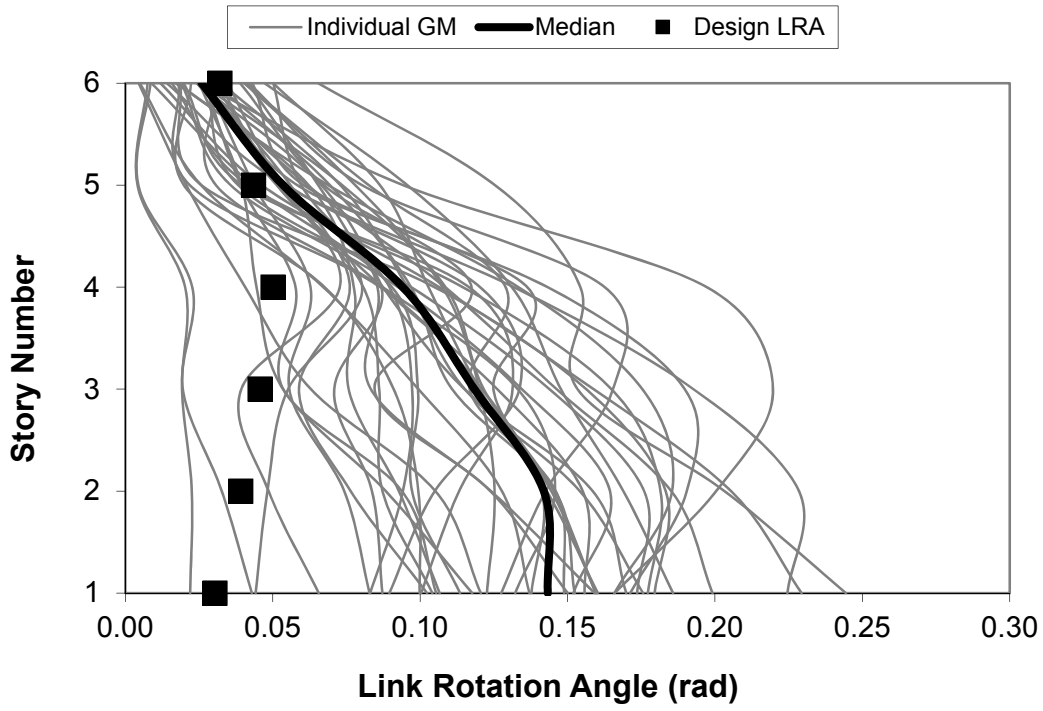


Figure 6.12 Response of 6 story archetype with $e/L=0.15$

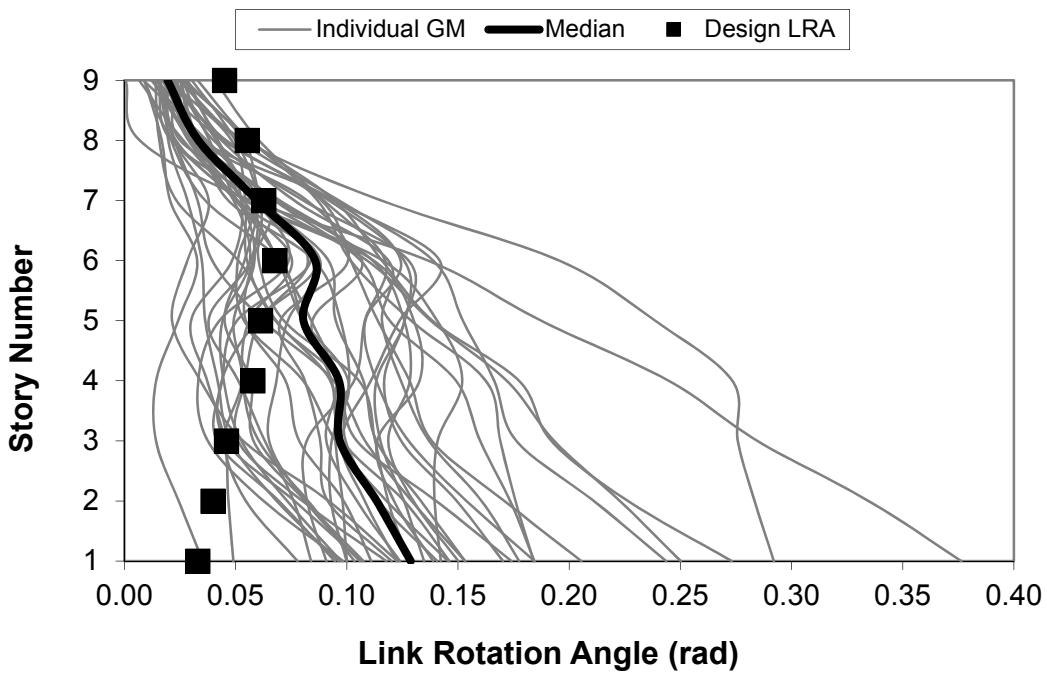


Figure 6.13 Response of 9 story archetype with $e/L=0.15$

The 3-story archetype with $e/L=0.1$ was found to be problematic when the cumulative link rotation angles are considered. The median cumulative link rotation angle was calculated as 1.81 radians for the bottom story which exceed the limit of 1.76 radians. For all other archetypes the median of the cumulative link rotation angle varied between 0.99 and 1.60 radians for the bottom stories. The results indicate that fracture of bottom story link is likely for the 3-story EBF with $e/L=0.1$. In addition, the results do not guarantee that the bottom story links do not fracture for the other cases considered based on the cumulative link rotation angle criterion. It is worthwhile to note that the limit of 1.76 radians can be unconservative for links that are not stiffened for higher demands. This limit was determined based on results from six specimens tested by Okazaki et al. (2005). All of these specimens were stiffened according to the rules presented by AISC341-10 (2010) and designed for a link rotation angle of 0.08 radians. On the other hand, the design link rotation angles for the six archetypes considered in this study vary between 0.030 and 0.047 radians which are well below the limit of 0.08 radians. This means that the archetype designs require fewer stiffeners than would be required for a link rotation angle of 0.08 radians. It is expected that the cumulative link rotation angle capacity reduces as the number of stiffeners are decreased. Available experimental data reported to date does not encompass shear links with A992 steel stiffened for link rotation angle demands that are less than 0.08 radians. More definite conclusions can be drawn on this issue when such data becomes available.

6.6. PROPOSED MODIFICATIONS

The results of the evaluation phase indicate that current values of response factors for EBFs need to be revised for satisfactory behavior. It has long been recognized that the links in the first floor undergo largest inelastic deformation (Popov et al., 1989). As mentioned before, the Commentary to AISC 341-10 (2010) recommends

designing the links in the first two or three stories to demands that are 10 percent greater. Although the archetypes were designed to have shear strengths that are 10 percent greater than the demands, the results indicate that link rotation angles can still exceed the predefined limits. The problem stems from the fact that increasing the strength of the link does not provide a remedy unless the stiffness of the link is increased. In Chapter 5, the details of deflection amplification factor study were presented. The results on the deflection amplification factor indicate that using the current value of $C_d=4$ results in significant underestimations of the deflections for lower stories. Richards and Thompson (2009) also reported that the value of deflection amplification factor is too low to accurately estimate inelastic drifts in low-rise buildings.

As presented in Chapter 5, a total of 72 EBFs were studied to develop recommendations on the deflection amplification factor. Three, 6, 9, and 12 story EBFs with bay widths of 8m, 11m, and 14m and e/L ratios of 0.1, 0.2, and 0.3 were considered. The EBFs were analyzed using inelastic time history analysis under design level ground motions (2/3 of MCE level). Deflections from inelastic time history analysis were normalized by the deflections obtained using equivalent lateral force method to arrive at the deflection amplification factors. The results are averaged by grouping the EBFs according to their number of stories. The results are given in Figure 6.14 where the deflection amplification factor is normalized by its current value of 4 ($C_d/4$) and is plotted along the height of the structure. The results indicate that the value of deflection amplification factor reaches to its value of 4 at higher floors. For lower floors, however, the calculated value of C_d is more than twice its current value.

In general, the response factors are single valued parameters and are not given as a function of the number of stories or the height of the structure. Proposing a single C_d value, such as 8, that is based on the lower stories results in significant over-design of high-rise EBFs. On the other hand, providing a modifier (ϕ_i) to the existing C_d value can be a practical solution. The very same value of $C_d=4$ can still be kept

in the ASCE7-10 (2010) document while a recommendation for its modification can be provided by the Commentary to the AISC341. A similar approach is currently in use and the Commentary recommends amplifying the shear force demand on the links of the first two or three stories. The following modification to C_d is proposed herein to be adopted by the Commentary to AISC341.

$$C_d = 4\phi_i \quad \text{where} \quad \phi_i = 1 + 1.6\left(\frac{8-i}{8}\right) \geq 1.0 \quad (6.1)$$

where $i = i^{\text{th}}$ story.

The modification factor (ϕ_i) was developed by considering the data presented in Figure 6.14. A linear variation of C_d was adopted which envelopes the computed response. The proposed modifications replace any modification that is required for the strength of the links in the first two or three stories. In other words, the deflections of an EBF should be calculated using the proposed C_d factor which takes into account the variation of C_d along the height of the structure. The link rotation angles can in turn be calculated using these deflections and the rigid-plastic mechanism.

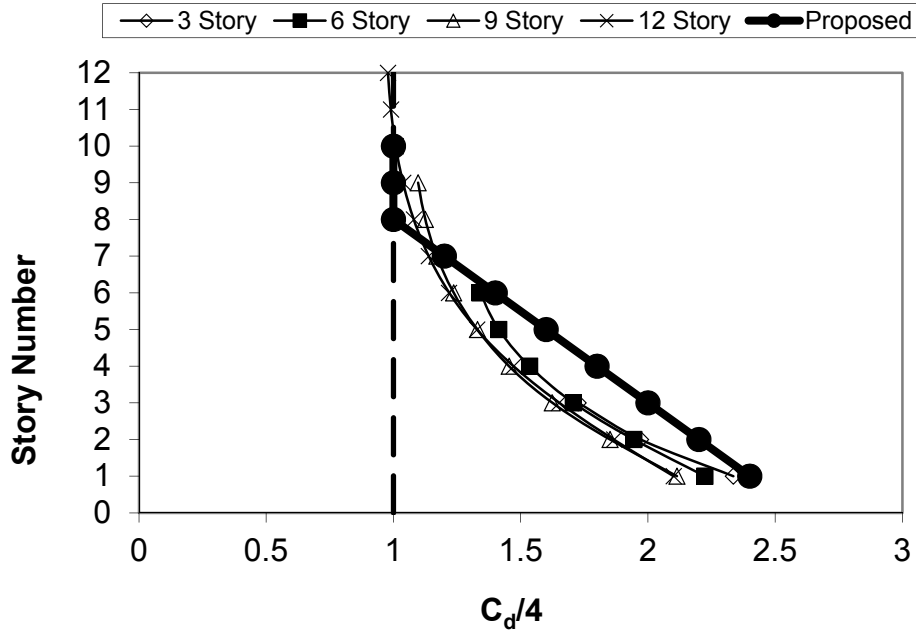


Figure 6.14 Variation of deflection amplification factor

6.7. RE-EVALUATION OF SEISMIC RESPONSE FACTORS

Proposed modification to the C_d factor was evaluated using the Methodology. The same archetypes were redesigned considering the deflection amplification factor proposed in Equation (6.1). The resulting member sizes are given in Table 6.3. In this table the redesigned EBFs are denoted by the archetype number followed by a suffix “R”. Contrary to the designs based on unmodified C_d , the revised designs are generally governed by link rotation angle limit of 0.08 radians. The design over-strength of the shear links are reported in Table 6.3 and the values indicate that the links in the first few stories need to be significantly over-designed to meet the stringent link rotation angle limit. The bottom story link design over-strength of EBFs with $e/L=0.1$ varied between 1.99 and 2.32 whereas the over-strengths varied between 1.54 and 1.78 for EBFs with $e/L=0.15$. These values indicate that

increasing the link strength by 10 percent is not sufficient and in some cases the link must be more than doubled.

Fundamental periods, period based ductility and scaling factors for these redesigned archetypes are given in Table 6.1. These archetypes were analyzed under the ground motion set recommended by the Methodology and link rotation angle histories were collected. The median of the maximum link rotation angle and median cumulative link rotation angle are reported in Table 6.3. Variations of link rotation angle along the height of EBFs are given in Figure 6.15, Figure 6.16 and Figure 6.17 for 3, 6 and 9 story EBFs with $e/L=0.1$, respectively. Similarly, Figure 6.18, Figure 6.19 and Figure 6.20 shows variation of link rotation angle for 3, 6 and 9 story EBFs with $e/L=0.15$, respectively. The results indicate that the median of the link rotation angles reach to a maximum of 0.14 radians for 6-story archetype with $e/L=0.1$. For all other archetypes the median stayed below the limit of 0.14 radians. Similarly, the maximum cumulative link rotation angle was calculated to be equal to 1.43 radians indicating that for all archetypes the cumulative link rotation angle stayed below the predefined limit of 1.76 radians. It is worthwhile to note that the proposed modifications will have an impact on the sizing as well as stiffening of the link sections. As compared with the previous designs the new designs have design link rotation angles close to 0.08 radians indicating that closely spaced stiffeners would be needed. Stiffening the link to meet the 0.08 radian criterion will lead to larger cumulative rotation capacities such as the one reported by Okazaki et al. (2005).

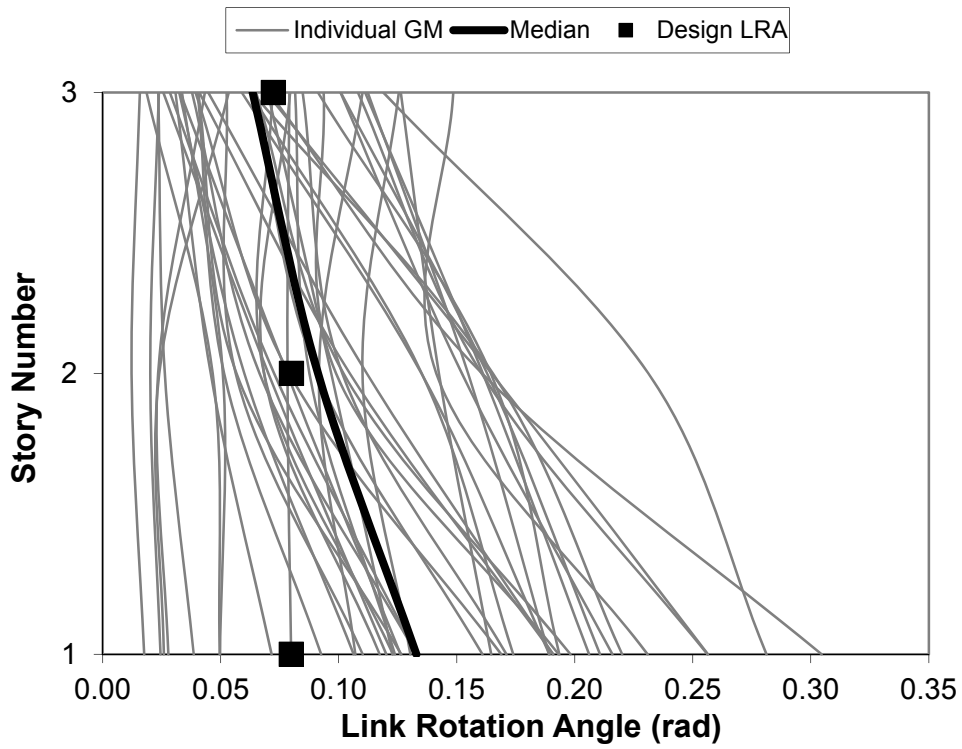


Figure 6.15 Response of 3 story redesigned archetype with $e/L=0.1$

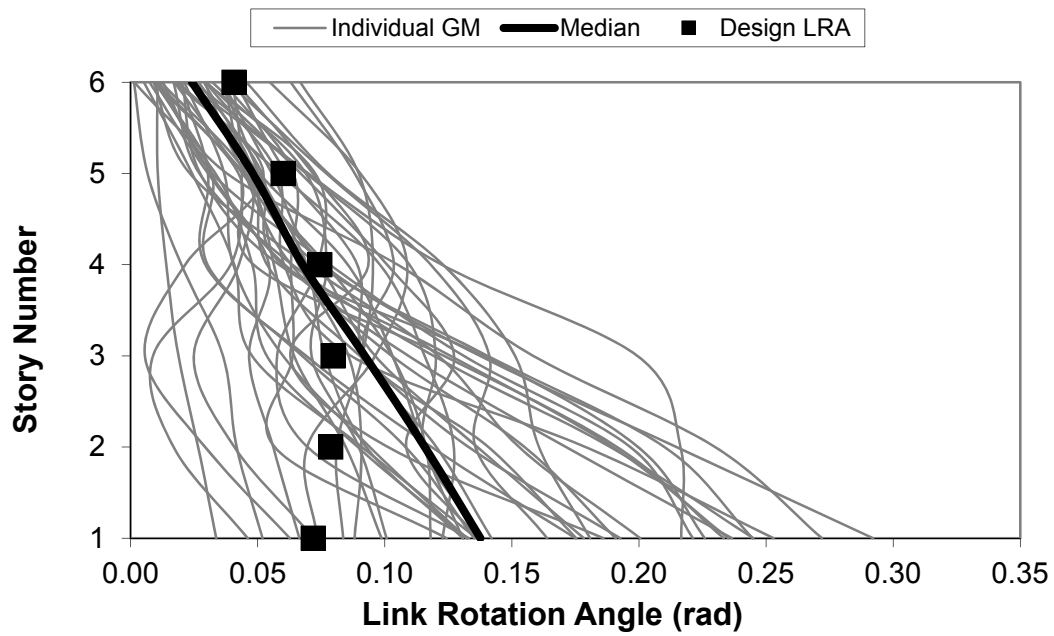


Figure 6.16 Response of 6 story redesigned archetype with $e/L=0.1$

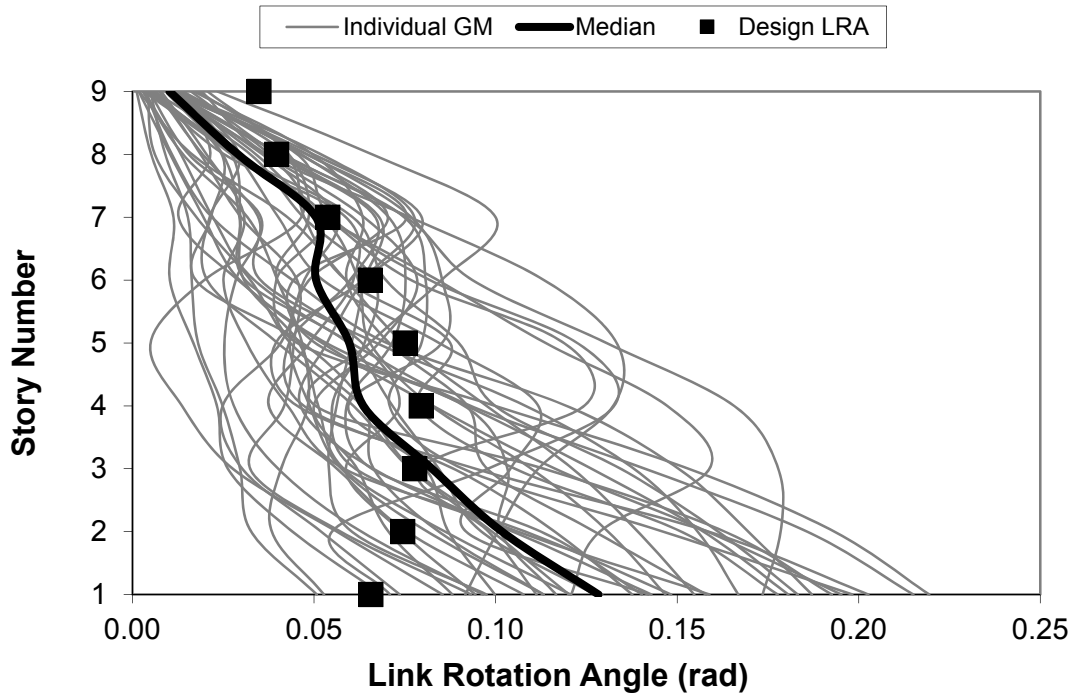


Figure 6.17 Response of 9 story redesigned archetype with $e/L=0.1$

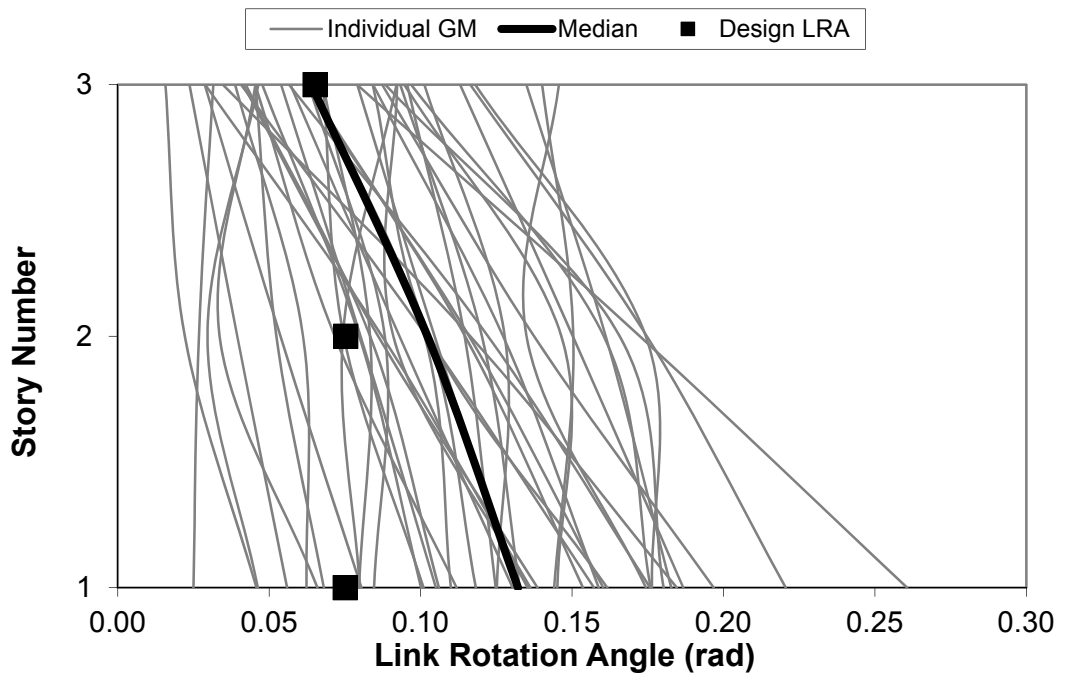


Figure 6.18 Response of 3 story redesigned archetype with $e/L=0.15$

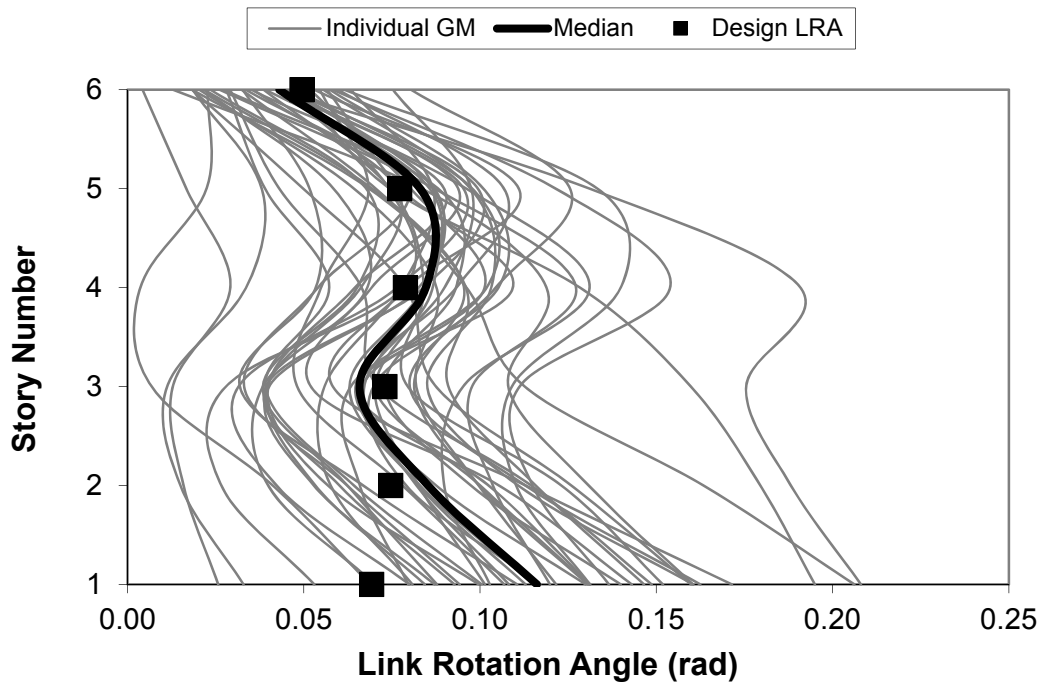


Figure 6.19 Response of 6 story redesigned archetype with $e/L=0.15$

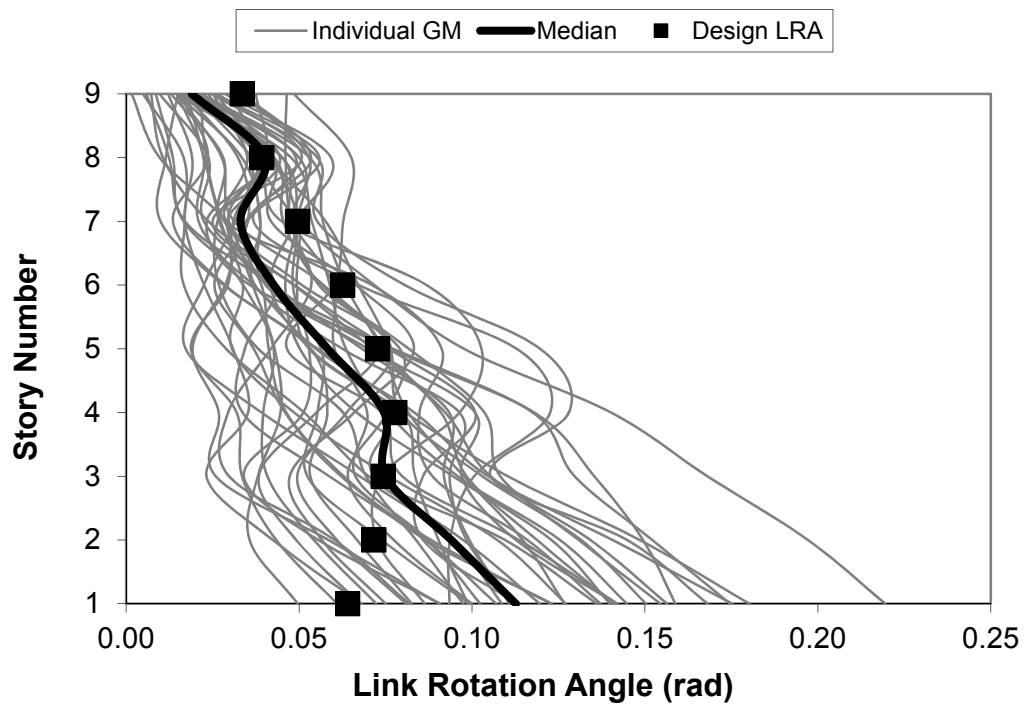


Figure 6.20 Response of 9 story redesigned archetype with $e/L=0.15$

Table 6.3 Member Sizes of Revised Archetypes and Link Rotation Angles from Design and Analysis

AT	Story	Link	Brace	Column	Link OS	DLRA	MLRA	CLRA
1R	1	W18×46	W12×72	W14×74	1.99	0.080	0.13	1.43
	2	W16×45	W10×68	W14×74	2.00	0.080	0.09	1.16
	3	W14×34	W10×49	W14×74	2.38	0.072	0.06	1.17
2R	1	W21×62	W12×79	W14×176	2.17	0.072	0.14	1.11
	2	W21×62	W12×79	W14×176	2.24	0.079	0.12	0.77
	3	W21×55	W12×79	W14×176	2.28	0.080	0.09	0.65
	4	W21×44	W12×79	W14×132	2.50	0.074	0.07	0.63
	5	W18×46	W12×72	W14×132	2.91	0.060	0.05	0.55
	6	W18×46	W12×72	W14×132	5.21	0.041	0.02	0.24
3R	1	W24×68	W12×96	W14×311	2.32	0.066	0.13	0.95
	2	W24×68	W12×96	W14×311	2.34	0.074	0.10	0.69
	3	W24×68	W12×96	W14×311	2.40	0.078	0.08	0.53
	4	W24×55	W12×96	W14×193	2.41	0.080	0.06	0.44
	5	W24×55	W12×96	W14×193	2.62	0.075	0.06	0.36
	6	W24×55	W12×96	W14×193	2.97	0.066	0.05	0.34
	7	W21×57	W12×87	W14×132	3.24	0.054	0.05	0.34
	8	W21×57	W12×87	W14×132	4.45	0.040	0.03	0.20
	9	W21×62	W12×79	W14×132	8.07	0.035	0.01	0.03
4R	1	W14×61	W10×68	W14×68	1.54	0.075	0.13	1.34
	2	W12×58	W12×58	W14×68	1.52	0.075	0.10	1.27
	3	W10×49	W10×49	W14×68	1.92	0.065	0.06	1.27
5R	1	W16×67	W12×72	W14×132	1.62	0.069	0.12	0.95
	2	W16×67	W12×72	W14×132	1.68	0.075	0.09	0.70
	3	W16×67	W12×72	W14×132	1.82	0.073	0.07	0.47
	4	W12×58	W12×58	W14×68	1.42	0.079	0.08	0.86
	5	W10×49	W10×49	W14×68	1.45	0.077	0.08	1.28
	6	W10×49	W10×49	W14×68	2.59	0.049	0.04	0.82
6R	1	W18×76	W12×79	W14×233	1.78	0.064	0.11	0.86
	2	W18×76	W12×79	W14×233	1.79	0.072	0.09	0.66
	3	W18×76	W12×79	W14×233	1.84	0.074	0.07	0.46
	4	W16×67	W12×72	W14×145	1.60	0.078	0.07	0.54
	5	W16×67	W12×72	W14×145	1.73	0.073	0.06	0.43
	6	W16×67	W12×72	W14×145	1.97	0.063	0.04	0.37
	7	W16×67	W12×72	W14×74	2.39	0.050	0.03	0.32
	8	W14×61	W10×68	W14×74	2.62	0.039	0.04	0.46
	9	W14×61	W10×68	W14×74	4.82	0.034	0.02	0.28

CHAPTER 7

CONCLUSIONS AND RECOMMENDATIONS

7.1. SUMMARY

In this thesis, seismic performance factors of EBFs are evaluated numerically and dynamic characteristics of EBFs are examined. Pursuant to this goal a computer program which facilitates seismic resistant design of EBFs was developed. The algorithm of the program adopts the lightest uniform frame design and library of link-beam-brace sub-assemblages concepts. The design output from the program was compared with published solutions and the results indicate that the algorithm developed as a part of this study is capable of providing lighter framing solutions.

The formulation of a hand method used to predict computed periods of buildings has been presented. The formulation requires roof drift ratio under seismic forces as a parameter. A parametric study has been conducted to obtain roof drift ratios for steel eccentrically braced frames. A model used to predict the roof drift ratios was developed as a result of the parametric study. The model adopts the rigid plastic deformation mechanism of typical EBFs as a basis and requires prior knowledge of the normalized link length averaged over all stories.

An analytical study aimed at quantifying design overstrength of EBFs is presented. The study adopts an EBF design procedure specifically developed as a part of this research program. The design procedure was implemented into a computer program which was used to conduct a parametric study. The designs obtained using the developed algorithm were compared with published solutions. The geometrical properties and seismic hazard were considered as the variables and a total of 16640 EBFs were designed using the developed computer program to evaluate design overstrength of EBFs.

A numerical study undertaken to evaluate the displacement amplification factor given in ASCE7-10 (2010) for EBFs and link rotation angle estimation procedure given in AISC341 (2005). A total of 72 EBFs were designed by considering the number of stories, the bay width, the link length to bay width ratio, and the seismic hazard level as the prime variables. All structures were analyzed using elastic and inelastic time history analysis. Based on the results of the numerical study a new set of displacement amplification factors that vary along the height of the structure and more accurate procedures to estimate the link rotation angles were developed. In light of the proposed modifications, the EBFs were redesigned and analyzed using inelastic time history analysis.

Lastly, a numerical study undertaken to evaluate seismic response factors steel eccentrically braced frames (EBFs) using the FEMA P695 (2009) methodology. Six archetypes were designed by making use of the current US Specifications and their behavior was assessed by making use of non-simulated collapse models. A dual criterion was adopted for performance assessment which includes the maximum and the cumulative link rotation angle experienced by the link beam. Results indicate that the current values of response factors result in designs with higher collapse probabilities than expected. In majority of the archetypes the link rotation angle exceeds the maximum limit whereas the cumulative link rotation angle limit is exceeded in only one archetype. A modification to the deflection amplification factor was developed to bring the collapse probability of these archetypes to

acceptable levels. The modifications result in deflection amplification factors that vary along the height of the structure. Six archetypes were redesigned using the proposed modifications and re-evaluated using the FEMA P695 (2009) methodology. The results indicate that the proposed modifications are adequate to satisfy the target collapse probability. Maximum and cumulative link rotation angles were observed to be less than the predefined limits.

7.2. CONCLUSIONS

The following conclusions are reached according to the results obtained in this study.

Conclusions of Chapter 2;

- The design algorithm which adopts lightest uniform frame design and library of link-beam-brace sub-assembly concepts proves to be useful and efficient in design of EBFs. When compared with the published solutions the proposed algorithm offers lighter framing solutions.

Conclusions of Chapter 3;

- The normalized link lengths were found to depend on the seismic hazard, braced bay width and height of the building. Regression analyses were conducted to arrive at simplified equations which can be used to predict the normalized link length. The model developed for drift ratios was used in the proposed formulation to estimate the computed periods. Comparisons with data from the parametric study and with data published in literature show that the proposed method has the potential to estimate the computed periods. The proposed method significantly improves the estimates when compared with the estimates provided by the current expression given in ASCE7-10 (2010).

- The proposed formulation has been extended to derive new period-height relationships for steel eccentrically braced frames located in regions of different seismicities. The estimates offered by the new relationship for high seismic regions were compared against the apparent periods of 4 EBF buildings. Comparisons indicate that the proposed period-height relationship can be an alternative to the existing relationship.

Conclusions of Chapter 4;

- The average and minimum design overstrength of EBFs considered in this study were found to be 2.36 and 1.16, respectively. The average and minimum structural overstrength values were estimated to be 3.25 and 1.6. The average is well over the codified value of 2.0 indicating that the ductility demands on EBFs are lower than expected due to the presence of higher overstrength.
- The design overstrength is primarily influenced by the link length to bay width ratio (e/L) and the bay width. Design overstrength increases as the link length to bay width ratio or the bay width increases.
- The design overstrength is secondarily influenced by the building height and seismic hazard level. In general, the design overstrength decreases as the building height or seismic hazard level decreases.

Conclusions of Chapter 5;

- The existing design rules can result in calculated link rotation angles from inelastic time history analysis which are greater than the design link rotation angles.
- The differences were found to be dependent on the C_d value adopted and the link rotation angle calculation procedure. The C_d factor given in ASCE7-10 (2005) provides unconservative estimates of the lateral displacements. The

procedure recommended in AISC341 (2005) provides conservative estimates of the link rotation angle.

- An equation to represent displacement amplification factor along the height of an EBF (Equation (5.2)) is developed herein based on inelastic time history analysis results. The proposed equation provides C_d values equal to the R value of 8.0 at lower stories and C_d values that reach to 5.0 at the upper stories.
- Two methods were developed to be used in conjunction with the rigid-plastic mechanism recommended by AISC341 (2005) to calculate link rotation angles from lateral displacements. The first method is used for total link rotation angle while the second method is used for plastic link rotation angle. These modifications take into account the elastic deformations of the members other than the links and reduce the conservatism provided by the AISC341 (2005) procedure.
- The proposed modifications were applied to 72 EBFs with various geometric properties and seismic hazard level. The results indicate that the proposed modifications improve the quality of estimates. In general, the proposed modifications result in designs where the calculated link rotation angles do not exceed their design values.

Conclusions of Chapter 6;

- Six archetypes were evaluated using FEMA P695 (2009) methodology and the results indicate that the current response factors result in link rotation angles that exceed the limit defined by ASCE41-06 (2007). In addition, cumulative link rotation angles were found to exceed the cumulative link rotation angle capacities reported by Okazaki et al. (2005).
- A modification to the C_d factor was developed as a part of this study. The modifications include amplification of the current C_d factor and the amount

of amplification varies along the height of an EBF. All six archetypes were redesigned and evaluated using the Methodology. The results indicate that the proposed modifications are adequate. Link rotation angles of the redesigned frames stayed below the limit proposed by ASCE41-06 (2007) resulting in satisfying the target collapse performance levels defined in FEMA P695 (2009).

- The proposed modifications are simple to implement. By keeping the current value of 4 for the deflection amplification factor, the modifications can be codified into the Commentary to the AISC341 Specification.
- The proposed modifications result in link sections designed to experience lower amounts of link rotation angle during seismic events and stiffening of these sections that increase the cumulative link rotation angle capacity.

7.3. RECOMMENDATIONS FOR FURTHER RESEARCH

This study aims at evaluating seismic performance of EBFs designed according to the US provisions. The differences between design philosophies affect dynamic characteristics of resulting frames. Future research should consider assessment of seismic modification factors given in Turkish Earthquake Code and Eurocode 8.

REFERENCES

American Institute of Steel Construction (AISC) (1997), “Seismic Provisions for Structural Steel Buildings”, Publication No S341, American Institute of Steel Construction, Chicago, IL.

American Institute of Steel Construction (AISC) (2002), “Seismic Provisions for Structural Steel Buildings”, ANSI/AISC 341-02, American Institute of Steel Construction, Chicago, IL.

American Institute of Steel Construction (AISC) (2005), “Seismic Provisions for Structural Steel Buildings”, ANSI/AISC 341-05, American Institute of Steel Construction, Chicago, IL

American Institute of Steel Construction (AISC) (2005), “Specification for Structural Steel Buildings”, ANSI/AISC 360-05, American Institute of Steel Construction, Chicago, IL.

American Institute of Steel Construction (AISC) (2005), “Seismic Design Manual”, ANSI/AISC 327-05, American Institute of Steel Construction and the Structural Steel Education Council, Chicago, IL.

American Institute of Steel Construction (AISC) (2010), “Seismic Provisions for Structural Steel Buildings ANSI/AISC 341-10, American Institute of Steel Construction, Chicago, IL.

American Institute of Steel Construction (AISC) (2010), “Specification for Structural Steel Buildings”, ANSI/AISC 360-10, American Institute of Steel Construction, Chicago, IL.

American Society of Civil Engineers and Structural Engineering Institute (ASCE/SEI) (2010), “Minimum Design Loads for Buildings and Other Structures”, ASCE/SEI 7-10, American Society of Civil Engineers, Reston, VA.

American Society of Civil Engineers and Structural Engineering Institute (ASCE/SEI) (2010), “Seismic rehabilitation of existing buildings”, ASCE/SEI-41-06, American Society of Civil Engineers, Reston, VA.

Applied Technology Council (1978), “Tentative Provisions for the Development of Seismic Regulations for Buildings”, Publication ATC 3-06, NBS Special Publication 78-8, U.S. Government Printing Office, Washington, DC.

Arce, G. (2002), “Impact of Higher Strength Steels on Local Buckling and Overstrength of Links in Eccentrically Braced Frames”, Master’s Thesis, Department of Civil Engineering, University of Texas at Austin, Austin, TX.

Becker R., Ishler M. (1996), “Seismic design practice for eccentrically braced frames based on the 1994 UBC”, Steel Tips, Structural Steel Education Council, USA.

Clifton, C., Bruneau, M., MacRae, G., Leon, R., Fussell, A. (2011), “Steel Structures Damage from the Christchurch Earthquake Series of 2010 and 2011”, Bulletin of The New Zealand Society for Earthquake Engineering, 44(4), 297-318.

CSA (2005), “Limit states design of steel structures, including CSA-S16S1-05 Supplement No. 1, CAN/CSA S16-01”, Canadian Standards Association, Ontario, Canada.

Chopra A.K. (1995), “Dynamics of Structures: Theory and Applications to Earthquake Engineering”, Prentice Hall, Englewood Cliffs, NJ.

Clough, R. W., Benuska, K. L., and Lin, T. Y. (1966), "FHA Study of Seismic Design Criteria for High-Rise Buildings", HUDTS-3, Federal Housing Administration, Washington, D.C.

Dusicka P., Itani A.M., Buckle I.G. (2010), "Cyclic behaviour of shear links of various grades of plate steel", *Journal of Structural Engineering*, 136(4), 370–378.

Engelhardt, M. D. and Popov, E. P. (1989), "Behavior of Long Links in Eccentrically Braced Frames", Report No. UCB/EERC-89/01, Earthquake Engineering Research Center, University of California at Berkeley, California, CA.

Engelhardt, M. D. and Popov, E. P. (1992), "Experimental Performance of Long Links in Eccentrically Braced Frames", *Journal of Structural Engineering*, 118 (11), 3067-3088.

Engelhardt, M.D., Winneberger T., Zekany A.J., Potyraj, T. (1998), "Experimental Investigation of Dogbone Moment Connections", *AISC Engineering Journal*, 35(4), 128-139.

Eurocode 8 (1993), "Design of structures for earthquake resistance – Part 1: General Rules, seismic actions and rules for buildings", European Standard EN 1998-1, European Committee for Standardization, Brussels, Belgium.

Eurocode 8 (2004), "Design of structures for earthquake resistance – Part 1: General Rules, seismic actions and rules for buildings", European Standard EN 1998-1, European Committee for Standardization, Brussels, Belgium.

Federal Emergency Management Agency (2000), "State of the Art Report on Systems Performance of Steel Moment Frames Subject to Earthquake Ground Shaking", FEMA-355C, Washington, DC.

Federal Emergency Management Agency (2003), “NEHRP Recommended Provisions for Seismic Regulations for New Buildings and Other Structures”, FEMA 450-2, Part 2: Commentary, Washington, DC.

Federal Emergency Management Agency (2009), “Quantification of Building Seismic Performance Factors FEMA P695 ATC-63 Project Report”, FEMA P695, Washington, DC.

Filippou, F.C., FedeeasLab (2001), “Finite Elements in Design, Evaluation and Analysis of Structures”, University of California, Berkeley, California, CA.

Foutch, D. A. (1989), “Seismic behavior of eccentrically braced steel building”, *Journal of Structural Engineering*, 115 (8), 1857-1876.

Gálvez, P. (2004), “Investigation of Factors Affecting Web Fractures in Shear Links”, Master’s Thesis, Department of Civil Engineering, University of Texas at Austin, Austin, TX.

Ghobarah A., Ramadan T. (1991), “Seismic analysis of links of various lengths in eccentrically braced frames”. *Canadian Journal of Civil Engineering*, 18(1), 140–8.

Gilbertson, M. F. (1969), "Two nonlinear beams with definitions of ductility", *Journal of Structural Engineering*, 95(2), 137-157.

Goel R.K., Chopra A.K. (1997), “Period formulas for moment-resisting frame buildings”, *Journal of Structural Engineering*, 123(11), 1454–1461.

Goel R.K., Chopra A.K. (1998), “Period formulas for concrete shear wall buildings”, *Journal of Structural Engineering*, 124(4), 426-433.

Goel S.C., Itani A.M. (1994), "Seismic resistant special truss moment frames". ASCE Journal of Structural Engineering, 120(6), 1781-1797.

Goel S.C., Shao S.H. (2005), "Performance-Based Seismic Design of EBF Using Target Drift and Yield Mechanism as Performance Criteria", AISC Report.

Günaydın E., Topkaya C. (2013), "Fundamental periods of steel concentrically braced frames designed to Eurocode 8", Earthquake Engineering and Structural Dynamics, 42 (10), 1415-1433.

Hjelmstad, K. D. and Popov, E. P. (1983), "Seismic Behavior of Active Beam Links in Eccentrically Braced Frames", Report No. UCB/EERC-83/15, Earthquake Engineering Research Center, University of California at Berkeley, California, CA.

Hjelmstad K.D., Popov E.P. (1984), "Characteristics of eccentrically braced frames", Journal of Structural Engineering, 110(2), 340–53.

Hjelmstad K.D., Lee S.G. (1989), "Lateral buckling of beams in eccentrically-braced frames", Journal of Constructional Steel Research, 14, 251-272.

International Conference of Building Officials (1988), "Uniform Building Code", International Conference of Building Officials, Pasadena, CA.

Itani A., Douglas B. M., and El-Fass S. (1998), "Cyclic behavior of shear links in retrofitted Richmond-San Rafael Bridge towers." Proc., 1st World Congress on Structural Engineering-San Francisco, Paper No. T155-3, Elsevier, New York.

Kasai K. and Popov E. P. (1986), "A Study of Seismically Resistant Eccentrically Braced Steel Frame Systems," Report No. UCB/EERC-86/01, Earthquake Engineering Research Center, University of California at Berkeley, California, CA.

Koboevic S., Redwood R. (1997), "Design and seismic response of shear critical eccentrically braced frames", *Canadian Journal of Civil Engineering*, 24(5), 761-771.

Kwon O., Kim E. (2010), "Evaluation of Building Period Formulas for Seismic Design", *Earthquake Engineering and Structural Dynamics*, 39(14), 1569-1583.

Kuşylmaz A., Topkaya C. (2013), "Design Overstrength of Steel Eccentrically Braced Frames", *International Journal of Steel Structures*, 13 (3) , 529-545.

Manheim, D. N. (1982), "On the Design of Eccentrically Braced Frames", Thesis, D. Eng, Department of Civil Engineering, University of California at Berkeley.

Malley J. O. and Popov, E. P. (1983), "Design Considerations for Shear Links in Eccentrically Braced Frames", Report No. UCB/EERC-83/24, Earthquake Engineering Research Center, University of California at Berkeley, California, CA.

Malley J. O. and Popov, E. P. (1984), "Shear Links in Eccentrically Braced Frames", *Journal of Structural Engineering*, 110 (9), 2275-2295.

MathWorks, Inc. (2010), "MATLAB r2010b User's Guide", Natick, MA.

Mazzolani F.M, Della Corte G., D'Aniello M. (2009), "Experimental analysis of steel dissipative bracing systems for seismic upgrading", *Journal of Civil Engineering and Management*, 15(1), 7–19.

McDaniel C. C., Uang C. M. and Seible F. (2003), "Cyclic Testing of Built-Up Steel Shear Links for the New Bay Bridge", *Journal of Structural Engineering*, ASCE, 129 (6), 801-809.

Medina R.A., Krawinkler H. (2005), "Evaluation of drift demands for the seismic performance assessment of frames", *Journal of Structural Engineering*, 131(7), 1003-1013.

Miranda E. and Bertero V.V. (1994), "Evaluation of strength reduction factors for earthquake resistant design", *Earthquake Spectra*, 10(2), 357-379.

Miranda E. (2001), "Estimation of inelastic deformation demands of SDOF systems", *Journal of Structural Engineering*, 127(9), 1005-1012.

Miranda E. , Ruiz-Garcia J. (2002), "Evaluation of approximate methods to estimate maximum inelastic maximum displacement demands", *Earthquake Engineering and Structural Dynamics*, 31, 539-560.

Newmark N.M., Hall W.J. (1982), "Earthquake Spectra and Design", *Earthquake Engineering Research Institute, Berkeley, California, CA.*

Okazaki T. (2004), "Seismic performance of link-to-column connections in steel eccentrically braced frames", PhD Dissertation, Department of Civil Engineering, University of Texas at Austin, Austin, Texas.

Okazaki T., Arce G., Ryu H.C., Engelhardt M.D. (2005) , "Experimental study of local buckling, overstrength, and fracture of links in eccentrically braced frames", *Journal of Structural Engineering*, 131(10), 1526–35.

Okazaki T., Engelhardt M.D., Nakashima M, Suita K. (2006), "Experimental performance of link-to-column connections in eccentrically braced frames", *Journal of Structural Engineering*, 132(8), 1201-1211.

Özhendekci D., Özhendekci N. (2008), “Effects of frame geometry on the weight and inelastic behavior of eccentrically braced chevron frames”, *Journal of Constructional Steel Research*, 64, 326-343.

Popov E.P., Engelhardt M.D. (1988), “Seismic eccentrically braced frames”, *Journal of Constructional Steel Research*, 10, 321-354.

Popov E.P., Engelhardt M.D., Ricles J.M. (1989), “Eccentrically braced frames: US Practice”, *AISC Engineering Journal*, 26(2), 66-80.

Popov, E. P., Ricles, J. M., and Kasai, K. (1992), “Methodology for optimum EBF Link Design”, *Proceedings, Tenth World Conference of Earthquake Engineering*, Vol. 7, Balkema, Rotterdam, 3983-3988.

Richards, P. W. and Uang, C. M. (2003), “Development of Testing Protocol for Short Links in Eccentrically Braced Frames,” Report No. SSRP-2003/08, Department of Structural Engineering, University of California, San Diego, La Jolla, CA.

Richards, P.W., Uang, C.M. (2005), “Effect of Flange Width-Thickness Ratio on Eccentrically Braced Frames Link Cyclic Rotation Capacity”, *Journal of Structural Engineering*, 131(10), 1546-1552.

Richards, P.W., Uang, C.M. (2006), “Testing Protocol for Short Links in Eccentrically Braced Frames”, *Journal of Structural Engineering*, 132(8), 1183-1191.

Richards P.W., Thompson B. (2009), “Estimating inelastic drifts and link rotation demands in EBFs”, *AISC Engineering Journal*, Third Quarter: 123-135.

Richards P.W. (2010), "Estimating the stiffness of eccentrically braced frames", ASCE Practice Periodical on Structural Design and Construction, 15(1), 91-95.

Ricles J. M. and Popov E. P. (1987), "Experiments on Eccentrically Braced Frames with Composite Floors," Report No. UCB/EERC-87/06, Earthquake Engineering Research Center, University of California at Berkeley, California, CA.

Ricles J. M. and Popov E. P. (1989), "Composite action in eccentrically braced steel frames", Journal of Structural Engineering, 115(8), 2046-2066.

Ricles J. M., and Bolin S. (1991), "Seismic performance of eccentrically braced frames", UCSD Structural Systems Report No. 91-09, Univ. of California, San Diego, CA.

Ricles J. M. and Popov E. P. (1994), "Inelastic Link Element for EBF Seismic Analysis", Journal of Structural Engineering, 120 (2), 441-463.

Roeder C. W. and Popov E. P. (1977), "Inelastic Behavior of Eccentrically Braced Steel Frames Under Cyclic Loadings," Report No. UCB/EERC-77/18, Earthquake Engineering Research Center, University of California at Berkeley, California, CA.

Roeder C.W., Popov E.P. (1978), "Eccentrically braced steel frames for earthquakes", Journal of the Structural Division, 104(ST3), 391-412.

Roeder C. W., Foutch D. A. and Goel S. C. (1987), "Seismic Testing of Full-Scale Steel Building—Part II", Journal of Structural Engineering, ASCE, 113 (11), 2130-2145.

Rossi P.P., Lombardo A. (2007), "Influence of the link overstrength factor on the seismic behavior of eccentrically braced frames", Journal of Constructional Steel Research, 63, 1529-1545.

Ryu H.-C. , Okazaki T. and Engelhardt M.D. (2004), “Cyclic loading tests on shear links for EBFs: Link performance under revised loading protocol”, Unpublished report.

Saritas A., Filippou F.C. (2009), “Frame element for metallic shear-yielding members under cyclic loading”, *Journal of Structural Engineering*, 135(9), 1115-1123.

Somerville P. G., Smith M., Punyamurthula S. and Sun, J. (1997), “Development of Ground Motion Time Histories for Phase 2 of the FEMA/SAC Steel Project”, Report No. SAC/BD-97/04, SAC Joint Venture, Sacramento, CA.

Tremblay R. (2005), “Fundamental periods of vibration of braced steel frames for seismic design”, *Earthquake Spectra*, 21(3), 833-860.

Uang C.M. (1991), “Establishing R (or R_w) and Cd factors for building seismic provisions”, *ASCE Journal of Structural Engineering*, 117(1), 19-28.

Uang C.M., Maarouf A. (1994), “Deflection amplification factor for seismic design provisions”, *Journal of Structural Engineering*, 120(8), 2423-2436.

Uniform Building Code (1994), International Conference of Building Officials, Whittier, CA.

Yang, M-S. (1982), “Seismic Behavior of an Eccentrically X-Braced Steel Structure”, Report No. UCB/EERC-82/14, Earthquake Engineering Research Center, University of California at Berkeley, California, CA.

CURRICULUM VITAE

PERSONAL INFORMATION

Surname, Name: Kuşyılmaz, Ahmet
Nationality: Turkish (TC)
Date and Place of Birth: 26 June 1984, Ankara
Marital Status: Single
Phone: +90 555 204 69 31
email: ahmetk32@yahoo.com

EDUCATION

Degree	Institution	Year of Graduation
MS	METU Civil Engineering	2008
BS	METU Civil Engineering	2006
High School	Atatürk High School, Ankara	2002

WORK EXPERIENCE

Year	Place	Enrollment
2013-Present	İller Bankası A.Ş.	Asst. Technical Expert
2006-2013	METU Dept. of Civil Engineering	Research Assistant
2005 July	Prota Mühendislik	Intern Engineering Student
2004 July	Türkerler İnşaat	Intern Engineering Student

FOREIGN LANGUAGES

English (advanced level), German (beginner level)

PUBLICATIONS

1. Kuşyılmaz A., Topkaya, C. (2014), “Fundamental Periods of Steel Eccentrically Braced Frames”, The Structural Design of Tall and Special Buildings (in press)
2. Kuşyılmaz A., Topkaya, C. (2013), “Design Overstrength of Steel Eccentrically Braced Frames”, International Journal of Steel Structures, 13 (3), 529-545.
3. Kuşyılmaz A., Topkaya, C. (2011), “A Numerical Study on Local Buckling and Energy Dissipation of CHS Seismic Bracing”, Thin Walled Structures, 49 (8), 984-996.

HOBBIES

Computer programs, table tennis, tennis, swimming